Design and Modeling of BLDC Motor Drive with Regenerative Braking System Based on Fuzzy-PID Controller for Electric Vehicle

Mahlet Melesse Wolde

A Thesis Submitted to

The Department of Electrical Power and Control Engineering

School of Electrical Engineering and Computing

Presented in Partial Fulfillment of the Requirements for the Master of Science Degree in Electrical Power and Control Engineering (Power Electronics)

Office of Graduate Studies

Adama Science and Technology University

October, 2020

Adama, Ethiopia

Design and Modeling of BLDC Motor Drive with Regenerative Braking System Based on Fuzzy-PID Controller for Electric Vehicle

Mahlet Melesse Wolde

Advisor: Tafesse Asrat (PhD)

A Thesis Submitted to

The Department of Electrical Power and Control Engineering

School of Electrical Engineering and Computing

Presented in Partial Fulfillment of the Requirements for the Master of Science Degree in Electrical Power and Control Engineering (Power Electronics)

Office of Graduate Studies

Adama Science and Technology University

October, 2020

Adama, Ethiopia

APPROVAL OF BOARD OF EXAMINERS

We, the undersigned, members of the Board of Examiners of the final open defense by Mahlet Melesse Wolde have read and evaluated her thesis entitled "Design and Modeling of BLDC Motor Drive with Regenerative Braking System Based on Fuzzy-PID Controller for Electric Vehicle'' and examined the candidate. This is, therefore, to certify that the thesis has been accepted in partial fulfillment of the requirement of the Degree of Master's in Electrical Power and Control Engineering (Power Electronics).

Name of Student	Signature	Date
Advisor / Supervisor /	Signature	Date
Yoseph Mekonnen (Ph.D)	[signature]	31/10/20
External Examiner	Signature	Date
Internal Examiner	Signature	Date
Chairperson	Signature	Date
Head of Department	Signature	Date
School Dean	Signature	Date
Postgraduate Dean	Signature	Date

DECLARATION

I hereby declare that this MSc thesis is my original work and has not been presented for a degree in any other university, and all sources of material used for this thesis have been duly acknowledged.

Name: Mahlet Melesse Wolde

Signature: ___________________

This MSc thesis has been submitted for examination with my approval as a thesis advisor.

Name: ______________________________

Signature: ___________________

Date of submission: ________________________

ADVISOR APPROVAL SHEET

To: Department of Electrical Power and Control Engineering (EPCE)

This is to certify that the thesis entitled "Design and Modeling of BLDC Motor Drive with Regenerative Braking System Based on Fuzzy-PID Controller for Electric Vehicle. (The Case of Nissan 530)" submitted in partial fulfillment of the requirements of the Master of Science Degree in Electrical Power and Control Engineering, postgraduate in Power Electronics, and has been carried out by Mahlet Melesse Wolde Id No. PGR/1894/11 under my supervision. Therefore, I recommend that the student has fulfilled the requirements and hereby he can submit the thesis to the department.

Dr. Tafesse Asrat	____________________	____________________
Name of Advisor	Signature	Date

ACKNOWLEDGMENT

It is a pleasant task to express my thanks to all those who contributed in many ways to the successful completion of this thesis.

First, I would like to thank more my God. I would like to express my deep and sincere gratitude to my advisor, **Dr. Tafesse Asrat** for giving me the opportunity to research under his guidance and supervision. Thank you for making me work in a comfortable place. I also wanted to share my appreciation for your support, valuable advice, friendly attitude, patience and help. I received motivation, comments, encouragement and continuous guidance from him during my graduate studies.

I would like to thank my best friends, class mates and dorm mates especially thanks to **Minyamer Gelawe (MSc.)** for helping in preparing the thesis documentation and discussions regarding everything.

Finally, my deep and sincere gratitude to my family for their continuous and unparalleled love, help and support. I am grateful to my lovely sister **Mekdes Melesse** for always being there for me as a friend. I am forever indebted to my parents for giving me the opportunities and experiences that have made me who I am. They selflessly encouraged me to explore new directions in life and seek my own destiny. This thesis would not have been possible if not for them, and I dedicate this milestone to them.

ABSTRACT

Due to the increase in demand of energy, new technologies have evolved to improve energy efficiency like regenerative braking. In this thesis, the energy storage device, battery, with converters and Brushless Direct Current (BLDC) motor are used to analyze regenerative braking. The fuzzy logic control was used in three phase BLDC motor in order to control the four quadrant operations without any loss of power. Brushless Direct Current (BLDC) motors are one of the motor types rapidly gaining popularity. BLDC motors are used in industries such as appliances, automotive, aerospace, medical, industrial automation equipment and instrumentation. BLDC motor with matching servo amplifiers offer many features than other motion control systems, like broader speed range, operation in special environments and mechanical advantages. Brushless dc motor and servo amplifier therefore presents a complete line of compatible; latest technology of brushless system components. The speed control is achieved by using fuzzy-proportional integral derivative controller. The fuzzy-PID control is used in three phase BLDC motor in order to control the four quadrants operations without any loss of power. In fact, energy is conserve during the regenerative period and storage of excess energy created during regenerative braking condition of the battery. When motoring mode battery state of charge decreasing and when braking mode battery SOC increasing with and without lode. The bidirectional DC-DC converters are often used for the battery charging and discharging application. The main aim of this thesis is to control the power flow under acceleration and braking conditions. During acceleration and normal modes, the power flows from battery to motor, and during braking or regenerative mode the kinetic energy of the motor is converted into electrical energy and fed back to the battery. The simulation will be done for Brushless DC motor with fuzzy-PID controller using MATLAB/Simulink software.

***Keywords**: BLDC motor, Regenerative braking, Fuzzy logic control, DC-DC Converter, Four quadrant operations*

TABLE OF CONTENTS

LIST OF FIGURES

LIST OF TABLES

ACRONYMS

AMC	American Motor Car Company
BLDC	Brushless DC
CD-RW	Compact Disc, Rewriteable
DC	Direct Current
EMF	Electromotive Force
EMI	Electromagnetic Interference
EV	Electric Vehicles
EVB	Electric-Vehicle Battery
FLC	Fuzzy Logic Controller
HEV	Hybrid Electric Vehicles
ICE	Internal Combustion Engine
IGBT	Insulated-Gate Bipolar Transistor
IM	Induction Motor
Li-ion	Lithium-ion Battery
Li-S	Lead-Acid
MOSFET	Metal Oxide Silicon Field Effect Transistor
Ni-cd	Nickel Cadmium
Ni--MH	Nickel-Metal Hydride
PI	Proportional Integral
PID	Proportional Integral Derivative
PMDC	Permanent Magnet DC
PMSM	Permanent Magnet Synchronous Motors
PWM	Pulse Width Modulation
RBS	Regenerative Braking System
SOC	State of Charge
SRM	Switched Reluctance Motor
VSI	Voltage Source Inverter
VVS	Variable Voltage Source

LIST OF SYMBOLS

Symbol	Meaning	Unit
C_d	Aerodynamic drag coefficient	
ρ_a	Air density	(kg/m^3)
e_{a}, e_{b}, and e_c	Back-EMF	
B	Damping constant	(N.m.s)
V_{dc}	Dc link voltage input	(V)
T_r	Delay time	Sec
A_f	Effective cross-sectional area	(m^2)
η	Efficiency	(%)
θ_r	Electrical rotor angle	(°)
S	Endurance mileage	
e	Error	
λ_m	Flux linkage	(Wb)
B	Friction coefficient	(N)
g	Gravity	(m/s^2)
E_{a}, E_{b}, and E_c	Induced Back EMF	
J	Inertia	$(kg.m^{2)}$
T_L	Load torque	(N-m)
m	Mass	(kg)
V_{cm}	Maximum control voltage	(V)
ω_m	Mechanical speed of the rotor	(rad/s)
M	Mutual inductance per phase	(H)
i_a, i_b and i_c	Per phase stator currents.	(A)

P	Power	(kW)
I^*	Reference current amplitude	(A)
i_a^*, i_b^*, i_c^*	Reference phase currents	(A)
α	Road gradient angle	(°)
C_r	Rolling resistance coefficient	
$f_{as, bs, cs}(\theta_r)$	Rotor angle functions	
J	Rotor inertia	(kgm^2)
θ	Rotor position	(°)
ω_m	Rotor speed	rpm
L	Stator inductance per phase	(H)
$V_{as, bs, cs}$	Stator per phase stator voltages	(V)
R_s	Stator resistance per phase	(R)
f_c	Switching (carrier) frequency	(Hz)
K_t	Torque constant	(N-m/A)
ν_{car}	Vehicle speed	(m/s)
ν_{wind}	Wind speed	(m/s)

CHAPTER ONE

INTRODUCTION

1.1. Background

In recent years, electric vehicles (EVs) have received much attention as an alternative to traditional internal combustion engine (ICE) vehicles. The unparalleled focus is mainly attributable to environmental and economic concerns linked to the consumption of fossil-based oil which is used as fuel in ICE-powered vehicles. With the development of battery and motor technology [1], the EVs become the most promising alternative to the ICE vehicles. Plug-in EVs use a battery system which can be recharged from standard power outlets. Since the performance features of EVs have become similar to, if not better than, those of traditional ICE vehicles, EVs present a realistic alternative. Regenerative braking can be used in EVs as a method for recycling the brake energy, which is incredible in the conventional internal combustion vehicles. Regenerative braking is the process of feeding energy from the drive motor back into the battery during the braking process, when the vehicle's inertia forces the motor into generator mode.

In this mode, the battery is considered as a load, thereby providing a braking force to EVs [2]. It is shown that the use of regenerative braking of EVs can increase the driving range up to 15% with respect to EVs without the regenerative braking system (RBS). However, regenerative braking does not work all times, e.g., when the battery is fully charged, braking needs to be affected by dissipating the energy in a resistive load. Therefore, the mechanical brake in the EV is still required. A mechanical brake system is also very significant for EVs safety and other operations [3]. Organization of EV mechanical braking and regenerative braking is accomplished by a single foot pedal: The first part of the foot pedal controls the regenerative braking, and the second part controls the mechanical brake. This is a continuous transition from regenerative braking to mechanical braking. It cannot be simply accomplished by traditional ICE vehicles [4]. In addition, the other main important of the electric driven vehicles is that, for a large capacity drives, the battery requirement increases drastically. Therefore, the main application is for the lower capacity drives. As the input power is electrical, the motor required shall be utilizing the electrical input and driven by a suitable controller. Therefore, the reliability of the motor is also very important so, it is important to choose the right motor. The electric motor plays an important role in any electric vehicle. The most appropriate motor among many electric motors for EV is BLDC motor because it has many advantages over brushed DC motor and induction motor [5].

BLDC motors are a type of synchronous motor. This indicates the magnetic field created by the stator and the magnetic fields generated by the rotor rotate at the same frequency. The brushless motor, not at all like the DC brushed motor, has the permanent magnets joined on the rotor. It has usually four magnets around the border. The stator of the engine is composed by the electromagnets, usually four of them, set in a cross design with 90° angle between them. The major advantage of the brushless motors is that, due to the reality that the rotor carries as it were the permanent magnets, no require of winding connections to be done with the rotor, no brush-commutator pair should be made. This is frequently how the brushless motors took their name from. This include gives the brushless motor incredible improvement in reliability, as the brushes wear off very quick. In addition, brushless motors are more silent and more efficient in terms of power consumption. The fast braking operation and speed controlling of BLDC motor drive required speed controller. Several techniques and algorithms have been proposed by researchers for the BLDC motor speed controller [6]. Among them are PI, PID, fuzzy and adaptive fuzzy PID controllers have been widely used for speed control of BLDC motor.

PID controllers are the known controllers used in many industrial processes because of simple structure and robust performance. PID controllers deal with both time and frequency responses if they are tuned suitably, but for complex systems the performance of conventional PID controllers are tend to reduce. The performance of the controllers changed extremely with the introduction of fuzzy logic controller. For extensive range of industrial applications fuzzy logic controllers are being used. This fuzzy logic controller shows improved performance when compared to PID controllers [6]. Fuzzy-PID controller is proposed which combines the fuzzy controller with the conventional PID controller and has the benefit of two methods.

In this thesis, the electric vehicle dynamics mathematical modeling is performed. Also, the mathematical model and the principle of a three-phase star-connected BLDC motor drive with ideal trapezoidal back-EMF waveform is discussed. The comparison of PID and Fuzzy-PID speed controllers for BLDC motor control is performed. The result shows Fuzzy-PID speed controller gives better speed performance than the others. Beside the motor is controlled in all the four quadrants without any loss of power; in fact, energy is conserved during the regenerative period. This energy is stored in a battery storage system through regenerative period and can be fed back to the inverter mains during shortage of supply from the source. The model of BLDC motor drive for the application of electric vehicle is designed and simulated using MATLAB/Simulink.

1.2. Statement of the Problem

Due to the emission of greenhouse gases the environmental pollution is increasing around the world. Besides, the cost of the fuel also increasing. To reduce certainly the above-mentioned problems fossil fuel-based vehicles must be replaced by electric vehicles. The motor and battery consumption are an important thing in electric vehicle which needs the efficient and appropriate control techniques. BLDC motor has better performance characteristics in many aspects. Depend on overall performance lithium-ion battery has better performance for electric vehicle. The life time of the battery was other problem in electric vehicle. To decrease overcome the above-mentioned problems using regenerative braking systems. In this research work, develop strategies in order to increase the regeneration of power being wasted during braking. The proposed control and drive systems are implemented and simulated by using MATLAB software.

1.3. Research Questions

In general, the research has been guided to address the following questions:

- ✓ How to analyze the specification of motor and battery for electric vehicle?
- ✓ How to model the BLDC motor drive for EV propulsion?
- ✓ How to control the speed of BLDC motor with regenerative braking system?

1.4. Objectives of the Study

1.3.1. General Objective

The general objective of this thesis is to design and model of BLDC motor drive based on fuzzy-PID controller with regenerative braking system for Nissan 530 electric vehicle.

1.3.2. Specific Objectives

The general objectives of this thesis are;

- To model three phase BLDC motor drive for Electric Vehicle.
- To design bidirectional DC-DC converter for regenerative braking system.
- To design fuzzy-PID controller for speed of BLDC motor drive.
- To control the speed of the BLDC motor with regenerative braking system.
- To simulate the system by using MATLAB software.

1.5. Significance of the Study

The worldwide are shifting the energy source usage from non-renewable source that will not available after a few decades to renewable energy source that can exist forever. In a similar ways center of transformation and vehicle engineering members are trying to develop EV in ASTU. Since the above-mentioned objectives are certainly full filled, this research study can support the trend started by center of transportation and vehicle engineering members.

1.6. Motivation of the Study

As the global economy strives towards clean energy in the face of climate change; the automotive industry is researching into improving the efficiency of automobiles. Electric Vehicles (EV) are an answer to the crisis the world is about to face in the near future. But the question that's being always asked is, how can the driving range of electric vehicles be increased? The answer to this question lies within the success of the investigate for an efficient and power packed energy source like an enchantment battery or success with fuel cells, efficient regenerative braking systems, etc. In regenerative braking, the kinetic energy can be changed over back into electrical energy that can be stored in batteries for reuse to move the vehicle during the driving cycle [5]. In this manner, regenerative braking has the potential to moderate energy which can improve fuel economy whereas reducing emissions that contribute to air pollution.

1.7. Scope of the Study

The research study includes modeling and simulation of speed control of BLDC motor drive with regenerative braking system by using MATLAB software. Regenerative braking is necessarily limited when the batteries are fully charged. Because the additional charge from regenerative braking would cause the voltage of a full battery to rise above a safe level. This thesis can be applicable for Nissan 530 EV. The study doesn't include the detail parts of other EV.

1.8. Limitation of the Study

The thesis is limited to the simulation of the system using MATLAB/Simulink by showing how the different components of the system interact with each other. This is because the implementation of a real system is difficult to procure the components. Along with it takes the additional time and cost incurred in making the actual prototype implementation. Also, because of Corona virus (COVD-19) don't access the internet freely. Then data collection well be difficult.

1.9. Thesis Outline

Chapter 1: The first chapter presents the introduction of BLDC motor drive, a statement of the problem, research questions, objectives of the study, Significance of study, motivation, scope, and limitation of the study.

Chapter 2: Reviewed literatures and papers on the background. And also cover advantage of BLDC motor compared with the other electric motors and existing control mechanism of BLDC motor are discussed. And also, compared lithium-ion battery with the other electric batteries.

Chapter 3: Covers the analyses of data's, BLDC motor drive modeling and the proposed system development are covered.

Chapter 4: The proposed system results are discussed in chapter four.

Chapter 5: Finally, conclusion and recommendation are made in chapter five.

CHAPTER TWO

THEORETICAL BACKGROUND AND LITERATURE REVIEW

2.1. Introduction

In this chapter the background and varieties of electric motors, advantage of brushless DC motor compared with the other electric motors and its todays word wide application, the existing controlling mechanism and other related applications of BLDC motor are reviewed and discussed.

2.2. Electric Vehicle

Electric vehicles are not something modern to this world, but with the innovative progression and increased concern on controlling pollution have given it a tag of future mobility. In EV's, electric energy is the most source of power for drive of a vehicle. In electric vehicles, electrical energy is changed over into mechanical (rotational) energy by electric motors. This rotational energy is connected to the wheels of a vehicle through an appropriate transmission system which in turn causes drive. A vehicle with four wheels can be considered as the foremost efficient show in electric vehicles [7]. Electric vehicles can utilize electric energy as a sole source of power or can utilize batteries in conjunction with gasoline engines to control the vehicle. Battery, electric motor and controller are the core components of any electric vehicle.

2.3. Electric Motors

An electric motor is an electrical machine that changes over electrical energy into mechanical energy. Most electric engines work through the interaction between the motor's magnetic field and electric current in a wire winding to produce force within the form of torque applied to the motor's shaft. Electric motors can be powered by coordinate current (DC) sources, such as from batteries, engine vehicles or rectifiers, or by alternating current (AC) sources, such as a power grid, inverters or electrical generators. A motor in an electric vehicle gives the vital force for the propulsion of a vehicle, which makes it the heart of electric vehicles. An electric generator is mechanically identical to an electric engine, but operates with a turned around flow of control, converting mechanical energy into electrical energy [8].

2.3.1. Various Types of Electric Motors used in Electric Vehicles

Different types of electric motors are compared on the basis of certain parameters which should be considered for selecting a particular motor type for electric vehicle application. The comparison is tabulated for some parameters. Also, on the characteristics chart different motors are included at some points.

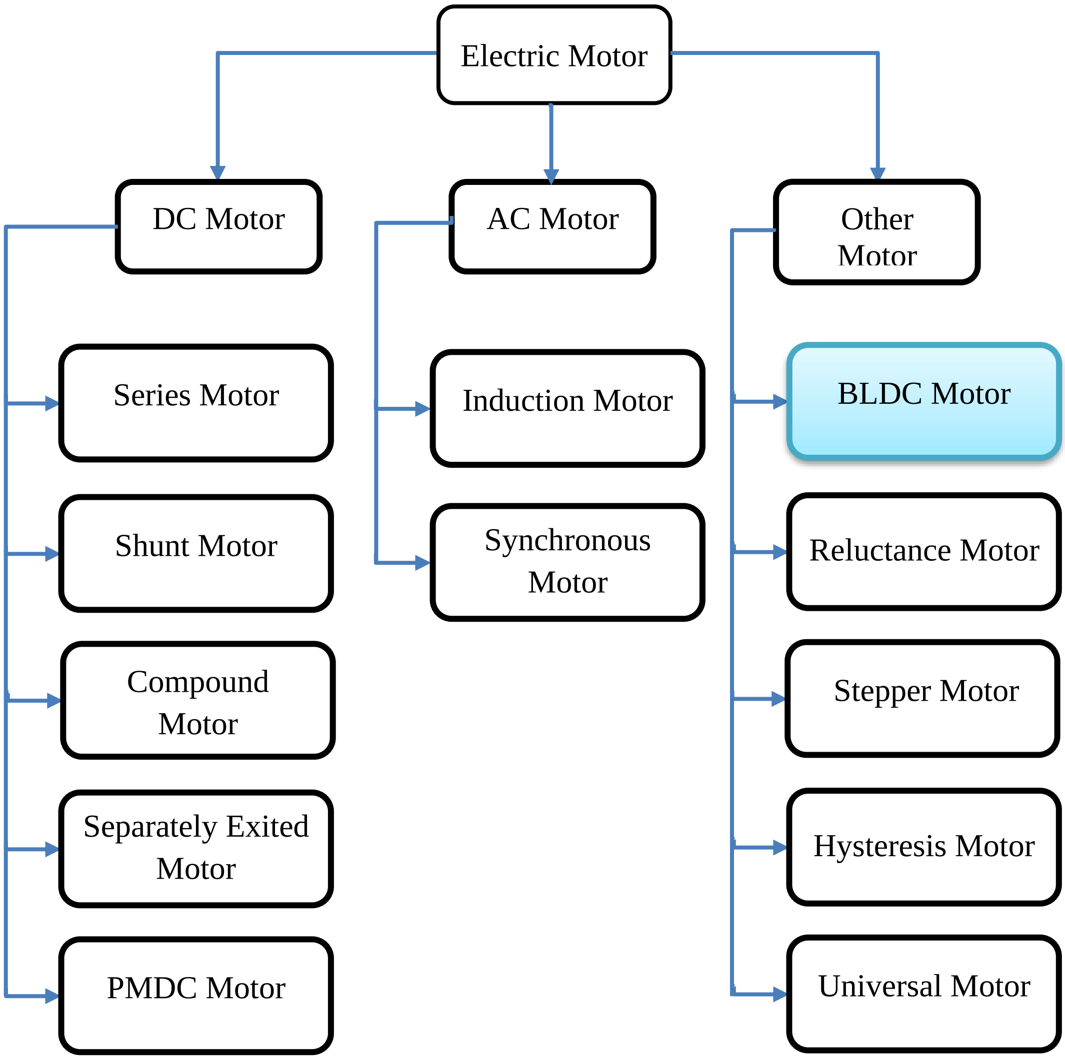

Figure 2.1 Types of motor

2.3.2. DC Brushed Motor

In DC brushed motor, brushes along with commutators provide a nexus between external supply circuit and armature of the motor. Brushes can be made up of carbon, copper, carbon graphite, metal graphite and are mostly rectangular in shape [9]. The Wearing of commutators due to continuous cutting with brushes is one of the main drawbacks of DC brushed motors. Also, friction between brushes and commutators, limits the maximum motor speed. DC brushed motors have the ability to achieve high torque at low speeds, which makes them suitable for traction system [10].

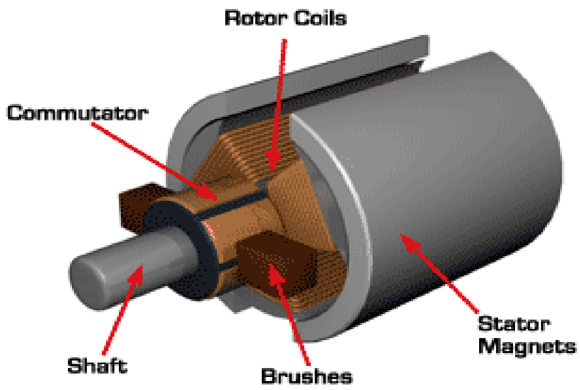

Figure 2.2 DC motor [L1]

2.3.3. Induction (Asynchronous) Motor

Three phase induction motors are widely used in electric vehicles because of high efficiency, good speed regulation and absence of commutators. Three phase AC supply is connected to stator winding, due to which revolving magnetic field is established. This revolving magnetic field interacts with stationary rotor conductors, and induced current flows through rotor conductors. Induced current establishes its own magnetic field. Interaction between revolving magnetic field and field due to induced currents gives rise to unidirectional torque [10]. As the speed of the rotor is different (less) than speed of revolving field (synchronous speed), these motors are also called as asynchronous motor.

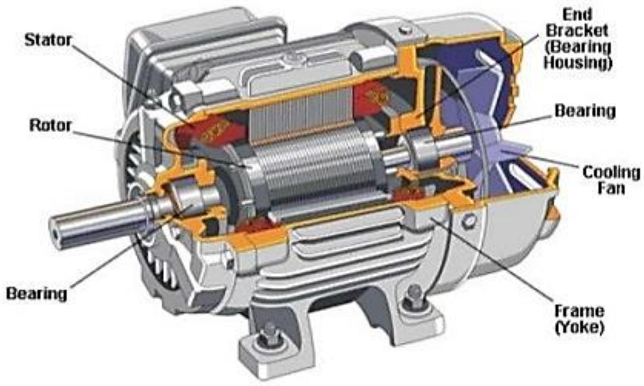

Figure 2.3 Induction motor [L1]

2.3.4. Switched Reluctance Motor (SRM)

Switched reluctance motor produces torque by variable reluctance method. When stator coils are energized, variable reluctance is set up in the air gap between the stator and the rotor. Rotor tends to move to a position of least reluctance thus causing torque. Switched reluctance motor has characteristics like high starting torque, wide speed range and better inherent fault-tolerance capability, which makes it suitable for electric vehicle application [11]. Some parameters that must be taken into account while comparing above motors for choosing a best suited motor for the required electric vehicle application are power-to-weight ratio, torque-speed characteristics, efficiency, cost of the controller, cost of motor [12].

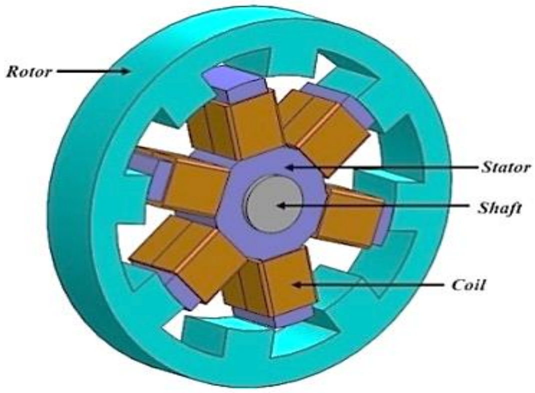

Figure 2.4 Switched reluctance motor [L1]

2.3.5. Brushless DC Motor (BLDC)

Brushless DC motor provides certain advantages over DC brushed motor, like less maintenance and higher efficiency. Mechanical commutation as in brushed DC motor is replaced by equivalent electronic commutation (inverter circuit and rotor-position sensing element) circuit in DC brushless motor [13], [14]. BLDC motor is defined as rotating self-synchronous machine with a permanent magnet rotor and known rotor shaft positions for electronic commutation [15]. BLDC motor provides higher torque at the peak values of current and voltage as compared to other motors [14]. Due to better operating characteristics at higher speeds, these motors find their application in compressors, pump and ventilation system.

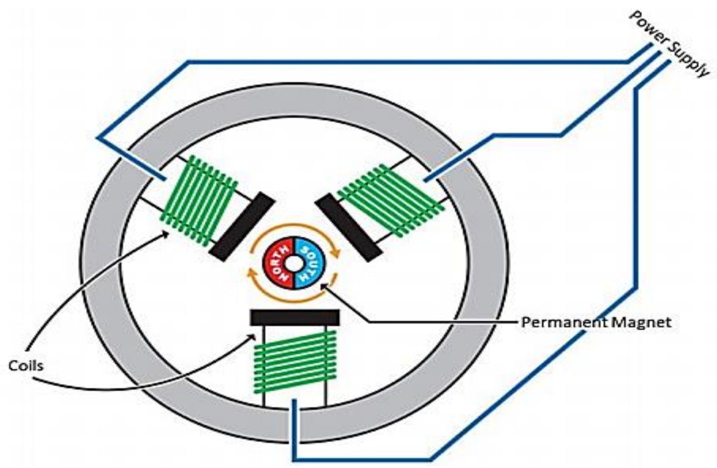

Figure 2.5 Brushless DC motor [L1]

2.3.6. Permanent Magnet Synchronous Motor (PMSM)

This motor is additionally kind of like a BLDC motor which has permanent magnets on the rotor. The same as BLDC motors, these motors even have traction characteristics like high power density and high efficiency. The difference is that PMSM has a sinusoidal back EMF whereas BLDC has a trapezoidal back EMF. Permanent magnet Synchronous motors are available for higher power ratings. PMSM is that the best option for high performance applications like cars, buses. Despite the high cost, PMSM is providing stiff competition to induction motors due to increased efficiency than the latter. PMSM is also costlier than BLDC motors. Most of the automotive manufacturers use PMSM motors for their hybrid and electric vehicles. As an example, Toyota Prius, Chevrolet Bolt EV, Ford Focus Electric, zero motorcycles S/SR, Nissan Leaf, Hinda Accord, BMW i3, etc. use PMSM motor for propulsion.

Figure 2.6 Permanent magnet synchronous motor [L1]

2.1. Comparison of BLDC Motor with Other Motors

The only difficulty of the electric driven vehicles is that, for a large capacity drives, the battery requirement increases drastically. Therefore, the main application is for the lower capacity drives. As the input power is electrical, the motor required shall be utilizing the electrical input and driven by a suitable controller. Therefore, the reliability of the motor is also very important so, it is important to choose the right motor. For single-speed applications, induction motors are more suitable, but if the speed has to be maintained with the variation in load, then because of the flat speed-torque curve of BLDC motor, BLDC motors are a good fit for such applications. BLDC motors become a more suitable fit for such applications because variable speed induction motors will also need an additional controller, thus adding to system cost. Brushed DC motors will also be a more expensive solution because of regular maintenance. Precise control is not required applications like an induction cooker and because of low maintenance; BLDC motors are a winner here too. However, for such applications, BLDC motors use optical encoders, and complex controllers are required to monitor torque, speed, and position. Brushed DC motors are known for generating more EMI noise, so BLDC is a better fit but controlling requirements for BLDC motors also generate EMI and audible noise. The selection of the BLDC as a suitable motor was based on comparative studies represented in Table 2.1, Table 2.2 and Table 2.3.

Table 2.1 Comparison of BLDC motor with DC motor and IM [16], [17]

Futures	**BLDC motor**	**DC motor**	**Induction motor (IM)**
Speed-torque characteristics	Flat in nature as the result it can operate at all speeds with rated load	Moderately flat, at higher speed brush friction increases reduction of useful torque.	Non-linear, it enables lower torque at lower speeds
Efficiency	High	Moderate	Less
Rotor inertia	Lower and hence better dynamic characteristics	Higher and hence limited dynamic response time.	Higher and hence Poor dynamic characteristics
Electric noise	Less	High– because of brushes	Less
Speed range	Higher - no losses in brushes	Moderate – loses in brushes	Lower – determined by the Ac line frequency; increases in load further reduces speed
Control requirements	A controller is always required to control the commutation sequence	No controller is required for a fixed speed; controller required for variable speed	No controller is enquired for a fixed speed; controller required for variable speed
Commutation method	Using solid state switches	Mechanical contacts between brushes and commutator	The special starting circuit is required
Maintenance	Less maintenance	Periodic maintenance because of brushes	Less maintenance
Cost	Expensive	Cheaper	Cheaper

Table 2.2 Comparison of BLDC motor and SRM **[16]**

Parameter	**BLDCM**	**SRM**
Power density	Higher	Lower
Air gap	Up to 1 mm or more	Small, fraction of mm
Efficiency	Over 90%	Low
Performance at low speed	Good	Torque is high, but low efficiency
Torque ripple	About 10%	Over 20%
Power electronics converter	Necessary	Necessary
Cost	Still expensive motor	Cost-effective motor

Table 2.3 Comparison of BLDC motor and PMSM [16], [18]

Parameter	**BLDCM**	**PMSM**
Machine type	Synchronous machine	Synchronous machine
Back emf	Trapezoidal	Sinusoidal
Rotor position sensor	Stator flux position commutation each 60º	Continuous stator flux position variation
Phase winding energized	Only two phases ON at the same time	Possible to have three phases ON at the same time
Torque ripple	High	Moderate
Switching losses	Less switching losses	High switching losses at the same switching frequency
Control algorithms	Control algorithms are relatively simple	Control algorithms are mathematically intensive
Control	Easier to control (six trapezoidal states)	More complex control
Controller/ driver cost	Less expensive	Very expensive

In general, the comparison performance of BLDC motor for EV propulsion can be summarized as shown in Figure 2.7 based on motor performance characteristics of each maximum of six points [16], [17] and [18].

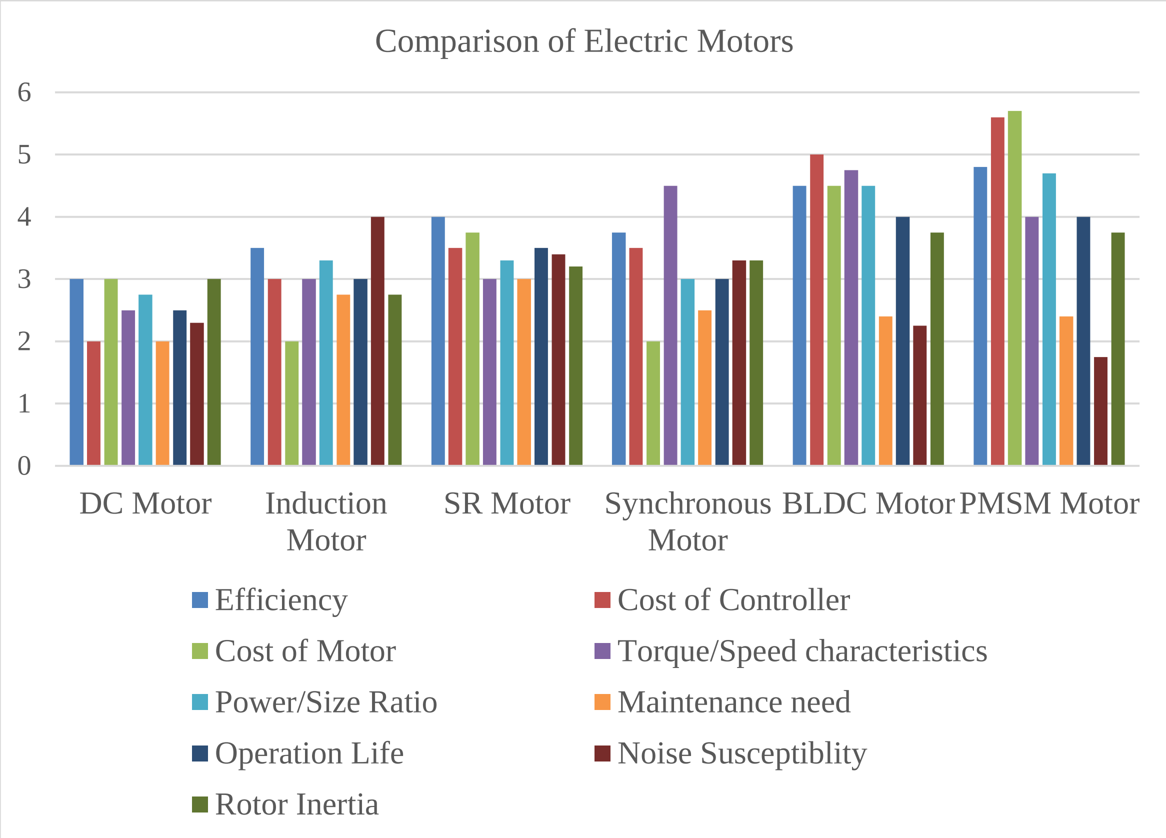

Figure 2.7 Comparison of electric motors

The above comparison shown that BLDC motor is the best selection for EV compared to an induction motor, SR motor, and DC brushed motor. PMSM motors are more efficient and produce less noise and torque ripple. But it is more complex to control, at the same switching frequency high switching losses, very expensive than BLDC motor for this reason, we can't use PMSM for electric vehicle.

2.2. Electric Vehicle Batteries

An electric-vehicle battery (EVB) in addition to the traction battery specialty systems used for industrial (or recreational) vehicles, are the batteries used to power the electric motors of a battery electric vehicle (BEVs). Batteries for electric vehicles are characterized by their relatively high power-to-weight ratio, specific energy and energy density; smaller, lighter batteries reduce the weight of the vehicle and improve its performance. Compared to liquid fuels, most current battery technologies have much lower specific energy, and this often impacts the maximal all-electric range of the vehicles. However, metal-air batteries have high specific energy because the cathode is provided by the surrounding oxygen in the air.

2.2.1. Types of Electric Battery

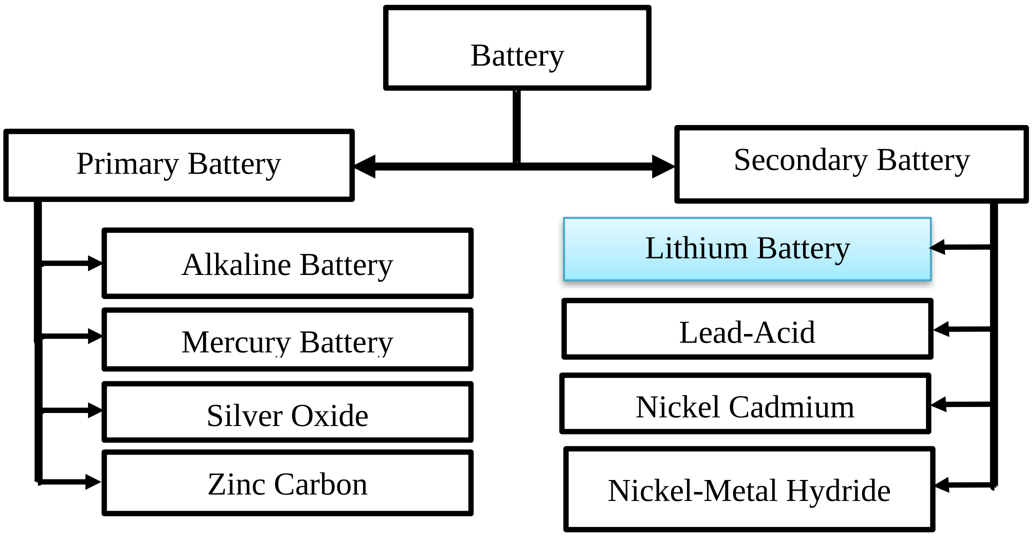

Figure 2.8 Types of electric battery

2.2.2. Comparison of Electric Batteries

Table 2.4 Comparison of electric batteries **[19]**

No.	**Types of Battery**	**Advantage**	**Disadvantage**
1	Lithium-ion Battery (Li-ion)	High energy density High power rate cycle life Longer run time High efficiency No loss of amp hours	Expensive Technology not properly developed
2	Lead-Acid (Li-S)	High power density Medium efficiency Loss of 15-amp hours	Low energy density High maintenance Vary large and old type

		Reliable and cheap	Bulky
3	Nickel Cadmium (Ni-cd)	Good life cycle Available in different size	Low output voltage Expensive and Toxic
4	Nickel-Metal Hydride (Ni-MH)	High capacity energy density Same size	More complex charging algorithm needed High self-discharging Low power rate

In general, the comparison performance of battery for EV propulsion can be summarized as shown in Figure 2.6 based on battery performance characteristics of each maximum of five points [19]. [20].

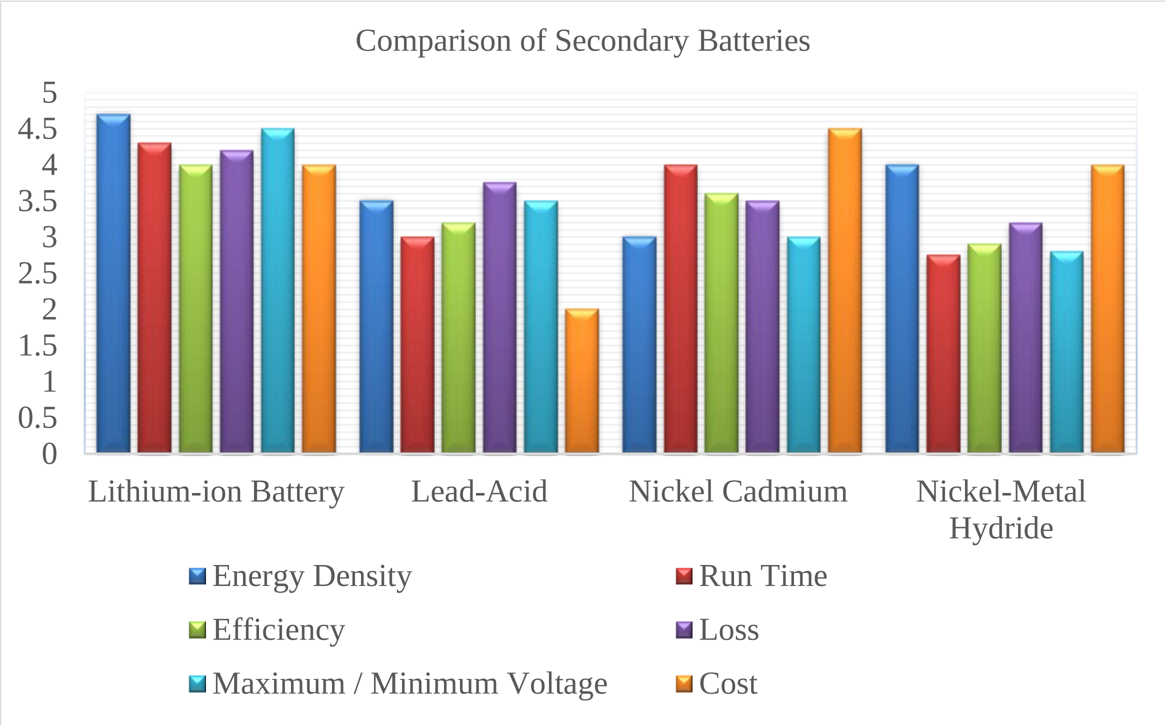

Figure 2.9 Comparison of secondary batteries

Lithium-ion batteries has good performance parameters than other type of batteries for EV. It has higher energy density, longer life span and higher power density than most other practical batteries. Complicating factors include safety, durability, thermal breakdown and cost. Li-ion batteries should be used within safe temperature and voltage ranges in order to operate safely and efficiently [21].

2.3. Bidirectional DC-DC Converter

A bidirectional buck-boost converter is shown in Figure 10. The main difference with a unidirectional DC/DC Converter is on the use of MOSFET or IGBT to switch the state of the current instead of all the diodes [22]. The magnitude of the voltage and current as well as the placement of the energy storage items, the bi-directional DC-DC converter can either operate as a Buck converter by stepping down a higher voltage to a lower voltage or as a Boost converter by stepping up from a lower voltage to a higher voltage. Indeed, diodes do not allow current to flow in both directions, but with MOSFET the period of each position can be easily controlled [23].

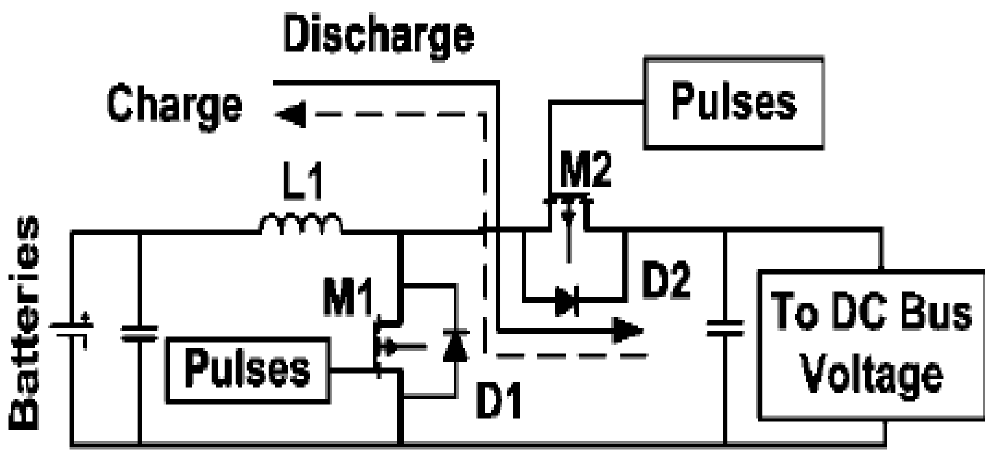

Figure 2.10 Bidirectional DC-DC converter [15], [L2]

The kinetic energy is wasted as heat energy in previous methods whereas this method involves the conversion of kinetic energy into electric energy which is rectified and stored in a chargeable battery in automotive applications most DC/DC converters have to exchange power between two voltage sources [24]. To accomplish this power, transfer the current must be able to go through the circuit in both directions.

There are a lot of for this kind of converters, because the use of a battery implies the capacity of charging and discharging so the use of a bidirectional converter allows avoiding a complex system of twin circuits to accomplish the charge and the discharge of the battery.

2.4. Four Quadrant Operation

There are four possible modes or quadrants of operation are possible in Brushless DC Motor which is depicted in Figure 2.11 In X-Y plot of speed versus torque, Quadrant 1 is forward speed and forward torque. The torque is propelling the motor in forward direction. Conversely, Quadrant 3 is reverse speed and reverse torque. Now the motor is "motoring" in the reverse direction, but torque is being applied in reverse. Torque is being used to "brake" the motor, and the motor is now generating power as a result.

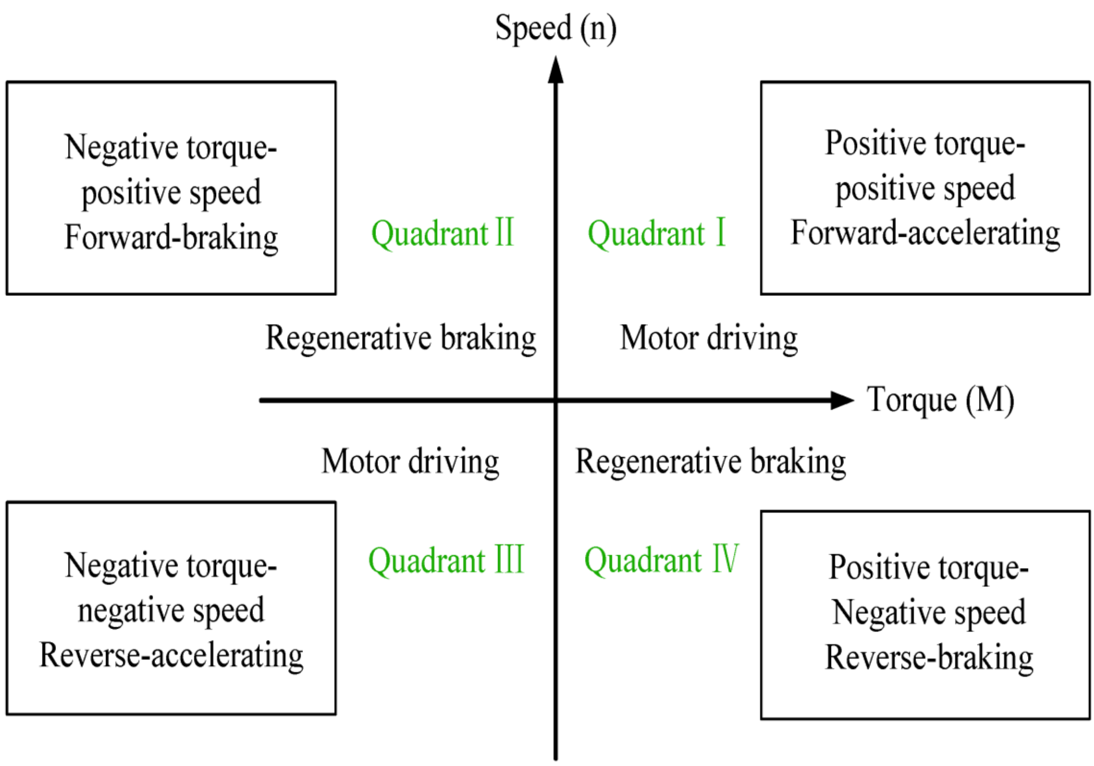

Figure 2.11 Four quadrant operation [L3]

Finally, Quadrant 4 is exactly the opposite. The motor spins in the direction, but the torque is being applied in the forward direction. Again, torque is being attempted to slow the motor and change its direction to forward again. Once again, power is being generated in the motor.

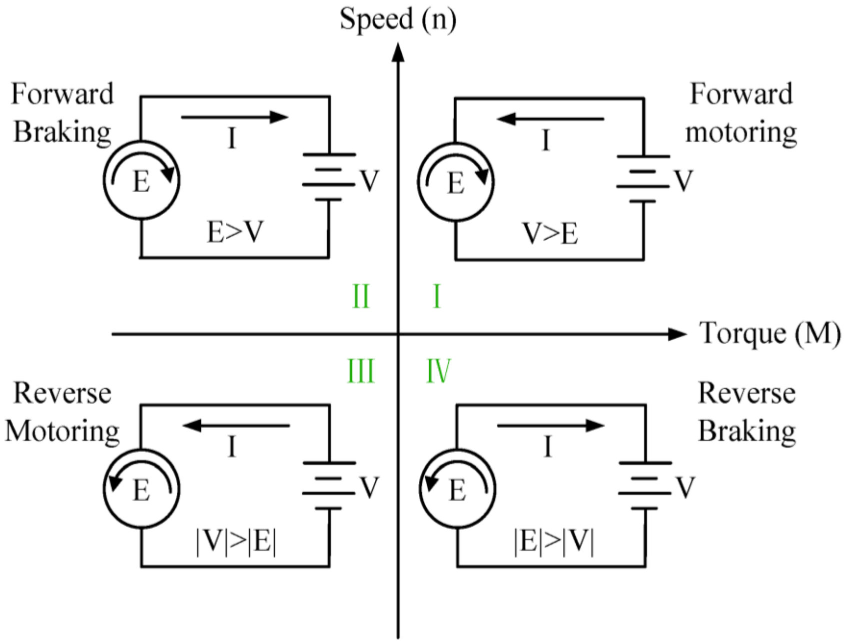

Figure 2.12 Operation modes [L3]

2.5. Depending on Inverter Controlling Technique

2.5.1. Six Step Inverter Feed VVS Based Speed Control of BLDC Motor Drive

This technique is applicable in the case of, if variable voltage source is used. The duty cycle of the speed controller output determines the input voltage to the inverter. The inverter switches will be controlled depending on rotor position. The hall sensor rotor position signal is decoded to the exact required duty cycle and generate zero and one via logical gates to drive the inverter switches.

2.5.2. Hysteresis Current Controller-Based BLDC Motor Drive

Hysteresis current control is a method of controlling a voltage source inverter so that an output current is generated to follow a reference current waveform. It is the easiest control method to be implemented. However, the disadvantage is that there is no limit to the switching frequency. Advantages of using hysteresis band control are excellent dynamic performance and ability to control the peak to peak value of current ripple in desired hysteresis band limit. It is also very simple for physically implementation. Hysteresis current controller can be used for trapezoidal BLDC motor drive. Differ from a six-step inverter feed VVS based BLDC motor drive, the output of speed regulator will not directly control input voltage but through the inverter switches control. The output of the speed regulator produces reference torque. The peck value of the reference current is produced by multiplying torque and torque constant. Then the reference current of each phase is produced multiplying the peak reference current and decoded hall sensor signal. Then it is the difference of reference current and phase current that determines the ON- OFF states of the inverter switches by using comparator and logical circuits.

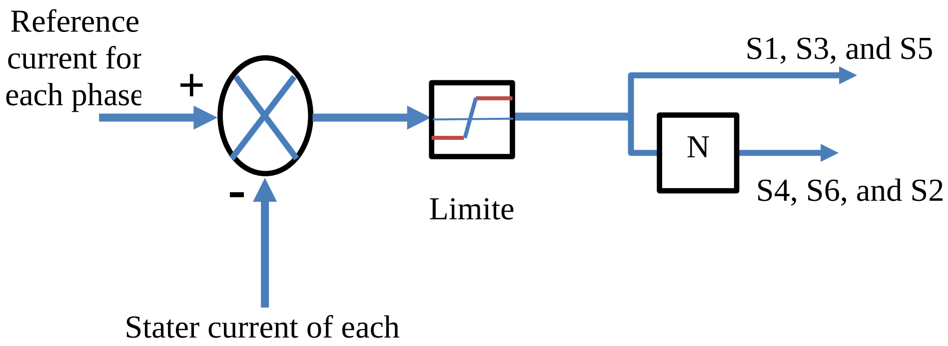

Figure 2.13 Hysteresis current controller-based BLDC motor drive for each phase

2.6. Related Work on Speed Control of BLDC Motor

In practice, the design of the BLDCM drive involves a complex process such as modeling, control scheme selection, simulation and parameters tuning etc. An expert knowledge of the system is required for tuning the controller parameters of servo system to get the optimal performance. Recently, various modern control solutions are proposed for the speed control design of BLDC motor [25]. However, Conventional PID controller algorithm is simple, stable, easy adjustment and high reliability, Conventional speed control system used in conventional PID control. Since, in fact, most industrial processes with different degrees of nonlinear, parameter variability and uncertainty of mathematical model of the system. Tuning PID control parameters is very difficult, poor robustness, therefore, it's difficult to achieve the optimal state under field conditions in the actual production. Fuzzy PID control method is a better method of controlling, to the complex and unclear model systems, it can give simple and effective control, play fuzzy control robustness, good dynamic response, rising time, overstrike characteristics [25].

2.7. Related Works on Regenerative Braking System

To understand the properties and requirements of a new system is more difficult and requires creative thinking and understanding of existing running system is also difficult, improper understanding of the present system can lead diversion from solution. Several research papers reported on regenerative braking system by using different motors and speed controllers.

In 1967, the American Motor Car Company (AMC) created an electrical energy regeneration brake for their concept electric car, the AMC Amitron. Toyota was the first car manufacturer to commercialize RBS technology in their Prius series hybrid cars [26].

The proposed system design involved the following research paper analysis: Paper presented on [27] includes the working principle and braking controller for RBS to increase its efficiency. The authors in [28] includes an introduction and working principle of the regenerative braking system in which all braking modes are described. The difference between conventional braking and regenerative braking system, its advantages disadvantages and applications conclude in literature [29].

The author in [30] presents “Modeling and Analysis of Bidirectional DC-DC Converter”. He applies the most common use control method for single phase isolated bidirectional full bridge DC-DC converter and compared this control method to efficiency way by with/without using snubber capacitors. In this paper, Isolated Bidirectional DC-DC Converter topology is modeled and controller algorithm is written in the FORTRAN programming language.

In a similar manner, “Modeling and Analysis of Regenerative Braking of an Induction Motor” [31]. Analyzes regenerative braking system by using, the energy storage device, battery, with converters and IM. She uses only battery and IM for easy to control, and she added converters for better performance result. The analysis is performed using a vector control method and MATLAB/SIMULINK as a simulation tool.

Author in [32], proposes “Modeling and Control of Bidirectional DC-DC Converter Fed PMDC Motor for Electric Vehicles (For HEV Applications)”. In this paper presented a battery operate bidirectional DC-DC converter fed PMDC motor for the electric vehicle application. The performance of the system has been verified by simulation using MATLAB/SIMULINK environment. The inductor operating in the discontinuous mode the current ripple has considerably risen. It can be reduced by multi-phase interleaved operation. It will also reduce the stress on the high side capacitor; thus, the capacitor value can also be reduced.

2.8. Related Work on Four Quadrant Operation System with Different Motors

DC/DC converters are widely used in telecommunication equipment power supplies, photovoltaic system, portable electronic devices and many other industrial applications [33], [34]. In some applications particularly when battery is used as an energy storage resource, a bidirectional DC/DC converter is required in order to provide an effective path to charge or discharge the battery. The bidirectional DC/DC converter can be realized easily if the active switch (transistor) and passive switch (diode) in conventional DC/DC converter are replaced with bidirectional switches [35], [36]. In addition, in recent years many bidirectional DC/DC converters with high performance and high voltage gain have been introduced [37, 38, 39, 40]. However, these converters do not provide a bipolar output voltage. In some special applications such as DC motor derive systems, a four quadrant DC/DC converter is required that provides the four quadrant operation modes that are include: forward and backward motoring mode and also forward and backward breaking mode. Four quadrant DC/DC converters have been found many applications, particularly in electrical transportation systems that the motor energy should back to source in breaking mode. In addition, four quadrant DC/DC converters can be utilized as one DC/AC inverter if their duty cycle is a sine wave.

In literature [41] Bi-directional dc-dc converter for a battery fed electric vehicle drive system. A closed loop speed control technique of the proposed battery fed electric vehicle is designed and implemented using PI controller.

CHAPTER THREE

METHODOLOGY

3.1. Introduction

This chapter include the methodology, data analysis, design of speed controller, mathematical modeling of the BLDC motor drive. The analysis of the identified motor specification and vehicle dynamics is performed. Finally, the system is simulated by using MATLAB/Simulink software.

3.2. Methods

The following method is used to meet the general and specific objectives of this thesis. First the closely related works are reviewed. Then the necessary data used throughout this study is collected from electric vehicle manufacturing company through their site. Then the collected data is analyzed for the purpose of understanding and developing the system modelling. The modelling BLDC motor drive with its speed controller is developed. Then the system is simulated by using both MATLAB/Simulink/ codes. In general, the method followed throughout the research study can be summarized as the following flow chart.

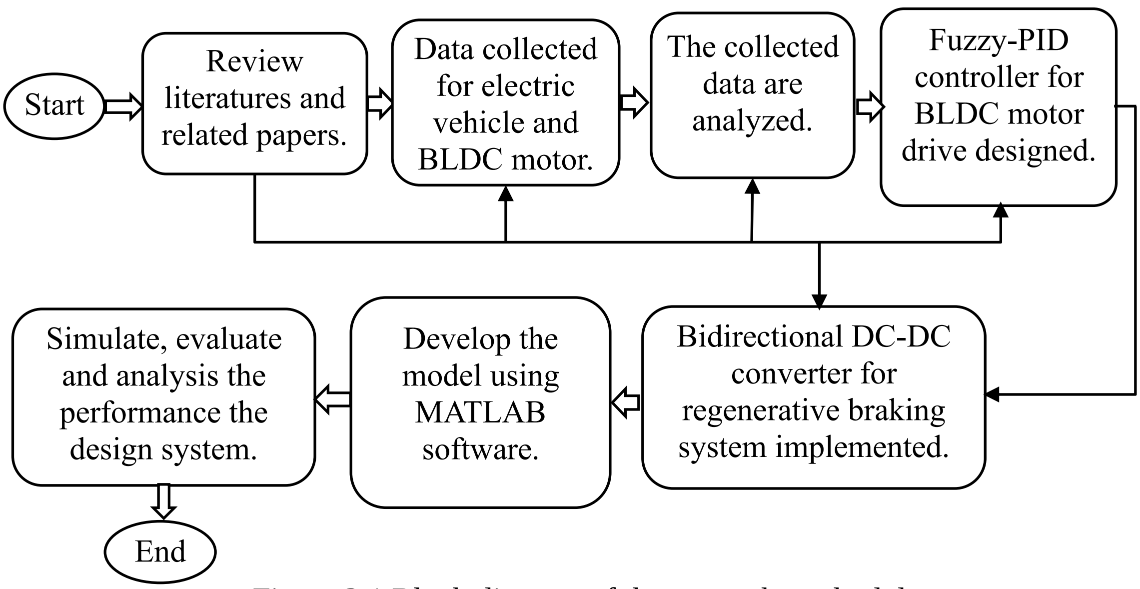

Figure 3.1 Block diagram of the research methodology

3.3. The Proposed Block Diagram of BLDC Motor Drive

The block diagram of the speed control of fuzzy based BLDC motor using bidirectional converter is shown in Figure 3.2. the DC-DC converter can be operated in two modes namely buck and boost mode. During boost mode, the converter boosts the voltage from battery and supplies the motor through the voltage source inverter [42]. The batteries need to be charged and discharging via bidirectional DC-DC power converter. The battery must be able to supply power to the BLDC motor drive. The brushless motor can operate in all four quadrants. The excess energy created during regenerative braking condition is stored in the battery.

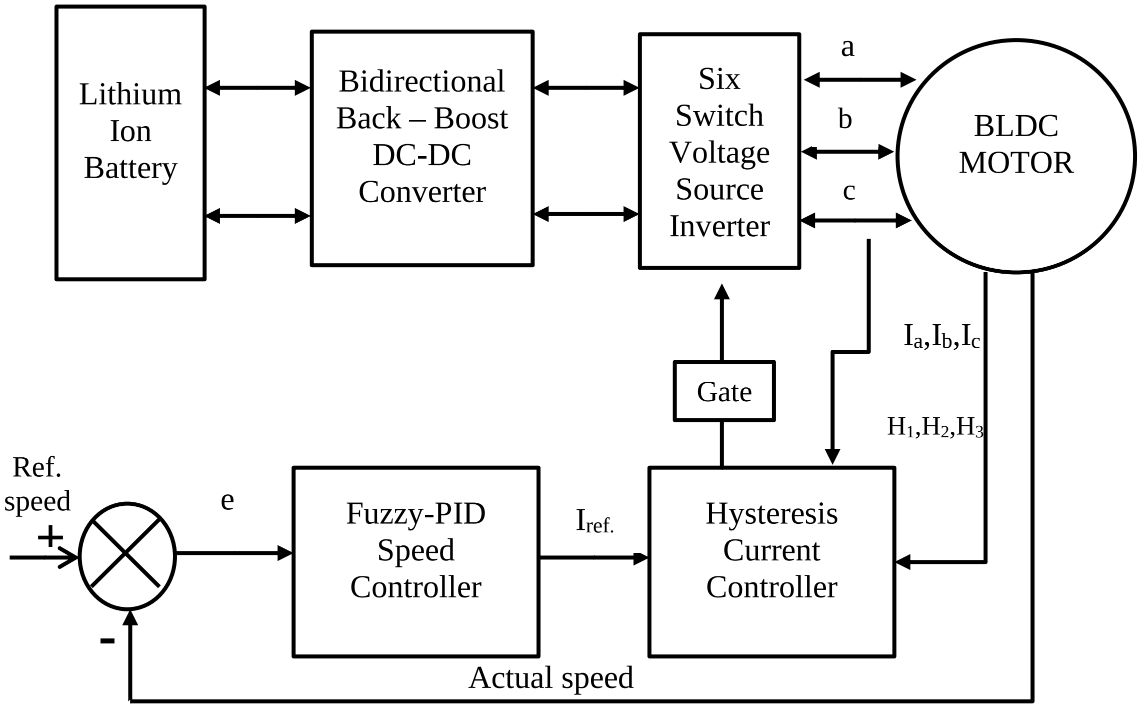

Figure 3.2 Block diagram of the proposed control system

The brushless motor is controlled using a fuzzy-PID controller. The difference between the actual speed and reference speed determine the error [43], [44]. The error signal is generated as the result of variation in the reference speed and the actual speed of the motor which is sensed by hall signal utilized for the formulation of fuzzy rules which results in the generation of the gate signals to drive the switching circuit [45]. The three-phase BLDC motor with built in Hall sensors is chosen for this work. The Hall sensors are required to detect the rotor position and they have to be fed back into the controller. The reference speed is fed as an input to the controller.

3.4. Analysis of an Electric Vehicle Dynamics

Vehicle dynamics aim to describe how a vehicle moves on a road surface while it is under the influence of forces between the tire and the road, as well as aerodynamics and gravity [46]. The pure electric vehicle power system train mainly includes: the electrical motor, battery, motor drive, battery controller and vehicle interface. The power system train of Electric Vehicle consists of an electric drive system with a battery serving as an energy buffer. Usually there is only one electric machine, typically of three phase AC type, connected to the wheel shaft via a gearbox and a differential. The energy is stored chemically in a battery, which is electrically connected to the machine via a DC/AC power electronic converter accompanied by a control system. The structure diagram of the pure electric vehicle power system is shown in Figure 3.3 The energy flow from the battery to the motor and vice versa converted to mechanical and electrical energy vice versa respectively.

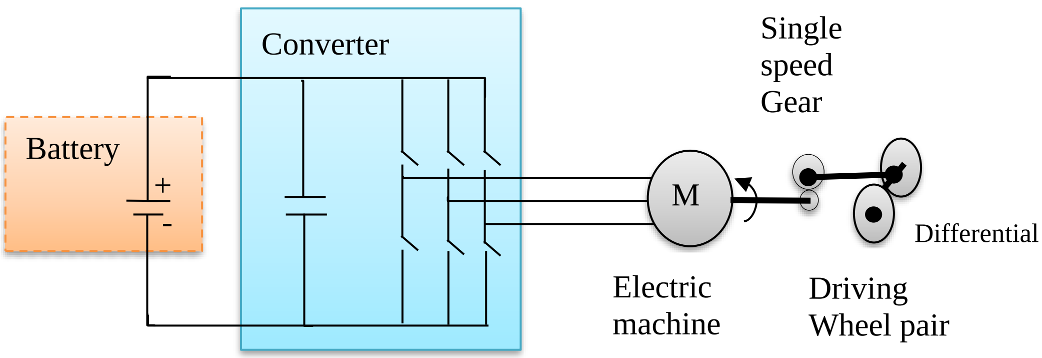

Figure 3.3 Electric vehicle power system structure

3.5.1. Driving Force and Power of Electric Vehicle

The force propelling the electric vehicle has to overcome the rolling resistance force (F_R), gradient (Clamping) resistance force (F_G) and aerodynamics drag force (F_A). In this thesis the car of gross weight 1500 kg is considered as per collected data in order to select the required motor power rating and another specification of electric motor. The total force required for driving a vehicle is calculated in Equation (3.1) [47], [48].

$$F_t = F_R + F_G + F_A \qquad (3.1)$$

The total force is the tractive force that the motor must overcome, in order to drive the vehicle therefore the selected motor must produce the force greater than total force so that there is no slipping of the wheels. It is seen in Figure 3.4 that, the changes of the inclination angle in the road surface introduce a disturbance to the system. Therefore, the controller must have the capability to eliminate disturbances.

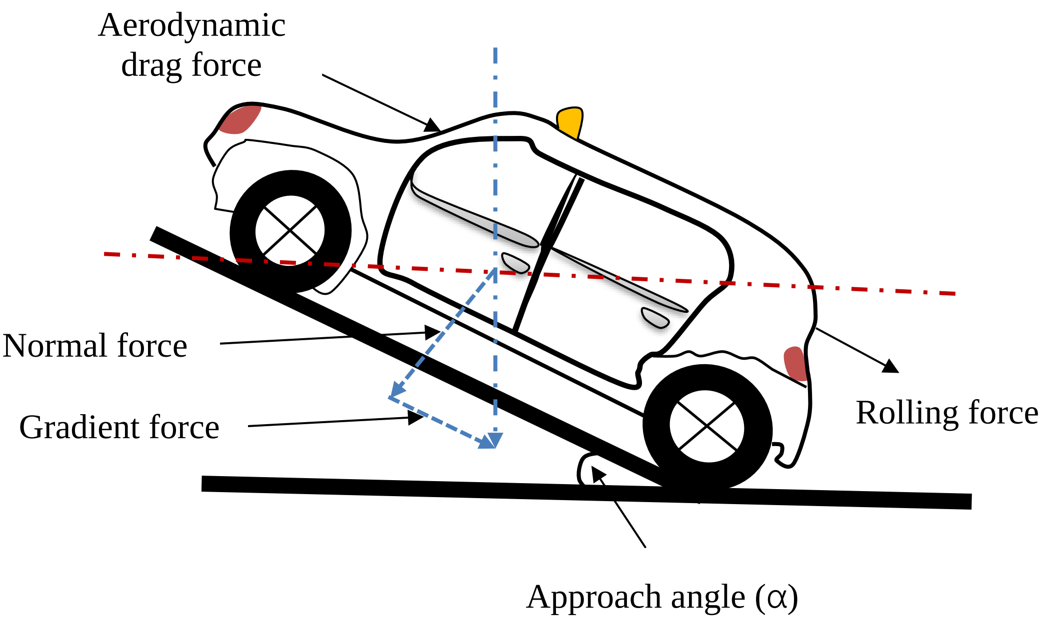

Figure 3.4 Forces acting on electric vehicle

3.4.1.1. Rolling Resistance Force

Rolling resistance is caused by a number of different phenomena taking place in and around the car tires during rolling [46]. Therefore, the rolling resistance force, F_r acting on a vehicle in the longitudinal direction, is usually expressed as the effective normal load of the vehicle multiplied by the dimensionless rolling resistance coefficient, as

$$F_R = m \times g \times C_r \times \cos(\alpha) \tag{3.2}$$

$$= 1500\text{kg} \times 9.81\,\text{m/s}^2 \times 0.01 \times \cos(25°)$$

$$= 133.3632\text{N}$$

where m (kg) is the vehicle mass, g (m/s^2) is the gravity constant, α (rad) is the road gradient angle and C_r rolling resistance coefficient. The power required to overcome the rolling resistance force is:

$$P_R = F_R \times \text{speed}\left(\frac{m}{\text{sec}}\right) \tag{3.3}$$

$$P_R = 133.3632\text{N} \times \left(\frac{120000\text{m}}{3600\text{sec}}\right)$$

$$P_R = 4.4454\text{kW}$$

The coefficient of friction of different types of surface used in the analysis of data is taken from literatures.

Table 3.1 The coefficient of friction for different types of surface [42] [43]

Contact surface	Coefficient of friction
Concrete surface (good/fair/poor)	0.010/0.015/0.02
Asphalt (good/fair/poor)	0.012/0.017/0.022
Macadam (good/fair/poor)	0.015/0.022/0.037
Snow/dirt	0.025/0.037
Mud (firm/medium/smooth)	0.037/0.09/0.15
Grass (firm/soft)	0.055/0.037
Sand (firm/soft/dune)	0.060/0.15/0.3

3.4.1.2. Gradient Resistance

In case of a road grade (or inclination), the vehicle's dynamics will be affected by the component of the gravitational force F_G that is parallel with the road [46].

$$F_G = m \times g \times \sin(\alpha) \tag{3.4}$$

$$= 1500\text{kg} \times 9.81\,\text{m}/\text{s}^2 \times \sin(25°)$$

$$= 6210.8277\text{N}$$

where m (kg) is the vehicle mass, g (m/s^2) is the gravity constant, α is the road gradient angle, road slope (rad.). The power required to overcome the gradient force at a speed of 60km/hr is:

$$P_G = F_G \times \text{speed}\left(\frac{\text{m}}{\text{sec}}\right) \tag{3.5}$$

$$P_G = 6210.8277\text{N} \times \left(\frac{60000\text{m}}{3600\text{sec}}\right)$$

$$P_G = 103.5138\text{kW}$$

3.4.1.3. Aerodynamic Drag

Aerodynamic drag is the resistive force offered due to viscous force acting on the vehicle. It is largely determined by the shape of the vehicle. A compromise often used to model the aerodynamical drag force, F_A, is the partly empirical model, partly based on the expression of dynamical pressure, which is showing a strong dependence on the square of the vehicle speed as

$$F_A = \frac{1}{2}\rho_a C_d A_f \left(\nu_{car} + \nu_{wind}\right)^2 \tag{3.6}$$

$$F_A = \frac{1}{2} \times 1.2 \times 0.2 \times 2 \times (33.33)^2$$

$$F_A = 266.613\text{N}$$

where ρ_a (kg/m^3) is the air density, C_d is the aerodynamic drag coefficient, A_f (m^2) is the effective cross sectional area of the vehicle, ν_{car} (m/s) is the vehicle speed and ν_{wind} (m/s) is the component of wind speed moving in the direction of the vehicle [49]. Equation (3.6) shows that, the aerodynamic force of the car is directly proportional to the square of the sum of the speed of the vehicle and the speed of the air. Substituting the values of constants in Equation (3.6), the aerodynamic force as the speed of the vehicle varies from 0 to 130 km/hr can be plotted as shown in Figure (3.5) by taking the assumption that the speed of the air is zero.

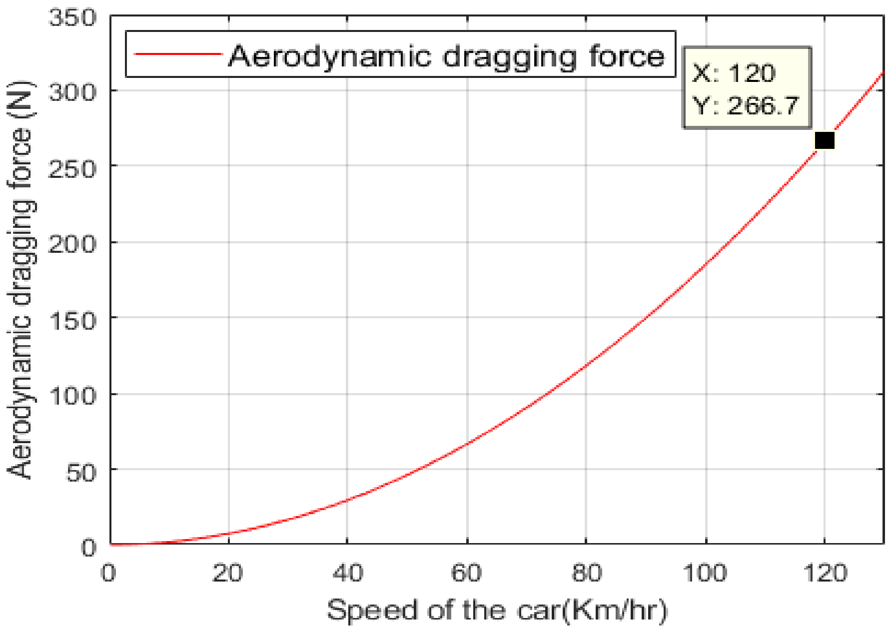

Figure 3.5 Aerodynamic dragging force versus speed of the car in Km/hr

The power applied on the vehicle due to aerodynamic drag force and aerodynamic lift force is calculated as by considering aerodynamic lift force is one fourth of aerodynamic drag force:

$$P_A = F_A \times \text{speed}\left(\frac{\text{m}}{\text{sec}}\right) \tag{3.7}$$

$$P_A = 266.7\text{N} \times \left(\frac{120000\text{m}}{3600\text{sec}}\right)$$

$$P_A = 8.89\text{kW}$$

3.4.1.4. Acceleration Forces

These are the three main force which act on the vehicle when it travels at constant speed, but the vehicle is accelerating or decelerating the effect of force due to inertia also acts up on the vehicle. Gradient forces increase as the approaching angle of the road increases and aerodynamic force is constant if the speed of the vehicle is assumed to be constant. The total motive force with each component of the vehicle is shown in Figure 3.6. In this Figure 3.6 the vehicle is assumed to move up a hill with constant speed of 60Km/hr and the velocity of the air is also assumed to zero.

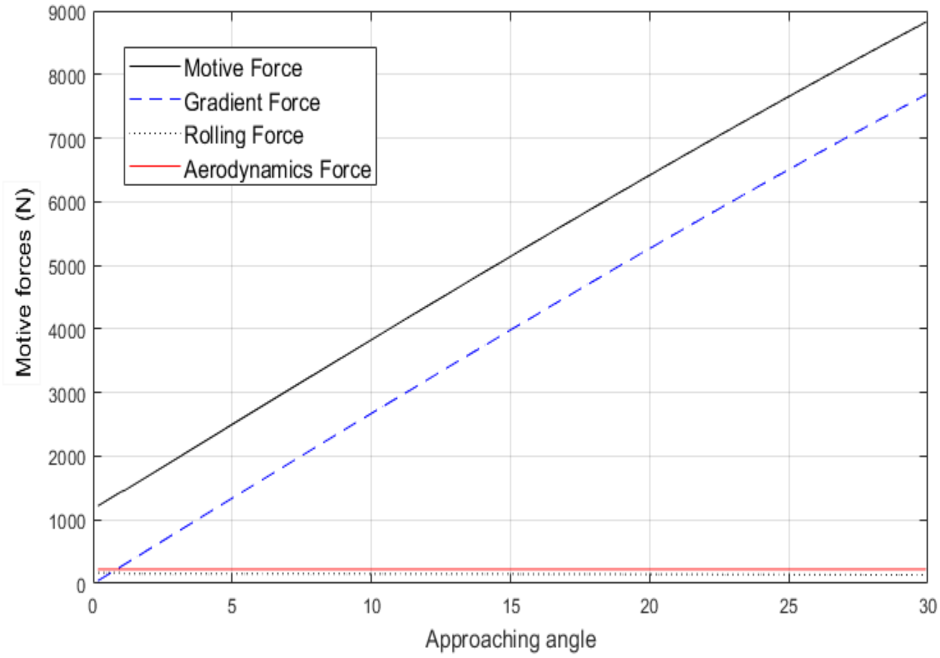

Figure 3.6 Motive force versus approaching angle of the vehicle

Hence, the air speed is less than the vehicle speed, and the power required to overcome it can be ignored. There are additional forces to consider when designing the Nissan 530 electric vehicle dynamics like aerodynamic lift force, wheel force, and others. Therefore, the required maximum power for BLDC motor to drive a four-wheel Nissan 530 electric vehicle in all conditions of motion, that is, the maximum tractive power required to drive the vehicle will be:

$$P_{total(max)} = 4.4454kW + 103.5138kW + 8.89kW \quad (3.8)$$

$$P_{total(max)} = 116.8492kW$$

From Equation (3.1) the total force acting on the vehicle will be:

$$F_t = 133.3632N + 6210.8277N + 266.613N$$

$$= 6610.8042N$$

But BLDC motor with output power rating of 116.8492kW should not be selected. The losses due to transmission of power to the wheel must be included. Therefore, the mechanical power output required to drive the vehicle is given by equation below:

$$M_{total(max)} = \frac{P_{total(max)}}{\eta_{transmission\ gear\ syasem}} \tag{3.9}$$

$$= \frac{116.6492}{0.95} \approx 123kW$$

Equation (3.9) shows the total driving power of the motor for the propulsion of the meter. Based on this result, the motor rated specifications are selected as shown in Table 3.2.

3.5. The Effect of Vehicle Speed on the Power Requirement

The relationship between the speed and driving power of the Nissan 530 is analyzed and plotted as shown in Figure 3.7. This shows that the vehicle power consumption and speed in km/hr have a linear relationship. As the speed of vehicle increases, its power consumption also increases [50] [51]. The vehicle can move at the speed of 120km/hr with a power consumption of 60kW. This relation fulfills with the identified maximum power requirement.

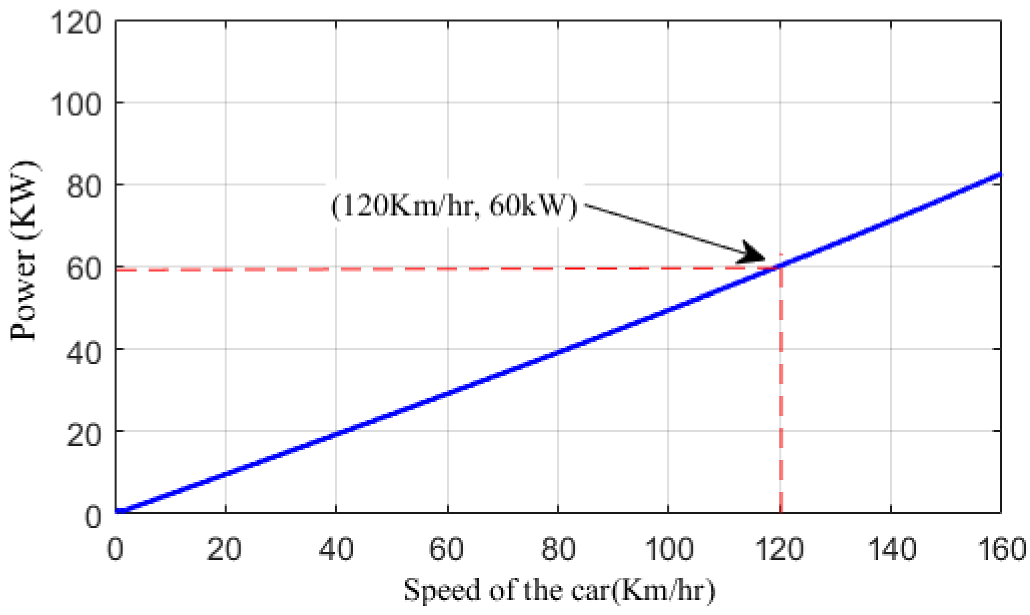

Figure 3.7 Driving power vs speed of the electric vehicle

3.5.1. Motor Rated Power and Peak Power Matching

The selection of rated speed, torque, and power of the BLDC motor should conform to the requirements of the torque versus speed characteristic curve [52]. When the vehicle starts, the motor speed is low and works in constant torque state, as long as the speed is higher than the rated speed, it works in constant power state [53]. The rated torque and power of the 3600rpm base speed electric vehicle BLDC motor have a value of 159.2Nm and 60kW respectively as shown in Figure 3.8.

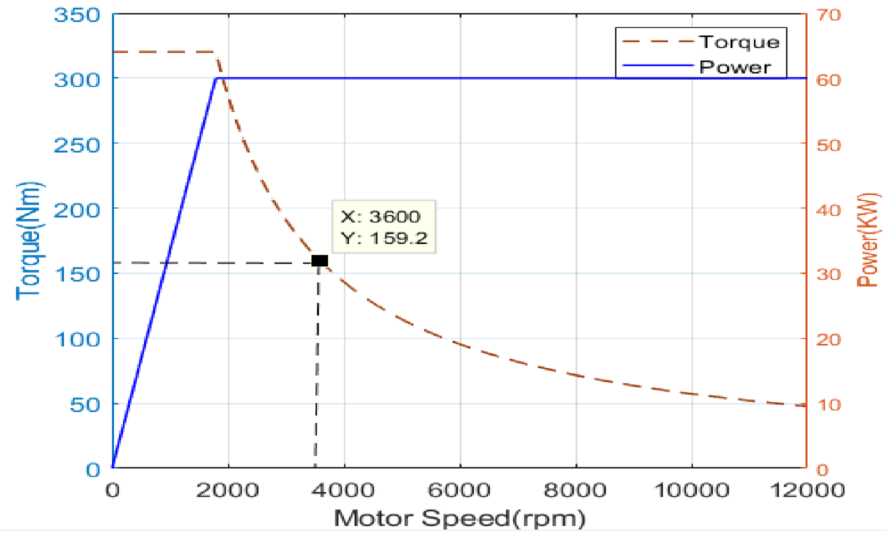

Figure 3.8 Torque versus speed characteristics of the BLDC motor

3.5.2. The Effect of Gradient Angle on the Power and Speed of Vehicle

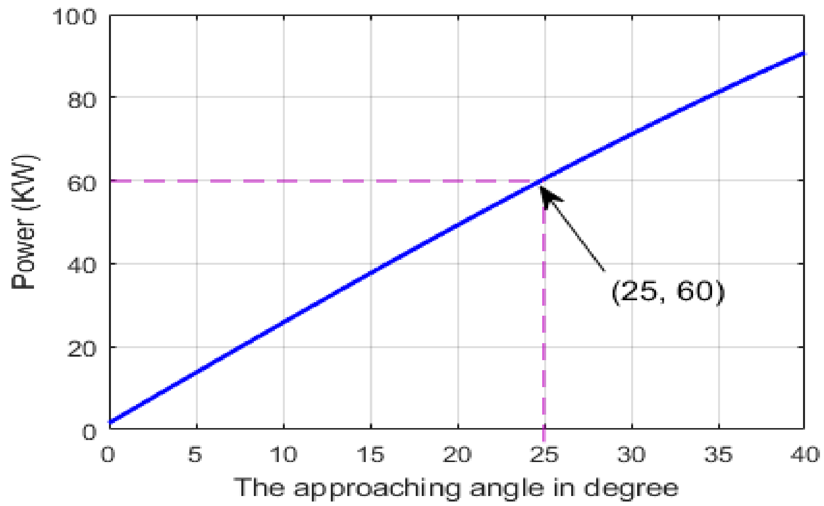

Figure 3.9 Driving power vs approaching angle of the vehicle

3.5.3. Electric Vehicle Specification

Table 3.2 Electric vehicle (Nissan 530) and driving motor specifications **[54]**

Parameters	Values
Maximum power	120 kW
Gross weight	1500 Kg
Rated power	60 kW
Maximum torque	320 N-m
Rated torque	159.2 N-m
Maximum speed	130 Km/hr.
Rated speed	3600 Km/hr.
Departure angle	25°
Seating capacity	5 persons

3.5.4. Traction Motor

3.5.4.1. Selection of Traction Motor

In literature [16], it is shown that BLDC motor is the best selection for EV compared to induction motor, RS motor and DC motors. PMSM motor is highly competent with BLDC motor especially in the case of weight, efficiency, having less torque ripple and so on. Even though these two motors are highly competent to each other BLDC motor has better futures in case of having a higher power output, higher torque density, cost and simplicity. The power output ratio of these two motors is derived as the following, based on equal cupper losses principle of their stators.

3.5.4.2. Traction Motor Specification

According to the maximum power of the electric vehicle some of the BLDC motor specifications are taken from the manufacturing company and the others are taken from literature. The torque and back EMF constants are determined by the following derivations from the motor two phase equations [54]. The rated power of the motor is expressed by the product of the motor current and the back EMF for considering two phases.

$$Power_{max} = 2E_m I_m \tag{3.10}$$

from Equation 3.10,

$$E_m = \frac{Power_{rated}}{2 * I_m}$$

$$= \frac{60kW}{2 \times 172A} = 174.186V$$

Hence, the back EMF of the motor is directly proportional to the motor speed.

$$\text{EMF constant}(K_b) = \frac{E_m}{\omega_{rated}} = \frac{174.186}{3600(\frac{2\pi}{60})} = 0.46204\left(\frac{V}{rad/sec}\right) \quad (3.11)$$

If two phase operating system of BLDCM is considered $K_b = 2 \times 0.46204 = 0.924$.

$$Torque_{rated} = K_t I_{m(rated)} = \frac{2 * E_{m(rated)} * I_{m(rated)}}{\omega_{rated}} \quad (3.12)$$

Then the torque constant of the motor is calculated by

$$K_t = \frac{2 * E_{m(rated)}}{\omega_{rated}} = \frac{2 \times 174.186}{376.9912\, rad/sec} = 0.924 \quad (3.13)$$

Then,

$$Torque_{rated} = K_t I_{m(rated)} = 0.924 \times 172 = 159N$$

In general, the BLDC motor specifications used in this thesis is given as in Table 3.3

Table 3.3 Parameters specification of BLDC motor used in this thesis **[54]**

Parameters	Values
Poles	4
Power factor	0.85
Efficiency at rated	90.4%
Rated motor power	60 kW
Control input rated voltage	350 V
Rated motor current	172 A
Rated speed	3600 rpm
Phase winding resistance	1.2 Ω
Phase inductance	0.00295 H
Viscous damping	0.001 N.m.s

Moment of inertia	0.008495 kg.m^2
Torque constant	0.924 N-m/A
EMF constant	0.46204 V·s/rad

3.5.5. Battery Specifications

3.5.5.1. Matching Power Battery Parameters

The power source of the pure electric vehicles is battery. The selection of battery parameters must meet the demand of endurance mileage requirements and maximum power of vehicle driving. Lithium ion battery is selected as the power source for electric vehicles due to its long life and mass energy density. In literature [21] depends on efficiency, energy density, safety, durability, run time and cost parameters select lithium-ion batterie for this thesis.

The lithium battery pack can able to store the DC power for EV. The lithium battery packs consist of standard lithium battery module in serial. The standard lithium battery module is connected in serial. Each battery module has 4kWh storage. The serially linked more than eight battery modules i.e. more than 32kWh total battery pack power with rated DC voltage of 350V is required for proposed EV. Accordingly, there are four serially linked battery modules to fulfill the requirement of total energy. Therefore, the selection of battery parameters must meet the demand for endurance mileage requirements and the maximum power of the vehicle [55].

$$P = P_{max} \times 0.15 + 0.85 \times P_{(@\text{ zero grad \& constant speed})} \tag{3.14}$$

$$P_m = \frac{P}{\eta_m} \tag{3.15}$$

$$W_{road} = P_m t = \frac{P_m S}{V} \tag{3.16}$$

$$SOC\% = \frac{\left(W_{rated} - W_{road}\right)}{W_{rated}} \times 100\% \tag{3.17}$$

Where P is the power required for the automobile at constant speed, S is endurance mileage, W_{rated} is the energy needed for mileage S, P_m is the input power of the motor drive and η_m is the motor and motor controller assembly efficiency.

Table 3.4 Parameter specifications of lithium-ion battery **[54]**

Parameters	**Values**
Cell type	Lithium-Ion
Total battery power pack	32 kWh
Rated DC power supply	350 V
Capacity	90 Ah
Mass	4.3 kg
Nominal voltage	4.2 V
Energy density	154 Wh/kg
Operating temperature	-10℃ to 50℃
Energy	666Wh

3.5.6. Selection of Power Semiconductor Device

A MOSFET is the preferable device used as a converter switch. The low power consumption, high switching speed and low current draw make the MOSFET an ideal device. N-type enhancement MOSFETs with bootstrapped half bridge MOSFET drivers have been selected.

3.6. Modeling of Brushless DC Motor Drive for Electric Vehicle

3.6.1. BLDC Motor Operation Principle

Permanent magnet DC motors use mechanical commutator and brushes to achieve the commutation. However, BLDC motors adopt Hall Effect sensors in place of mechanical commutator and brushes. The stators of BLDC motors are the coils, and the rotors are the permanent magnets. The stators develop the magnetic fields to make the rotor rotating. Hall-Effect sensors detect the rotor position as the commutating signals. Therefore, the BLDC motors use permanent magnets instead of coils in the armature and so do not need brushes. In this paper, a three-phase and four-pole BLDC motor is used. For the three phases BLDC motor the back-EMF and current waveforms with 120° conduction mode.

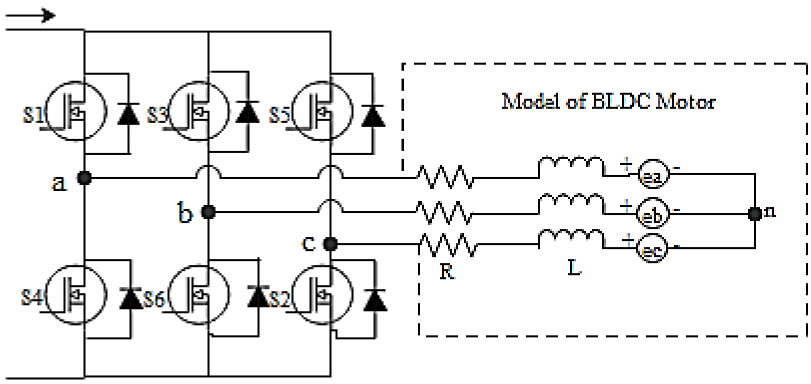

Figure 3.10 Configuration of BLDC motor drive system

3.6.2. Modeling of BLDC Motor

There are two possible methods to model a BLDC motor, one is abc phase variable model and the other is d-q axis model. BLDC motor is a permanent magnet motor with trapezoidal back EMF whereas synchronous motor has sinusoidal back EMF. Since trapezoidal the mutual inductance sandwiched between stator and rotor is non-sinusoidal. So, transforming to d-q axis does not provide any added benefit, thus abc phase variable model is chosen. In the present model, the motor is assumed to be star connected with isolated neutral. The analysis is based on the following assumptions:

- The motor is not saturated and should be operated with the rated current.
- Stator resistances of all the windings are equal.
- Self-inductance and mutual inductance are constant.
- Iron and stray losses are negligible.
- Three phases are balanced one.
- Uniform air gap.
- Hysteresis and eddy current losses are not considered.
- Power semiconductor devices in the inverter are ideal.

The equivalent circuit diagram of the BLDC motor is as shown in the Figure 3.11.

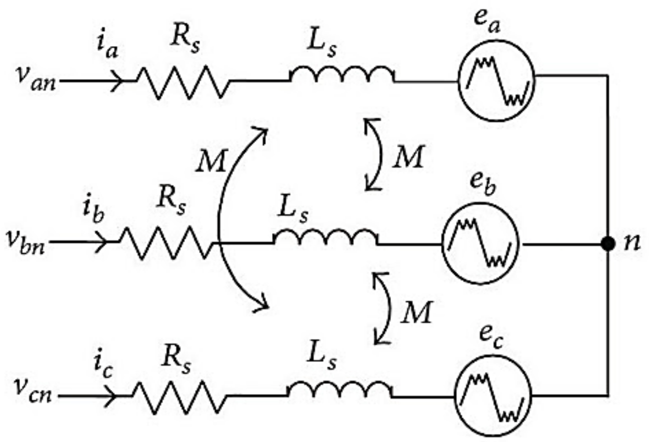

Figure 3.11 Equivalent circuit of BLDC motor [L5]

For simplification only phase A is taken under consideration during the modelling of the BLDC motor. The equivalent circuit of the phase A winding of the BLDC motor is given in Figure 3.12. The terminal voltage V_a is taken as V.

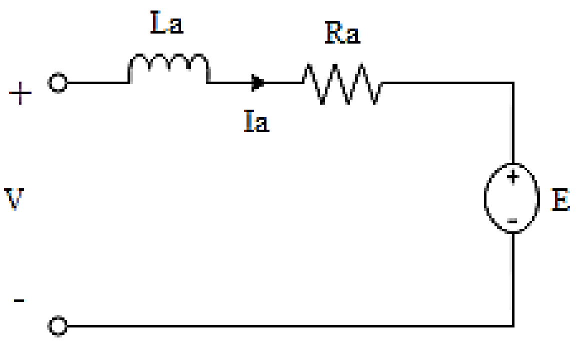

Figure 3.12 Equivalent circuit of the phase A

The circuit equations of the three windings in phase variables can be found in the literature [56]. The model of the armature winding for the BLDC motor is expressed as follows:

$$V_{as} = R_s i_a + L_a \frac{di_a}{dt} + L_{ab} \frac{di_b}{dt} + L_{ac} \frac{di_c}{dt} + e_a \tag{3.18}$$

$$V_{bs} = R_s i_b + L_b \frac{di_b}{dt} + L_{ba} \frac{di_a}{dt} + L_{bc} \frac{di_c}{dt} + e_b \tag{3.19}$$

$$V_{cs} = R_s i_a + L_c \frac{di_c}{dt} + L_{ca}\frac{di_a}{dt} + L_{cb}\frac{di_b}{dt} + e_a \quad (3.20)$$

It is assumed that resistances of all the windings are equal. It is also assumed that if there is no change in the rotor reluctance with angle because of no salient rotor and so that:

$$L_a = L_b = L_c = L \quad (3.21)$$

$$L_{ab} = L_{ba} = L_{ca} = L_{ac} = L_{bc} = L_{cb} = M \quad (3.22)$$

where R_s Stator resistance per phase, L Stator inductance per phase, V_{as}, V_{bs}, and V_{cs} are the stator per phase stator voltages, M is the mutual inductance per phase. i_a, i_b and i_c are the per phase stator currents. The stator phase currents are considered to be balanced.

$$i_a + i_b + i_c = 0 \quad (3.23)$$

Multiplying both sides by M gives:

$$Mi_a + Mi_b + Mi_c = 0 \quad (3.24)$$

Then, rearranging Equation (3.24)

$$-Mi_a = Mi_b + Mi_c \quad (3.25)$$

From Equations (3.18) and (3.22):

$$V_{as} = R_s i_a + L\frac{di_a}{dt} + M\frac{di_b}{dt} + M\frac{di_c}{dt} + e_a \quad (3.26)$$

$$V_{as} = R_s i_a + L\frac{di_a}{dt} + \frac{d}{dt}(Mi_b + Mi_c) + e_a \quad (3.27)$$

Substituting Equation (3.25) into (3.27) gives Equation (3.28):

$$V_{as} = R_s i_a + L\frac{di_a}{dt} + \frac{d}{dt}(-Mi_a) + e_a \quad (3.28)$$

The per-phase terminal voltage in terms of the motor armature parameters and back emf motor voltage is given by:

$$V_{as} = R_s i_a + \frac{di_a}{dt}(L - M) + e_a \quad (3.29)$$

The other phase voltage equations are obtained in a similar fashion:

$$V_{bs} = R_s i_b + \frac{di_b}{dt}(L - M) + e_b \quad (3.30)$$

$$V_{cs} = R_s i_c + \frac{di_c}{dt}(L - M) + e_c \tag{3.31}$$

Rearranging Equations (3.29), (3.30), and (3.31) gives the two phases of current differential equations as follows:

$$\frac{di_a}{dt} = \frac{V_{as}}{L - M} - \frac{R_s i_a}{L - M} - \frac{e_a}{L - M} \tag{3.32}$$

$$\frac{di_b}{dt} = \frac{V_{bs}}{L - M} - \frac{R_s i_b}{L - M} - \frac{e_b}{L - M} \tag{3.33}$$

$$\frac{di_c}{dt} = \frac{V_{cs}}{L - M} - \frac{R_s i_c}{L - M} - \frac{e_c}{L - M} \tag{3.34}$$

The modeling Equation (3.32), (3.33) and (3.34) can be represented in matrix form:

$$\frac{d}{dt}\begin{bmatrix} i_a \\ i_b \\ i_c \end{bmatrix} = \begin{bmatrix} -\frac{R_s}{L - M} & 0 & 0 \\ 0 & -\frac{R_s}{L - M} & 0 \\ 0 & 0 & -\frac{R_s}{L - M} \end{bmatrix}\begin{bmatrix} i_a \\ i_b \\ i_c \end{bmatrix} + \frac{1}{L - M}\begin{bmatrix} V_{as} \\ V_{bs} \\ V_{cs} \end{bmatrix} - \frac{1}{L - M}\begin{bmatrix} e_a \\ e_b \\ e_c \end{bmatrix} \tag{3.35}$$

The state space form is given by:

$$\frac{dx}{dt} = Ax + b(V - e) \tag{3.36}$$

where,

$$A = \begin{pmatrix} -\frac{R_s}{L - M} & 0 & 0 \\ 0 & -\frac{R_s}{L - M} & 0 \\ 0 & 0 & -\frac{R_s}{L - M} \end{pmatrix}, V = \begin{bmatrix} V_{as} \\ V_{bs} \\ V_{cs} \end{bmatrix}, e\begin{bmatrix} e_a \\ e_b \\ e_c \end{bmatrix}, b = \frac{1}{L - M} \tag{3.37}$$

3.6.3. Modeling of Ideal Back-EMF

When BLDC motor rotates, each winding generates a voltage known as Back EMF, which opposes the main voltage supplied to the winding according to Lenz's law. The polarity of the Back EMF is opposite direction of the source voltage. It is related to the function of rotor position and each phase has 120^0 phase difference.

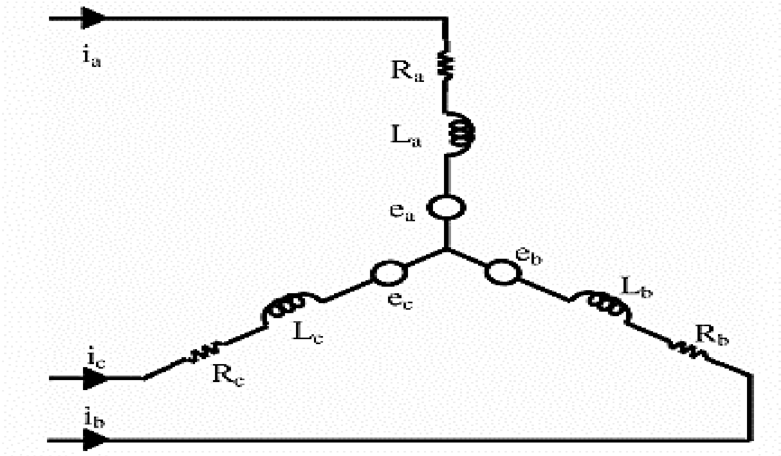

Figure 3.13 The equivalent circuit of BLDC Motor [L5]

Back EMF depends mainly on three factors (i) angular velocity of the rotor, (ii) magnetic field generated by the rotor magnets, (iii) the number of turns in the stator windings. The back-EMF and the motor current are drawn along with the rotor position sensor signals as shown in Figure 3.14. The induced-EMFs do not have sharp corners because these are in trapezoidal nature in trapezoidal based BLDC motor drive.

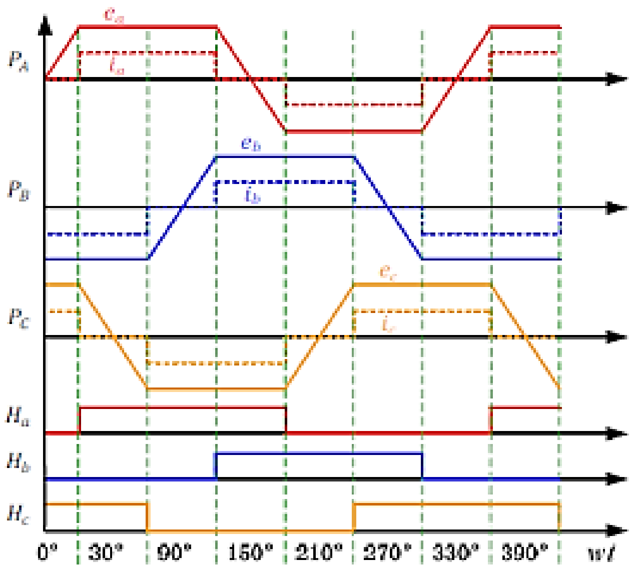

Figure 3.14 Trapezoidal back EMF and phase current variation with rotor electrical angle [L]

As mentioned before, it was assumed that back-EMF $e_{a,}\ e_{b,}$ and e_c have trapezoidal wave from. The three-phase BLDC motor back-EMF can be described by the following equations:

$$\begin{bmatrix} e_a \\ e_b \\ e_c \end{bmatrix} = \omega_m \lambda_m \begin{bmatrix} f_{as}(\theta_r) \\ f_{bs}(\theta_r) \\ f_{cs}(\theta_r) \end{bmatrix} \tag{3.38}$$

Equation of each phase as follows:

$$e_a = \omega_m.\lambda_m.f_{as}(\theta_r) \tag{3.39}$$

$$e_b = \omega_m.\lambda_m.f_{bs}(\theta_r) \tag{3.40}$$

$$e_c = \omega_m.\lambda_m.f_{cs}(\theta_r) \tag{3.41}$$

Where, $E_{a,}\ E_{b,}$ and E_c are the induced Back EMF and the expression of $e_{a,}\ e_{b,}$ and e_c will be given in Equations (3.39), (3.40) and (3.41). λ_m is flux linkage, θ_r is the electrical rotor angle, ω_m is the mechanical speed of the rotor [rad/s]. the rotor angle functions $f_{as}(\theta_r), f_{bs}(\theta_r),$ and $f_{cs}(\theta_r)$ have the same shape as $e_{a,}\ e_{b,}$ and e_c with a maximum magnitude of ±1. Equations (3.42), (3.43), and (3.44) show the mathematical functions of the rotor angle in a three-phase system.

$$f_{as}(\theta_r) = \begin{cases} (6/\pi)\theta_r & (0 < \theta_r \le \pi/6) \\ 1 & (\pi/6 < \theta_r \le 5\pi/6) \\ -(6/\pi)\theta_r + 6 & (5\pi/6 < \theta_r \le 7\pi/6) \\ -1 & (7\pi/6 < \theta_r \le 11\pi/6) \\ (6/\pi)\theta_r - 12 & (11\pi/6 < \theta_r \le 2\pi) \end{cases} \tag{3.42}$$

Since in the balanced three phase system each rotor position sensor is separated by 120^0, the rotor angle functions in phase-b and c are derived based on the function of the phase-a.

$$f_{bs}(\theta_r) = f_{as}\left(\theta_r + \frac{2\pi}{3}\right) \tag{3.43}$$

$$f_{cs}(\theta_r) = f_{as}\left(\theta_r - \frac{2\pi}{3}\right) \tag{3.44}$$

3.6.4. Dynamics Modeling of BLDC Motor

The electromagnetic torque for the three phase BLDC motor in Newton's is defined as:

$$T_e = \frac{P_{rotor}}{\omega_m} = \frac{i_a e_a + i_b e_b + i_c e_c}{\omega_m} \tag{3.45}$$

The resultant torque, T_e, can be obtained by the following expressions.

$$T_a = i_a.K_T.f(\theta) \tag{3.46}$$

$$T_b = i_b.K_T.f\left(\theta - \frac{2\pi}{3}\right) \tag{3.47}$$

$$T_c = i_c.K_T.f\left(\theta + \frac{2\pi}{3}\right) \tag{3.48}$$

$$T_e = T_a + T_b + T_c \tag{3.49}$$

$$T_e = i_a.K_T.f(\theta) + i_b.K_T.f\left(\theta - \frac{2\pi}{3}\right) + i_c.K_T.f\left(\theta + \frac{2\pi}{3}\right) \tag{3.50}$$

Moreover, the generation of electromagnetic torque can be written as:

$$T_e = J\frac{d\omega}{dt} + T_L + B\omega \tag{3.51}$$

The moment of inertia is described by:

$$J = J_m + J_1 \tag{3.52}$$

Where, J is the rotor inertia, [kgm^2], and B is damping constant and T_L is load torque in N-m. The resultant torque is:

$$T_e - T_L = J\frac{d\omega}{dt} + B\omega \tag{3.53}$$

Again, using Laplace transformation and we will get transfer function:

$$\frac{\omega(s)}{T_e(s) - T_L(s)} = \frac{1}{Js + \theta} \tag{3.54}$$

3.6.5. Reference Current Generator

Reference current generator determines reference phase currents (i_a^*, i_b^*, i_c^*) of the motor in regard to reference current amplitude (I^*), which is calculated using rotor position (θ). Reference current amplitude (I^*) can be obtained from Equations (3.55).

$$I^* = u/K_t \tag{3.55}$$

where u is the control signal and K_t is the torque constant. Phase currents given in Table 3.5 can be attained from Figure 3.14. These currents are input to PWM current control block [57].

Table 3.5 Reference currents of the BLDC motor

Rotor position (θ)	Reference currents (A)		
	i_a^*	i_b^*	i_c^*
0°-30°	0	$-I^*$	I^*
30°-90°	I^*	$-I^*$	0
90°-150°	I^*	0	$-I^*$
150°-210°	0	I^*	$-I^*$
210°-270°	$-I^*$	I^*	0
270°-330°	$-I^*$	0	I^*
330°-360°	0	I^*	I^*

3.6.6. Rotor Position Hall Sensors Modeling

Unlike a brushed DC motor, the commutation of a BLDC motor is controlled electronically. To rotate the BLDC motor the stator windings should be energized in a sequence. It is important to know the rotor position in order to understand which winding will be energized following the energizing sequence. Rotor position is sensed using Hall-effect sensors embedded into the stator [58]. Most BLDC motors have three Hall sensors inside the stator on the non-driving end of the motor. Whenever the rotor magnetic poles pass near the Hall sensors, they give a high or low signal indicating the N or S pole is passing near the sensors. Based on the combination of these three Hall sensor signals, the exact sequence of commutation can be determined.

Table 3.6 Hall effect signals and inverter switches status of the BLDC motor **[58]**

Electrical degree	Hall effect signals			Inverter switch status					
	Hall A	Hall B	Hall C	S_1	S_2	S_3	S_4	S_5	S_6
0°-60°	0	1	0	on	off	off	off	off	on
60°-120°	1	1	0	on	off	off	on	off	off
120°-180°	1	0	0	off	off	off	on	on	off
180°-240°	1	0	1	off	on	off	off	on	off
240°-300°	0	0	1	off	on	on	off	off	off
300°-360°	0	1	1	off	off	on	off	off	on

3.7. Transfer Function of BLDCM and the Load

BLDC motor is very similar to the DC motor. But the similarity holds only when two phases are conducted during the interval where the rotor flux linkages are constant as seen from these phases and all the phases are electrically symmetric and balanced [59]. During two phase conduction, the inverter output voltage, V_{is} is applied to the two phases having an impedance which is given by Equation (3.55).

$$Z = 2(R_s + \frac{d}{dt}(L - M)) = R_a + \frac{d}{dt}L_a \tag{3.56}$$

$$R_a = 2R_s \tag{3.57}$$

$$L_a = 2(L - M) \tag{3.58}$$

$$|Z| = \sqrt{R_a^2 + L_a^2} \tag{3.59}$$

The inverter output voltage is the same as the stator voltage and is given as:

$$V_{is} = (R_a + sI_a)I_{as} + E_{as} - E_{cs} \tag{3.60}$$

The induced emf in phase A and C are equal and opposite during the regular operation of the drive scheme and given as:

$$E_{as} = -E_{cs} = \lambda_m \omega_m \tag{3.61}$$

where, λ_m is the flux linkages per phase and ω_m is the rotor speed. Substituting Equation (3.61) to Equation (3.60) gives the stator voltage equation as:

$$V_{is} = (R_a + sI_a)I_{as} + \lambda_p \omega_m \tag{3.62}$$

$$V_{is} = (R_a + sI_a)I_{as} + 2\lambda_p \omega_m = (R_a + sI_a)I_{as} + K_b \omega_m \tag{3.63}$$

Where the emf constant for both the phases is combined into one constant as

$$K_b = 2\lambda_m \frac{V}{rad/sec} \tag{3.64}$$

The electromagnetic torque for two phases combined is given by

$$T_e = 2\lambda_m I_{as} = K_b I_{as} \tag{3.65}$$

$$\frac{I_{is}}{V_{is} - E_{is}} = \frac{1}{R_a + L_a s} = \frac{1}{1.2 + 0.00293s} \tag{3.66}$$

The load is assumed to be proportional to speed. If it is not proportional to the speed the load torque is truly a disturbance. In that case it is incorporated in the block diagram suitably but, ignored in the controller design for most of the applications.

$$T_1 = B_1 \omega_m \tag{3.67}$$

The speed to air gap torque or dynamics transfer function can be evaluated as:

$$\frac{\lambda_m(s)}{T_e(s) - T_1(s)} = \frac{1}{B + Js} = \frac{1}{0.001 + 0.008495s} \tag{3.68}$$

where B is the friction coefficient of the motor and J is the inertia of the machine.

3.7.1. Modeling of Three Phase Inverter Transfer Function

The transfer function of inverter is represented as a first-order lag with a gain given by Equation (3.69).

$$G_r(s) = \frac{V_{is}(s)}{V_c(s)} = \frac{K_r}{1 + sT_r} \tag{3.69}$$

Where K_r value of gain is evaluated for line to line output voltage and T_r delay time of the inverter switches which is calculated as:

$$K_r = 0.65 \frac{V_{dc}}{V_{cm}} = 0.65 \times \frac{350}{10} = 22.75 \tag{3.70}$$

$$T_r = \frac{1}{2f_c} = \frac{1}{2 \times 8000} = 6.25 \times 10^{-3} \tag{3.71}$$

Provided that, V_{dc} is the dc link voltage input to the inverter, V_{cm} is the maximum control voltage and f_c is the switching (carrier) frequency of the inverter.

$$G_r = \frac{22.75}{1+6.25\times10^{-5}s} \tag{3.72}$$

3.8. Bidirectional DC-DC Converter

This section will discuss the four-quadrant converter subsystem component selection. The converter subsystem is designed to operate under dynamic load conditions with variable output torque and speed. The four-quadrant converter operates from four control signals that control power magnitude and direction. The device construction consists primarily of four power semiconductor switches along with supporting switch drivers and input/output filters. The converter operates under four basic modes of operation: as a boost converter stepping up voltage to the motor from battery, as a buck converter stepping down voltage to the motor from the battery, as a boost converter stepping up voltage to the battery from the motor, and as a buck converter stepping down voltage from the motor to the battery. In each mode of operation, control signals are modified to each of the four power semiconducting switches.

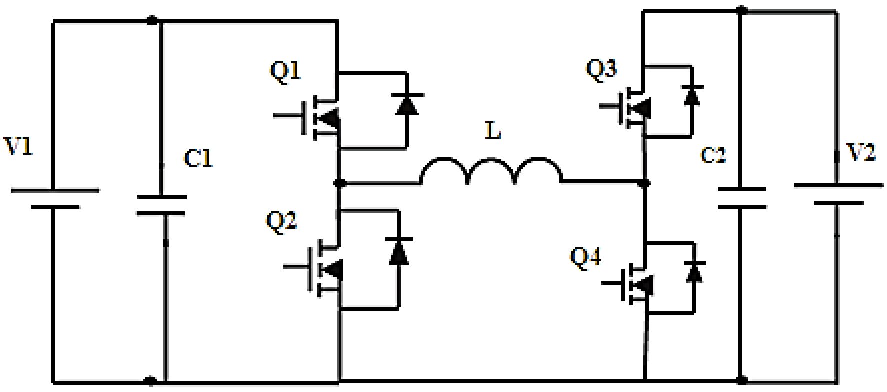

Figure 3.15 Bidirectional cascaded buck-boost converter [L6]

The Bidirectional topology as seen in the Figure 3.15 can be obtained by cascading the bidirectional buck converter with bidirectional boost converter. This topology allows the output voltage to be either higher or lower than the input voltage depending up on the switch combinations used and the direction of the current. For the step-up operation in the forward direction, the switch S1 is always on and S2 and S4 are always off, whereas the switch S2 is conducted depending on the duty cycle. During forward step-down operation the switch S1 is operated with the required duty cycle and the switch S2, S3, S4 are always off. Diode D2 and D3 are always reverse biased whereas the D3 is always forward biased. Diode D4 acts as a freewheeling diode. Similarly, in the backward step up operation, switch S3 is always on whereas the switch S4 is operated with the required duty cycle with the diode D1 acting as a freewheeling diode.

3.8.1. Component Selection

The first step in choosing component values, such as those for the output ripple capacitor and inductor, is to outline the necessary operating parameters of the system. The following parameters were realized based on the specific brushless DC motor specifications as well as nominal battery supply voltage and ratings.

1. Input voltage range: $V_{batterymin}$, $V_{battterymax}$, $V_{battery}$
   a. This can be described as the voltage supplied by the battery pack at the minimum and maximum states of charge in which the system can safely operate, as well as the nominal state of charge.
      i. $V_{batterymin}$ = 175V or 50% of the nominal state of charge
      ii. $V_{battterymax}$ = 400V
      iii. $V_{battery}$ = 350V nominal state of charge
2. Nominal output voltage: V_{out}
   a. The nominal output voltage desired in this case will be the maximum voltage rating of the motor.
      i. V_{motor} = 550V
3. Maximum output current: I_{out}
   a. The maximum output current is determined by motor ratings, as well as how much current that can be continuously supplied by the battery source in a safe manner.
      i. I_{out} = 172A
4. Estimated efficiency: η
   a. The efficiency of the converter is estimated from how much power is lost through switch on resistance, other impedances throughout the system, leakage flux from the inductor, as well as rise and fall times of switching components. Since the exact

efficiency cannot be calculated at this time without physical experimentation, A realistic efficiency of power throughput has been estimated to be 90.4%.

3.8.2. Duty Cycle Calculations

To calculate a capacitor value that will be sufficient to operate the converter under over necessary ranges, the optimal duty cycle in boost mode, and optimal duty cycle in a buck regenerative mode is used. The maximum and minimum duty cycle during a regenerative phase given a maximum voltage across the motor should be:

$$D_{buck(reg)min} = \frac{V_{batterymin} \times \eta \times 1.1}{V_{motor}} \tag{3.73}$$

$$D_{buck(reg)min} = \frac{175V \times 0.9 \times 1.1}{450V}$$

$$D_{buck(reg)min} = 0.385$$

$$D_{buck(reg)max} = \frac{V_{batterymax} \times \eta \times 1.1}{V_{motor}} \tag{3.74}$$

$$D_{buck(reg)max} = \frac{400V \times 0.9 \times 1.1}{450V}$$

$$D_{buck(reg)max} = 0.88$$

The maximum and minimum duty cycle during a motor drive phase with various battery states of charge should be:

$$D_{boostmax} = 1 - \frac{V_{batterymin} \times \eta}{V_{motor}} \tag{3.75}$$

$$D_{boostmax} = 1 - \frac{175V \times 0.9}{450V}$$

$$D_{boostmax} = 0.65$$

$$D_{boostmin} = 1 - \frac{V_{batterymax} \times \eta}{V_{motor}} \tag{3.76}$$

$$D_{boostmax} = 1 - \frac{400V \times 0.9}{450V}$$

$$D_{boostmax} = 0.2$$

3.8.3. Inductor Selection

High inductor values are ideal in order to operate the converter in continuous mode with higher output current and reduced output ripple. However high inductor values tend to be physically larger with greater equivalent series resistance without increasing the wire gauge and, as a result, significantly more expensive. Therefore, the minimum inductor value should be chosen to satisfy the given operational parameters. An acceptable inductance value is calculated for both boost and buck modes of operation, the largest value calculated is then used as a minimum value in the design. The following equation estimates a reasonable minimum inductance value for the regenerative mode of operation:

f_s = switch frequency

$I_{L\ ripple}$ = inductor ripple current (approximately 30% of the output current)

$$L > \frac{V_{motor} \times (V_{motor} - V_{batterymax})}{I_{L\ ripple} \times f_s \times V_{motor}} \tag{3.77}$$

$$L > \frac{400V \times (450V - 400V)}{50A \times 40000Hz \times 450V}$$

$$L > 22.22\mu H$$

The following equation estimates a reasonable minimum inductance value for the boost, motor drive mode of operation:

$$L > \frac{V_{battery\min}{}^2 \times (V_{motor} - V_{batterymin})}{I_{L\ ripple} \times f_s \times V_{motor}{}^2} \tag{3.78}$$

$$L > \frac{175V^2 \times (450V - 175V)}{50A \times 40000Hz \times 175V^2}$$

$$L > 1.375\mu H$$

Since the inductor will be shared during all modes of operation, the value of 22.22μH is used as an inductor minimum value.

3.8.4. Input/ Output Capacitor Selection

The following equations estimate appropriate values for input and output ripple capacitors in the converter. The maximum value derived from the following four equations is used for both the input and output capacitors. An appropriate ripple capacitor for regenerative mode is calculated using the following equations, the largest of which is used:

V_{ripple} = Desired output voltage ripple (should be as small as possible)

$$C_{min} > \frac{I_{Lripple}}{8 \times f_s \times V_{ripple}} \tag{3.79}$$

$$C_{min} > \frac{50A}{8 \times 40000Hz \times 0.1V}$$

$$C_{min} > 1562.5\mu H$$

The following equation can be used to find the minimum capacitor required during an overshoot situation in which the load is removed.

$$C_{min\ overshoot} > \frac{{I_{Lripple}}^2 \times L}{2 \times V_{motor} \times V_{ripple}} \tag{3.80}$$

$$C_{min\ overshoot} > \frac{50A^2 \times 22.22\mu H}{2 \times 450V \times 0.1V}$$

$$C_{min\ overshoot} > 617.2\mu F$$

The following equations are used to adjust output voltage ripple during a motor drive boost mode of operation:

$$C_{min} > \frac{I_{Lripple} \times D_{boostmax}}{f_s \times V_{ripple}} \tag{3.81}$$

$$C_{min} > \frac{50A \times 0.7}{40000Hz \times 0.1V}$$

$$C_{min} > 8750\mu F$$

The value of 8750µF is used as a guideline for selecting the output ripple capacitor. Control of the four quadrant DC-DC converter is accomplished by selecting which switching device in Figure 3.16 is actively switched via a PWM signal. The converter can boost or buck voltages in either direction based on the requirements of the vehicle system. A reference throttle signal specifies how much voltage should be supplied to the motor in the range of 0 to 350V. The controller compares the desired output voltage with the voltage of the battery and calculates the required PWM duty cycle. Based on this comparison, the controller either boosts or bucks the battery voltage into the motor. If the regenerative brake button is active, the power flow is reversed and voltage output from the slowing brushless motor (generator) is converted to the proper battery voltage for partial recharging. Table 3.7 details the signals sent to each switching transistor based on power flow and switching mode.

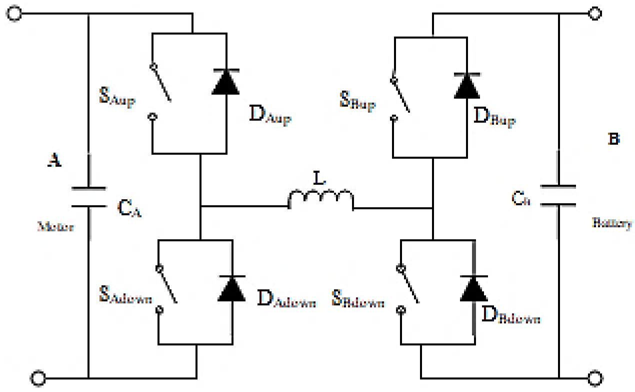

Figure 3.16 Four quadrant converter topology with four switching elements

V_A represents the motor voltage and V_B represents the battery voltage. V_{Aref} and V_{Bref} are the reference signals for the desired motor voltage (throttle) and the charging voltage for the battery respectively. The outputs to the switches correspond to the switch names in Figure 3.15.

Table 3.7 Modes of operation and switching states for the four-quadrant converter

Power Flow	**Mode**	**Switch S_{Aup}**	**Switch S_{Bdown}**	**Switch S_{Bup}**	**Switch S_{Adown}**
A to B	Buck	PWM(D)	0	0	0
A to B	Boost	1	PWM(D)	0	0
B to A	Buck	0	0	PWM(D)	0
B to A	Boost	0	0	1	PWM(D)

3.9. Design Speed Controller for BLDC Motor

There are several controllers available nowadays like proportional integral (PI), proportional integral derivative (PID), Fuzzy Logic Controller (FLC) or the combination between them: Fuzzy-PI, Fuzzy-PID, Fuzzy-Neural Networks, Fuzzy Genetic Algorithm, Fuzzy-Ants Colony, Fuzzy-Swarm. But as within the scope of this thesis discussion on the PID, Fuzzy Logic Controller and Fuzzy-PID will be discussed. The generalized block diagram of a BLDC Motor with a controller as shown in Figure 3.17, can be replaced by any other controller as required. Any control mechanism can be adopted in the system such as PID, Fuzzy Logic or fuzzy-PID Controller which will be suitable to maintain and control the speed of the BLDC Motor.

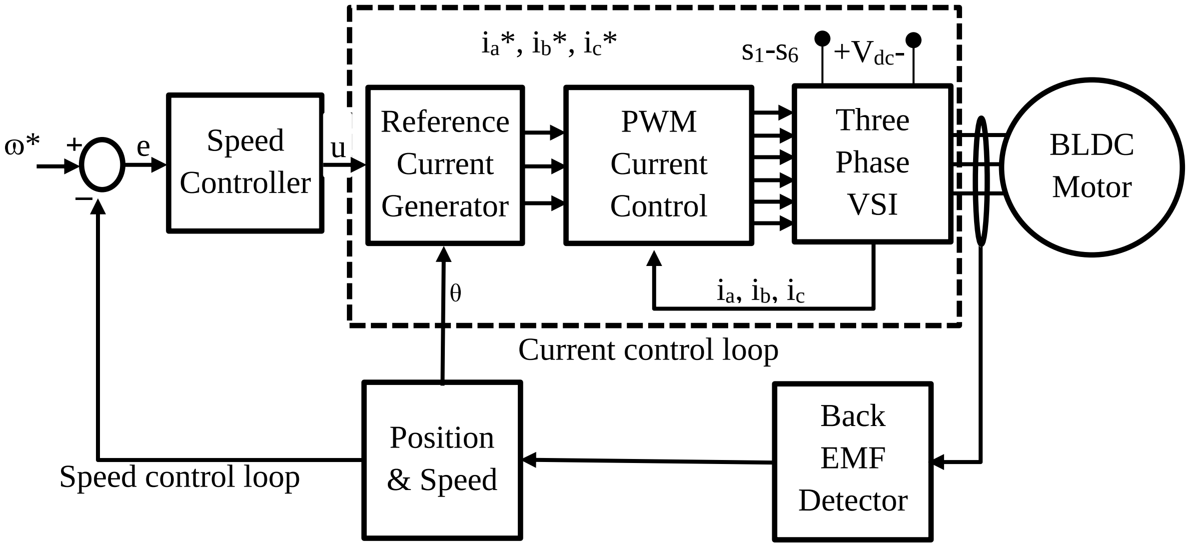

Figure 3.17 Block diagram of a BLDC motor with a speed controller

The block diagram speed control of brushless DC motor is shown in Figure 3.17. There are two loops that used in the block diagram. The first loop is used for six step inverter commutation and the second loop is used for speed control of brushless DC motor. Hall Effect sensor on the brushless DC motor has two functions, as position sensor and speed sensor. The Hall Effect sensor algorithm when detecting the rotor position is used as switching commutation on the inverter. When the coil is energized, the magnetic field will be form and the rotor will rotate. Meanwhile, hall Effect sensor as a speed sensor serves to obtain the current speed data which will be used to get the error value.

3.9.1. Design of Controller

The controller is used to return the desired set point value response, even if the set point value is changed. Stages of this controller planning include designing PID controllers and design of fuzzy logic controllers.

3.9.1.1. PID Controller for BLDC Motor Speed Control

In its basic form, PID involves three mathematical control functions working together: Proportional-Integral-Derivative. The most important of these, Proportional Control, determines the magnitude of the difference between the “set point” and the “process variable” (known as “error”), and then applies appropriate proportional changes to the “control variable” to eliminate “error”. Many control systems will, in fact, work quite well with only Proportional Control. Integral Control examines the offset of “setpoint” and the “process variable” over time and corrects it when and if necessary. Derivative Control monitors the rate of change of the “process variable” and consequently makes changes to the “output variable” to accommodate unusual changes.

The overview of the proposed speed control of BLDC motor using a Proportional plus Integral plus Derivative (PID) controller [60] is shown in Figure 3.18. Because the controller must direct the rotor rotation, the controller needs some means of determining the rotor's orientation/position relative to the stator coils. This is done by Hall Effect sensors to directly measure the rotor's position.

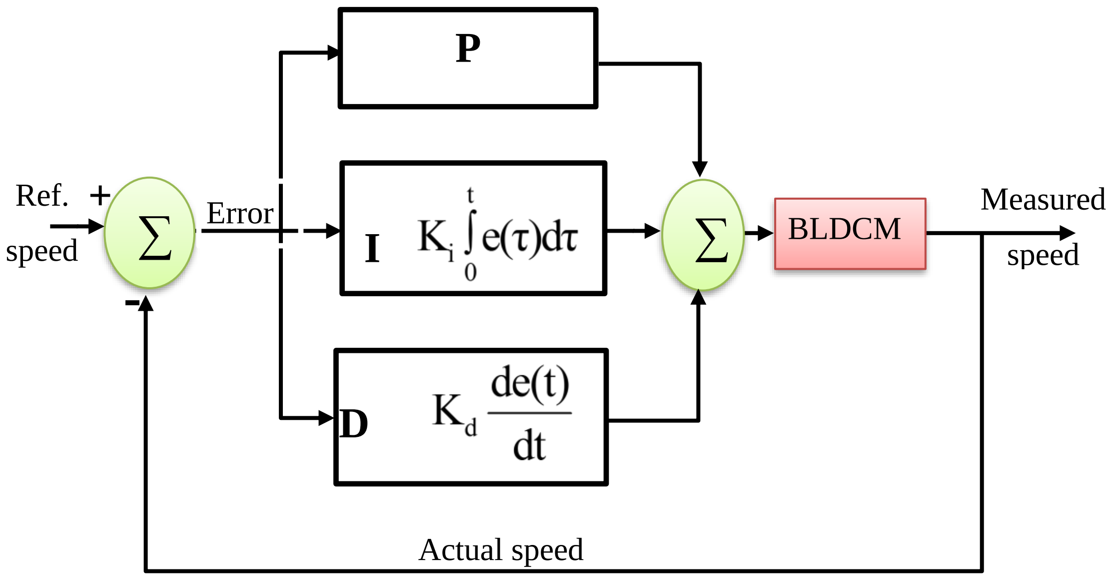

Figure 3.18 Overview of PID controller

Any excess on each parameter P, I, and D can be parallelly integrated into a PID controller. PID controller has characteristics that can accelerate the rise time, reduce the steady state error in the system, and also reduce the oscillation.

The transfer function of the PID Controller [61] is shown as

$$y(t) = \left(K_p e(t) + \frac{1}{K_i} \int e(t)dt + K_d \frac{d}{dt} e(t) \right) \tag{3.82}$$

Where, e(t) = Set point Measurement(t) is the error signal, and K_p, K_i, and K_d are constant that are used to tune the PID control loop. K_p is proportional gain, K_i is integral gain and K_d is derivative gain. Larger K_p typically means faster response since the larger the error, the larger the feedback to compensate. Larger K_i implies steady state errors are eliminated quicker. Larger K_d decreases overshoot, but slows down transient response. Therefore, the kp, ki and kd values can also be calculated using trial and error method in MATLAB Simulink.

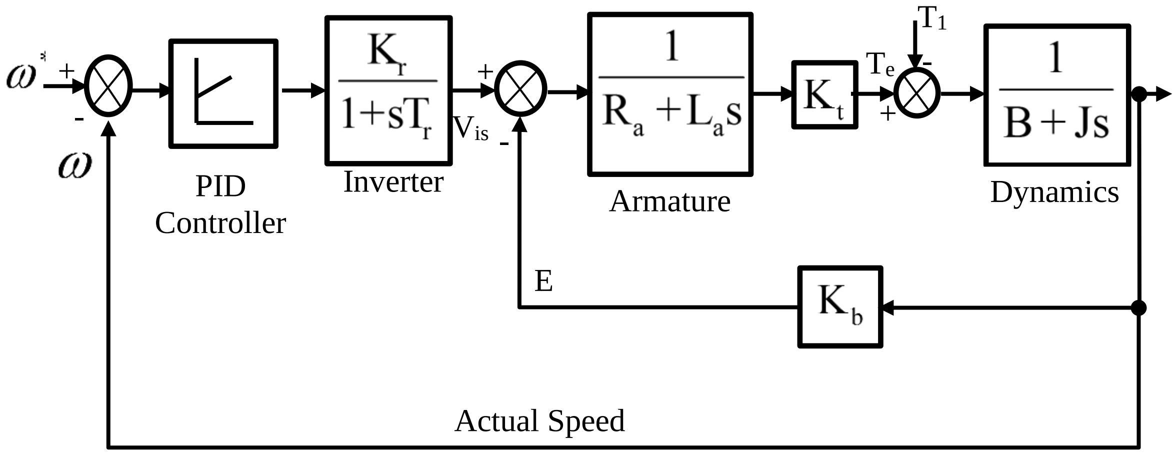

Table 3.8 Effects of increasing a parameter independently

Parameter	Rise time	Overshoot	Settling time	Steady-state error	Stability
K_p	Decrease	Increase	Small change	Decrease	Degrade
K_i	Decrease	Increase	Increase	Decrease significantly	Degrade
K_d	Minor decrease	Minor decrease	Minor decrease	NO effect in theory	Improve if K_i small

3.9.1.2. Automatically Tune PID Controller

PID tuning is the process of finding the values of proportional, integral, and derivative gains of a PID controller to achieve desired performance and meet design requirements. PID controller tuning appears easy, but finding the set of gains that ensures the best performance of your control system is a complex task. Traditionally, PID controllers are tuned either manually or using rule-based methods. Manual tuning methods are iterative and time-consuming, and if used on hardware, they can cause damage. Rule-based methods also have serious limitations: they do not support certain types of plant models, such as unstable plants, high-order plants, or plants with little or no time delay. Automatically tune PID controllers using software tools to achieve the optimal system design and to meet design requirements, even for plant models that traditional rule-based methods cannot handle well.

Figure 3.19 Tune PID controller with MATLAB/Simulink

3.9.1.3. Fuzzy-PID Controller for BLDC Motor

Fuzzy logic is a mathematical environment, based on fuzzy set theory, which admits the degrees of truth or falsehood opposition to “binary logic” that must be either true or false. Fuzzy Logic is an approach that is gaining interest both in the academic world and the industrial fields. Its capability to mimic the human minds makes it a useful scheme for plants experiencing issues with driving scientific models or having execution limitation with classical controllers. Fuzzy logic is multi-valued logic dealing with uncertainty and approximate reasoning [62]. Fuzzy logic control (FLC) deal with rule-base. Its algorithm is based on linguistic variable which tries to mimic human's knowledge about how to control a system without requiring a mathematical model.

3.9.1.4. Structure of a Fuzzy Controller

The Fuzzy logic controller comprises of four stages as appeared in the Figure 3.20. They are Fuzzification, Rule-based, Inference Engine, and Defuzzification.

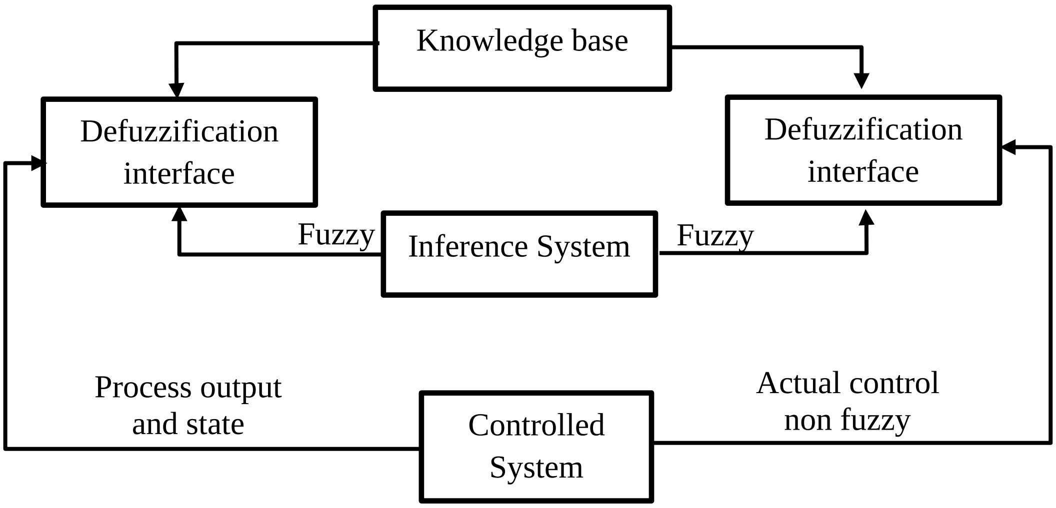

Figure 3.20 fuzzy logic controller Structure

Fuzzy Membership functions are utilized as a tool used to convert numerical variable to linguistic variable. A fuzzy variable can contain many fuzzy subsets inside, contingent upon what numbers of linguistic terms are utilized. Each fuzzy subset represents one linguistic term. To define fuzzy membership function, the designer picks a wide range of shapes Such as triangle, a trapezoid, etc. [63].

3.9.1.5. Fuzzification

Fuzzy logic utilizes linguistic variables rather than numerical factors. The process of converting a numerical variable into a linguistic variable is called Fuzzification. To perform fuzzy calculation, the sources of info must be changed over from numerical or crisp value into fuzzy variables, and the output should be change from fuzzy variables to crisp value, the fuzzy variables i.e. Error, change in error and output are quantized using the following linguistic terms. Negative large (NL), Negative Small (NS), Zero (ZE), Positive Small (PS), positive Large (PL), positive Very Small (PVS), Positive Small (PS), Positive Medium Small (PMS), Positive Medium Large (PML), Positive Large (PL), Positive Very Large (PVL). The membership function for speed error (e), change in speed error (Δe) shown in Figure 3.21 and Figure 3.22.

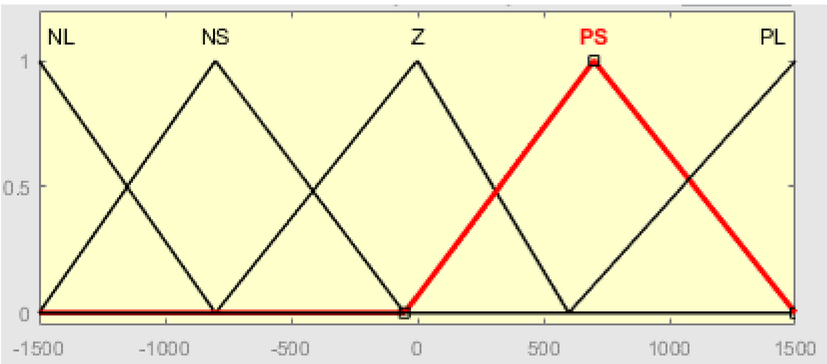

Figure 3.21 Membership functions for error

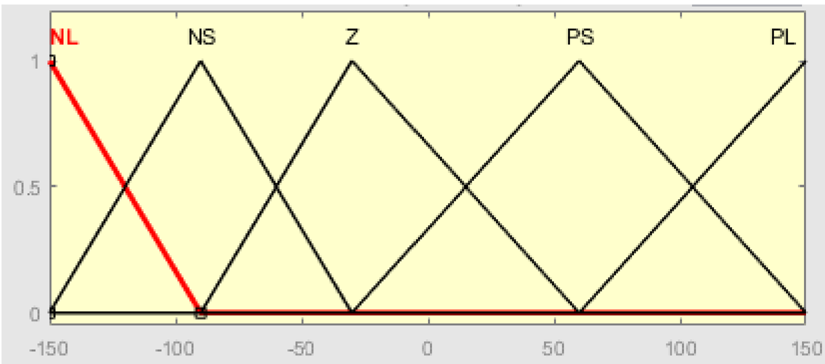

Figure 3.22 Membership functions for change in error

The membership functions of output variable shown in Figure 3.23, Figure 3.24 and Figure 3.25.

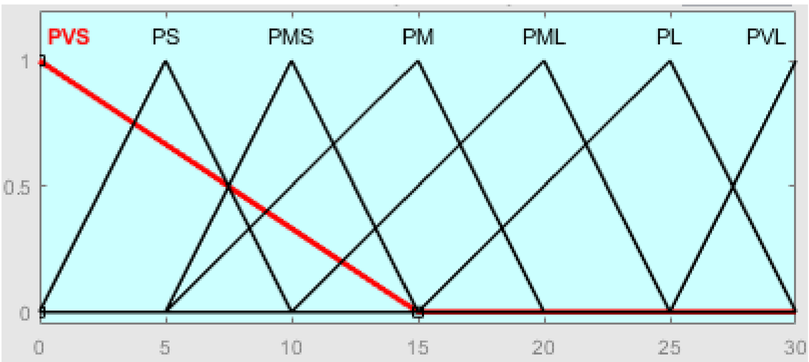

Figure 3.23 Membership function for Kp

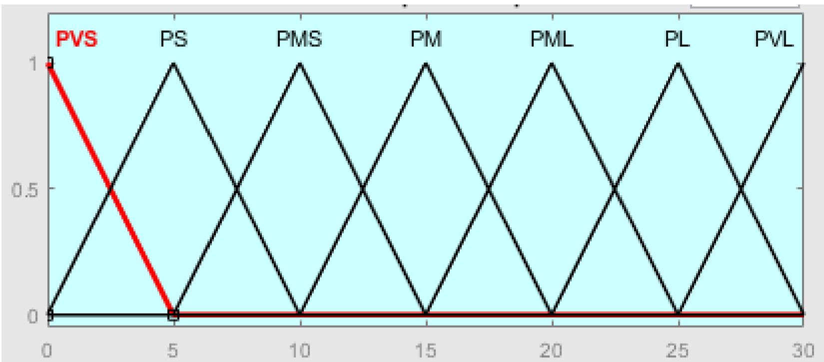

Figure 3.24 Membership function for Ki

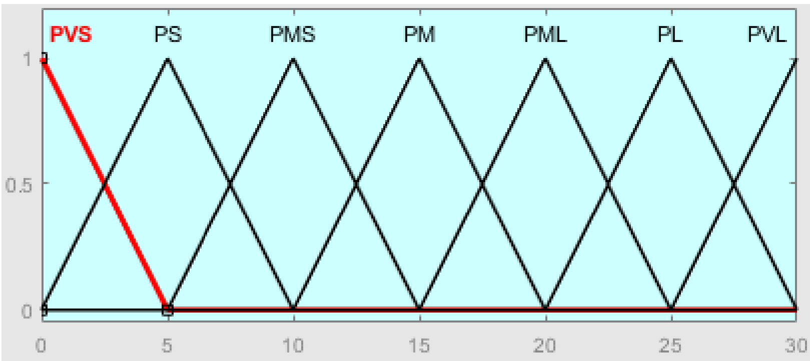

Figure 3.25 Membership function for Kd

3.9.1.6. Defuzzification

Defuzzification is when all the actions that have been activated are combined and Converted into a single non-fuzzy output signal which is the control signal of the system the output levels are depending on the rules that the systems have and the positions depending on the non-linearity existing to the systems [63].

3.9.1.7. Rule Base and Inference Engine

Rather than utilizing a numerical equation, FLC utilizes fuzzy principles to settle on a choice and produce the control activity. The rules are in the form of IF-THEN statements. Inference engine is used to compute the rules generated from the rule base [63]. Fuzzy logic control (FLC) has demonstrated compelling for complex, non-linear and imprecisely characterized forms for which standard model-based control systems are impractical or incomprehensible. Fuzzy logic manages issues that have vagueness, vulnerability and uses membership functions with values varying between 0 and 1 [64]. Recently, a combination of fuzzy logic and PID controller has achieved superior performance as clearly demonstrated by several authors including. [65]. In this thesis proposes fuzzy-PID and PID controller for the speed control of a BLDC motor. Fuzzy will be utilized to tune the parameters of PID according to the error and change of error.

3.9.1.8. Fuzzy Tuned PID Controller

Tuning the gain of a PID controller is extremely significance in PID control. Ziegler and Nichols proposed the outstanding tuning techniques but cannot guaranty better performance for nonlinear system always. Since BLDCM is nonlinear in nature, linear controllers such as PID failed to yield better results. Therefore, fuzzy logic controller is used in this paper to dynamically tune the parameter of the PID during operating condition. The Proportional, Integral and derivative (K_P, K_I and K_D) are the gains of PID controller which, tuned on line to force the system to follow the specified reference point, the structure of fuzzy tuned PID controller is shown in Figure 3.20.

PID controller finds its application in industrial control system due to feedback control loop mechanism. The integral action of PID controller helps in achieving the target value by providing equality between measured value and desired value with constant error which increases the controller output. The combination between PID controller and fuzzy controller might be a good choice for tuning the PID parameter according to the error and change of error. The relationship between error input e(t) and the output y(t) of PID controller is given in Equation (3.77).

The PID controller can be tuned by various methods. The most commonly used closed loop manual tuning method is Ziegler Nichols tuning. Complete elimination of steady state error of any process is not possible by manual tuning. The drawback of manual tuning method was overcome by the development of soft computing tuning methodology (Fuzzy Tuning). According to the principle of fuzzy self-tuning, error is changed in the entire process to adjust the three parameters (K_p, K_i, and K_d) of the PID controller online so that good dynamic and static performance can be achieved [66]. When compared to conventional PID controller it helps to achieve the desired response with minimum settling time and rise time. PID-Fuzzy is a controller to optimize the work of PID controllers when the set point and load are dynamic. Fuzzy logic works to determine Kp, Ki and Kd parameters. Fuzzy-PID has two inputs consisting of error and delta error, and three outputs are Kp, Ki, and Kd. The fuzzy-PID control scheme is shown in Figure 3.26.

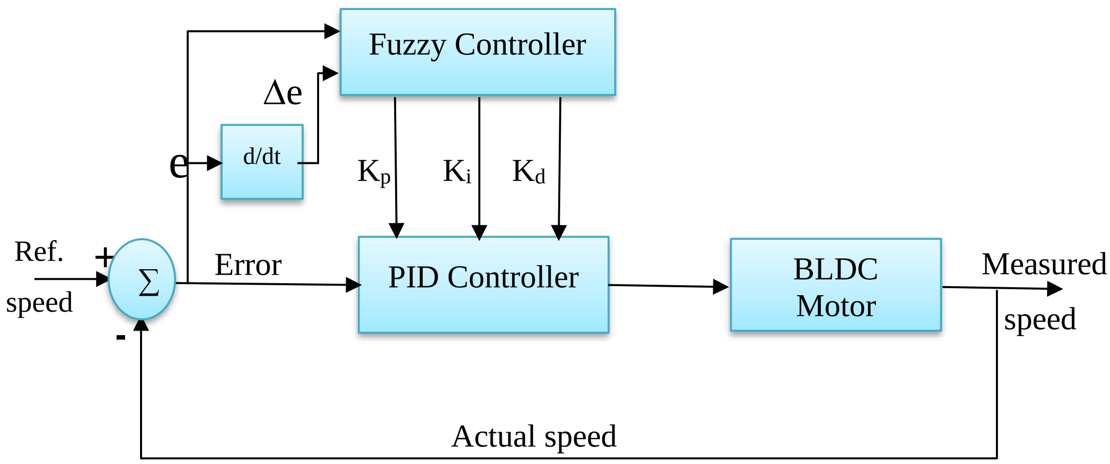

Figure 3.26 Fuzzy tuned PID controller

Error (E) and change in Error (CE) are the input of Fuzzy, and the three output from Fuzzy controller are KP, KI, and KD. The Fuzzy guidelines are extricated from major learning and human experience about the system. These rules contain the input and output information and yield connections that characterize the control technique. Each control input has seven fuzzy sets so that there are at most 49 fuzzy rules. In this thesis the rule base is simplify from 49 to 25 rule base. The fuzzy rules explain between relationship of input and output variables. The output of fuzzy logic controller is obtained by evaluation of reporting statues and behavior rules. Rules are created by defining system variables ‘IF’ and defining control variables ‘THEN’.

Table 3.9 The Rule base of Kp

e/Δe	NL	NS	Z	PS	PL
NL	PVL	PVL	PVL	PVL	PVL
NS	PML	PML	PS	PL	PVL
Z	PVS	PVS	PS	PMS	PMS
PS	PML	PML	PML	PL	PVL
PL	PVL	PVL	PVL	PVL	PVL

Table 3.10 The Rule base of Ki

e/Δe	NL	NS	Z	PS	PL
NL	PM	PM	PM	PM	PM
NS	PMS	PMS	PMS	PMS	PMS
Z	PS	PS	PVS	PS	PS
PS	PMS	PMS	PMS	PMS	PMS
PL	PM	PM	PM	PM	PM

Table 3.11 The Rule base of Kd

e/Δe	NL	NS	Z	PS	PL
NL	PVS	PMS	PM	PL	PVL
NS	PMS	PML	PL	PVL	PVL
Z	PMS	PL	PL	PVL	PVL
PS	PML	PVL	PVL	PVL	PVL
PL	PVL	PVL	PVL	PVL	PVL

The portion ‘IF’ of the rule is reference to membership degree of input part of fuzzy sets. ‘THEN’ is reference to output. Total number of rules equals total sum of products of fuzzy subsets which characterizes system. The number of rules and accuracy is one of the most significant factors affecting the performance of the system. Because speed error and change of speed errors are seven sets, there are 25 control rules in this fuzzy base. The rule base is shown in Table 3.9, Table 3.10 and Table 3.11. The speed of BLDC motor is designed by using rule base. This rule base is designed by using MATLAB fuzzy Logic Toolbox. After rule base is created, emerging surface and rule viewer are shown in Figure 3.27 and 3.28.

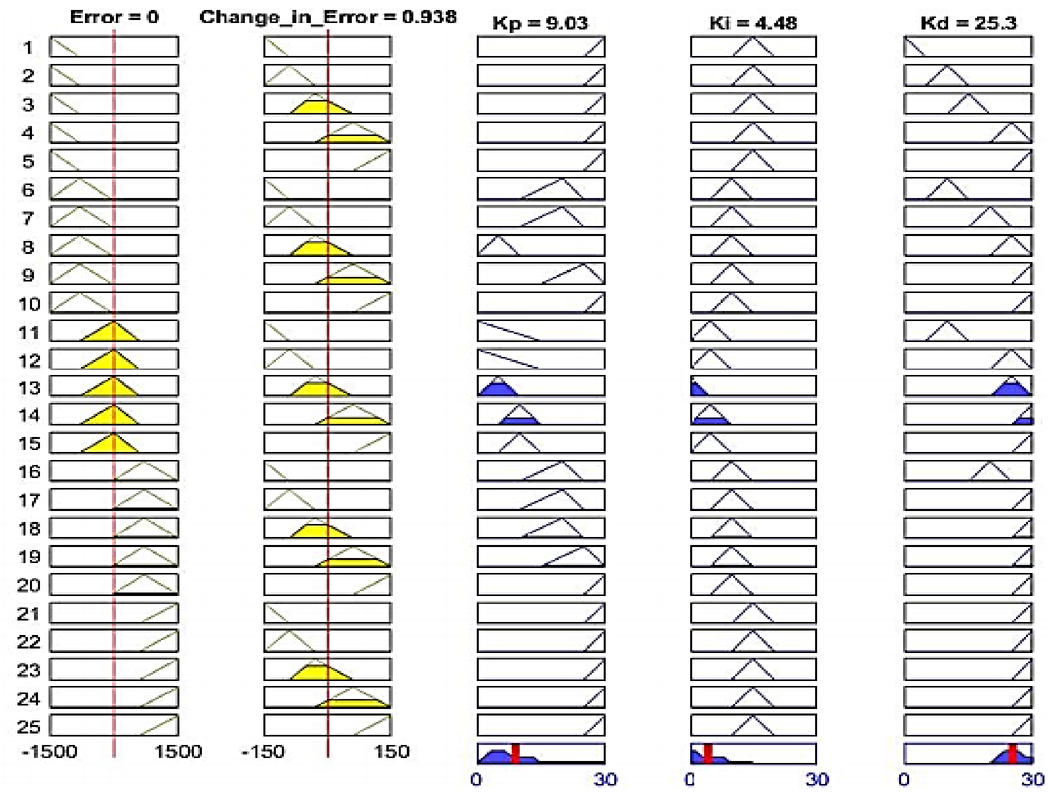

Figure 3.27 Rule Viewer

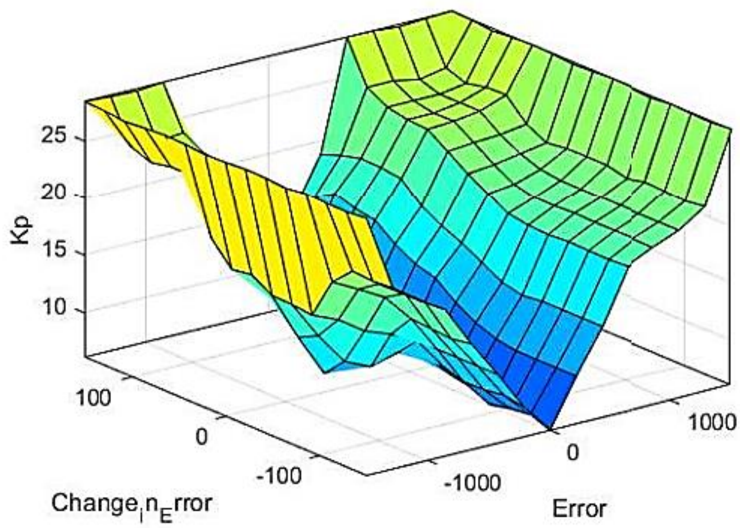

Figure 3.28 Surface viewer

CHAPTER FOUR

RESULTS AND DISCUSSIONS

The simulation results explained in this chapter is performed for the same values of the system parameters under study. The Simulation is done for confirming the viability of Fuzzy tuned PID controller, the simulation results were compared with the classical PID controller and found a tangible improvement in the performance characteristic. The system is simulated at no lode and the load torque of 20N-m and the speed response of BLDC Motor at 3000 rpm with PID and Fuzzy Tuned PID controller.

4.1. Result

For verifying the control technique performance on speed response, the simulation test is done with various operating condition (no load and with load) and speed response with step change in reference speed.

4.1.1. Comparison of Speed Controller-Based BLDC Motor Driving Output

In the PID controller design when the transfer function of BLDC motor is initialized to the controller firstly the signal is process for all three controller Proportional Controller, Integral Controller and Derivative controller at the same time, and in the last the sum of all the three controllers signal is process as resulted signal for the PID Controller. In Fuzzy-PID Controller Fuzzy Controller calculate the gain parameters by its self-tuning ability. There is no need to put gain parameters they were also found from the Controller in the terms of kp, ki and kd and performance parameters were measured from the responses.

Reference speed is taken different step reference signals. Speed response of BLDC motor is shown for fuzzy-PID and PID controller under no load condition in Figure 4.1. And on Figure 4.2 Fuzzy self-calculated Gain parameters were kp = 1.503, ki = 0.1763, kd = 7.503 and performance parameters were found as rise time in 0.04974sec, 1.96% overshoot and vary good stability whereas for PID Controllers These Parameters were k_P = 0.082119, k_i =

10.374485, k_d = 0.0001368 and for PID Controller performance parameters were found as rise time in 0.05192sec, 34.845% overshoot and good stability.

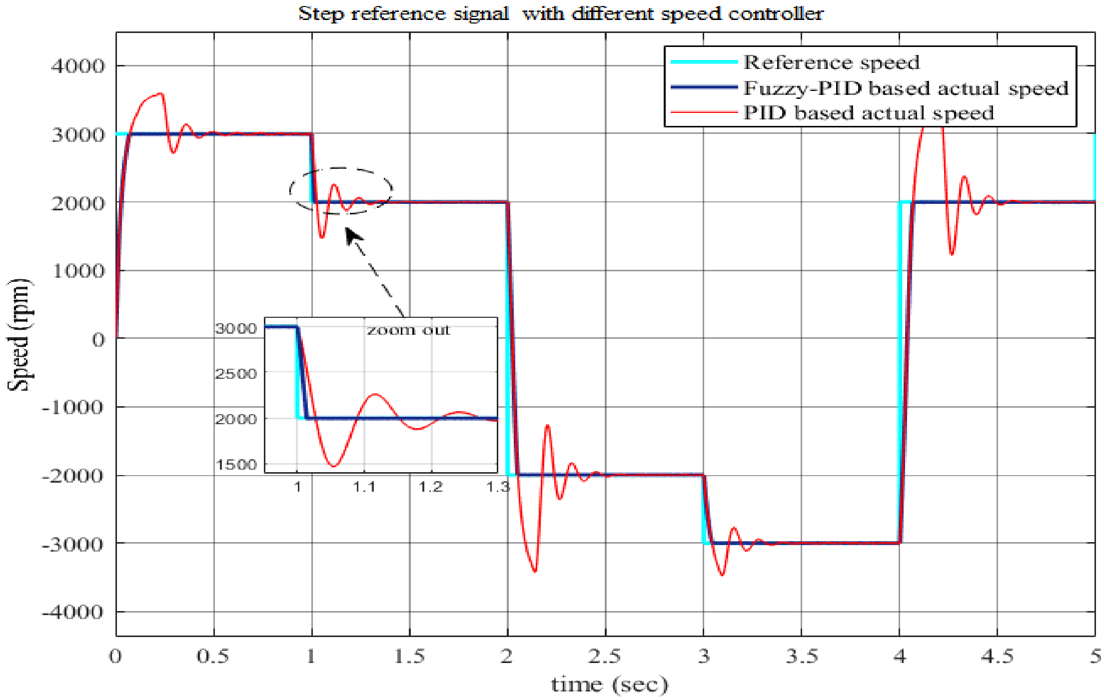

Figure 4.1 Step reference signal and rotor speed responses of PID and Fuzzy-PID controller

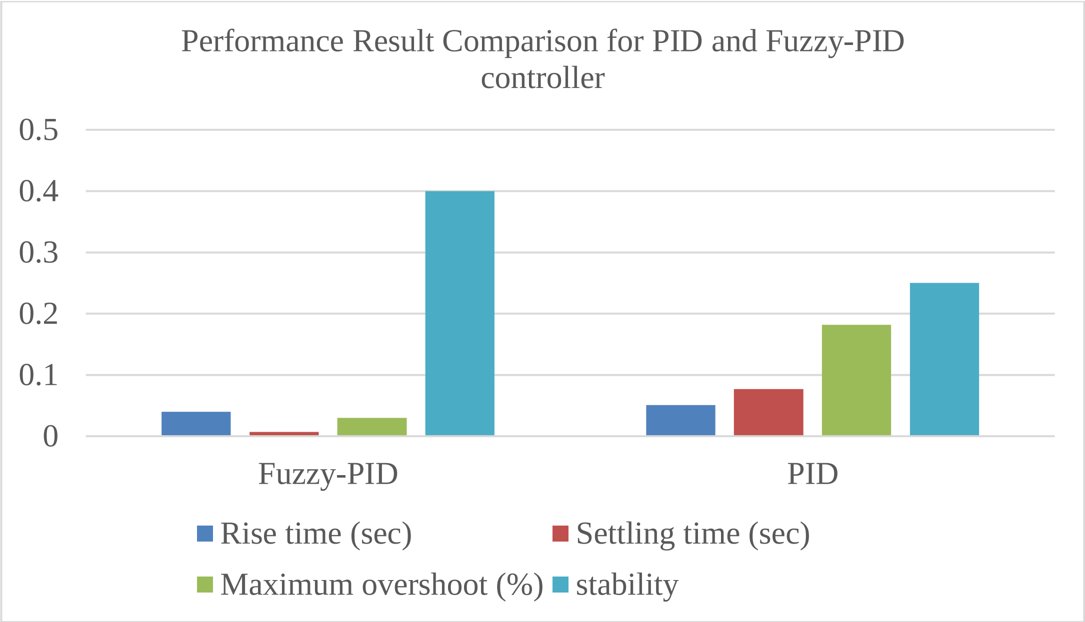

Figure 4.2 Performance comparison results for PID and Fuzzy-PID controller

4.1.1.1. Comparison of Speed Controller with and without Load at Constant Speed

Reference signal is taken at constant speed 3000 rpm. Speed response of BLDC motor is shown for fuzzy-PID and PID controller under no load condition in Figure 4.3. Settling time is 0.017 seconds for PID controller, but for fuzzy-PID controller this time is 0.013 seconds. Overshoot is 9.8% for PID control, however, there is no overshoot for fuzzy-PID control.

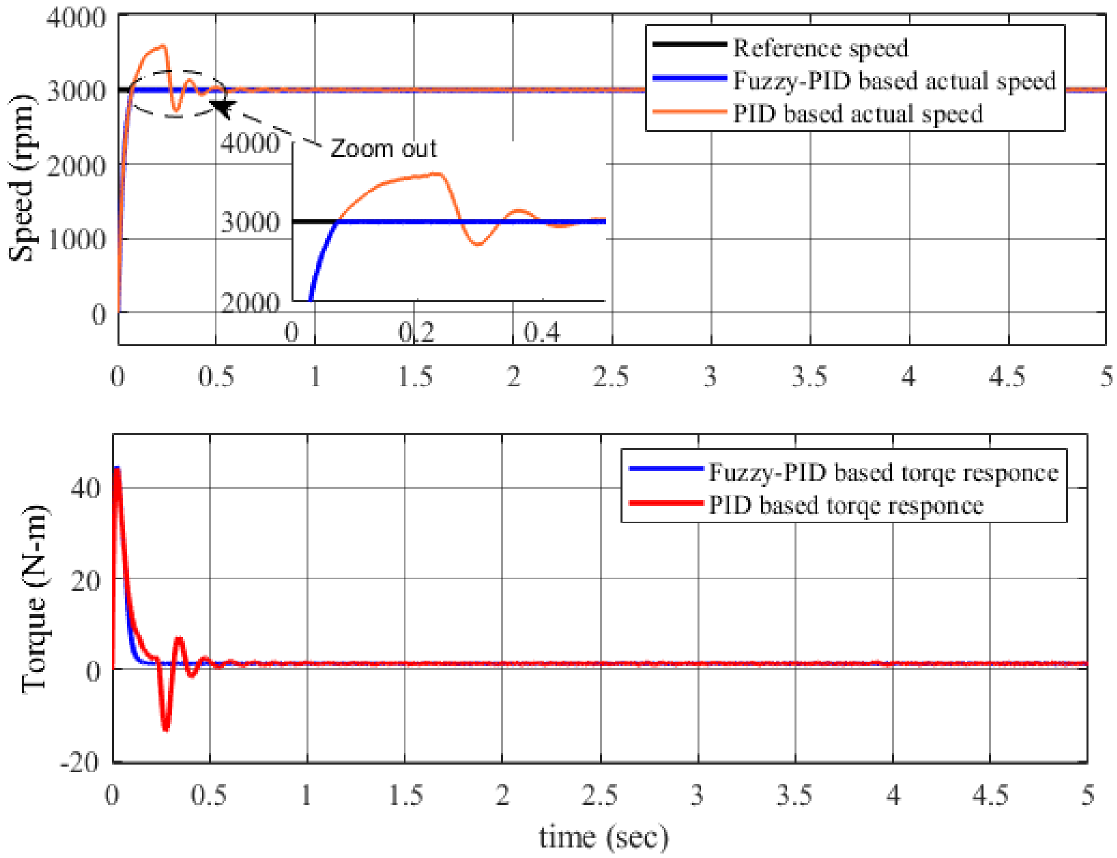

Figure 4.3 Speed and torque response under no load condition

Speed response of BLDC motor is shown for fuzzy-PID and PID controller under high load condition in Figure 4.4. Settle time is 0.01 seconds for PID controller after high load is applied to the system. However, settling time is 0.004 seconds for fuzzy logic controller after high load is applied to the system.

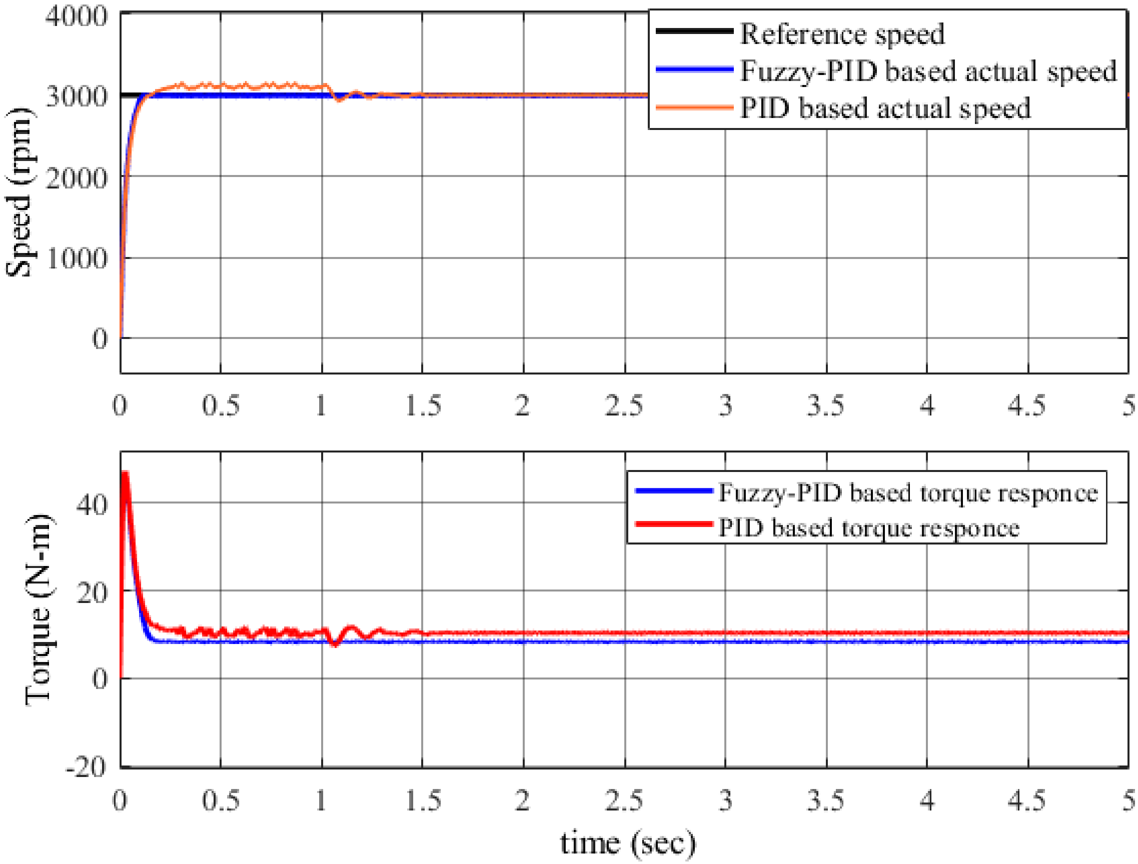

Figure 4.4 Speed and torque response under high load condition

4.1.1. Four Quadrant Operations of the BLDC Motor

For checking the behavior of the proposed system in the four quadrants of the speed-torque profile of the motor, the reference speed and the applied load torque to the motor are presented in Table 4.1.

Table 4.1 Quadrant determination

Time (s)	0	1	1.5	2.5	2.6	3	4	5	6.5
Reference speed (rpm)	0	3000	3000	3000	3000	0	-3000	-3000	0
Applied load torque (N-m)	0.1	0.1	20	0	-20	-20	-20	10	10
Quadrant		I	I	I	II	II	III	IV	-

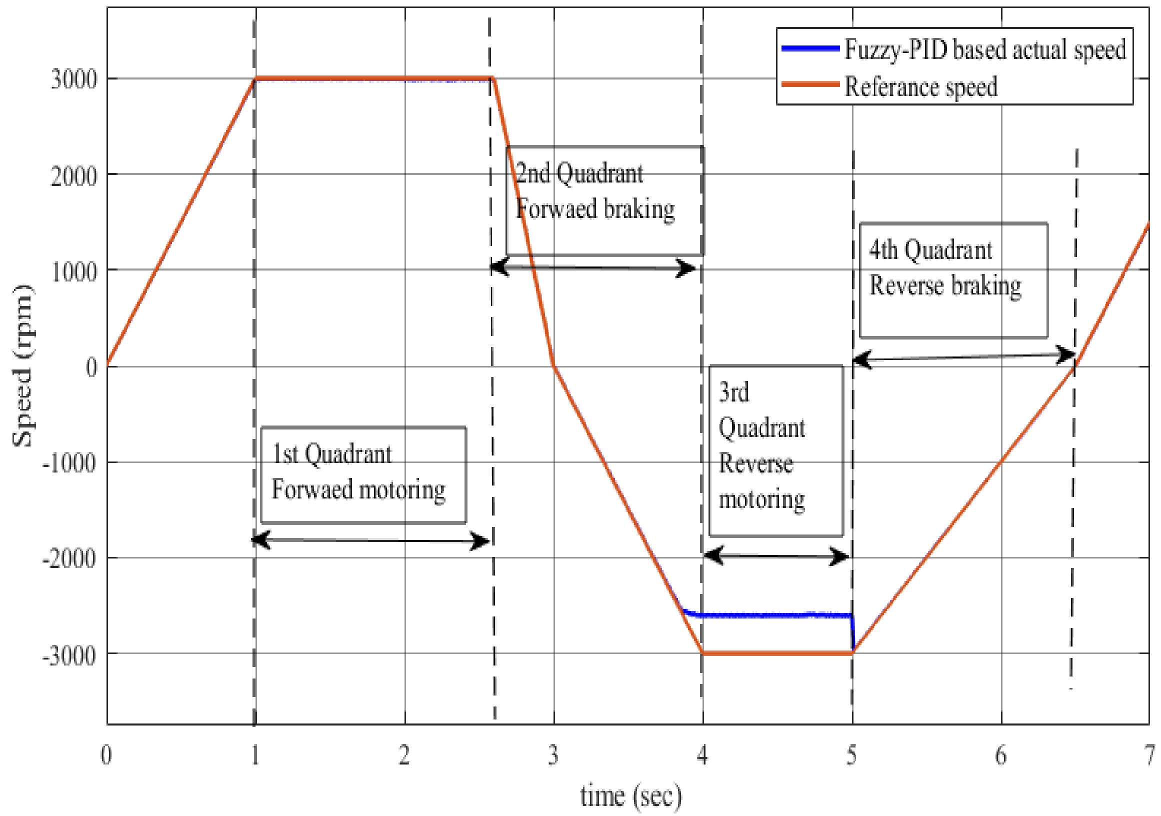

Figure 4.5 Rotor speed (four quadrant operation)

Figures 4.5 - 4.8 show the simulation results for the four quadrants operation of the motor. The speed set point and the torque set point are also shown. From time t = 1 s to 2.6 s, the speed set point is 3000 rpm and the applied load torque is positive. That is, the machine is operating in the first quadrant; forward motoring. As can be seen in Figure 4.6, the actual speed is precisely following the reference with the acceleration ramp. From time t = 2.6 s to 4 s, negative load torque is applied to the motor, while the speed set point is still positive. This implies that a brake is applied, and that the machine is operating in the second quadrant; forward braking. Figure 4.5 shows a deceleration in the rotor speed. At that time, the motor acts as a generator.

During the time t = 2 s to 2.5 s, both the speed set point and the applied load torque to the motor are negative. That is, the machine is operating in the third quadrant; reverse motoring. As can be seen in Figure 4.5, the actual speed tries to follow the speed set point ramp by decreasing the speed to zero and starting to speed up with a rotation in reverse direction.

At time t = 5s, the speed set point is commanded to reach zero value, but due to the 500 rpm/s rate limiter, it returned to zero value at 6.5 s. From time t = 5 s to 6.5 s, positive load torque is applied to the motor, while the speed set point is still negative. This implies that a brake is applied, and that the machine is operating in the fourth quadrant; reverse braking.

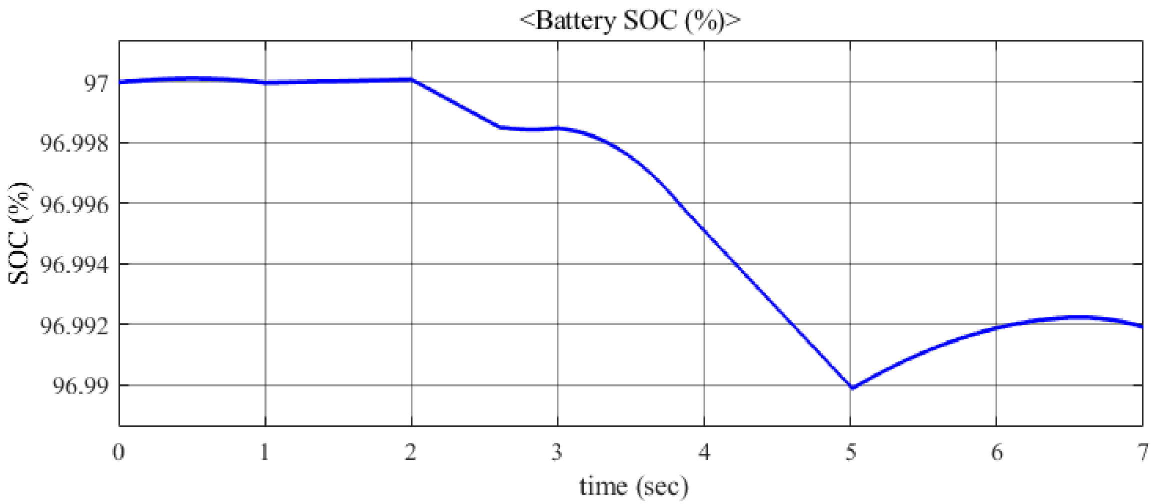

Figure 4.6 Battery state-of-charge

At initial conditions, the motor is operated in (Quad-I) Forward motoring mode. When a speed reversal command is issued, the motor undergoes braking operation in forward direction, with speed tending to zero and starts rotating in reverse direction as soon as the speed is zero as shown in Figure 4.7.

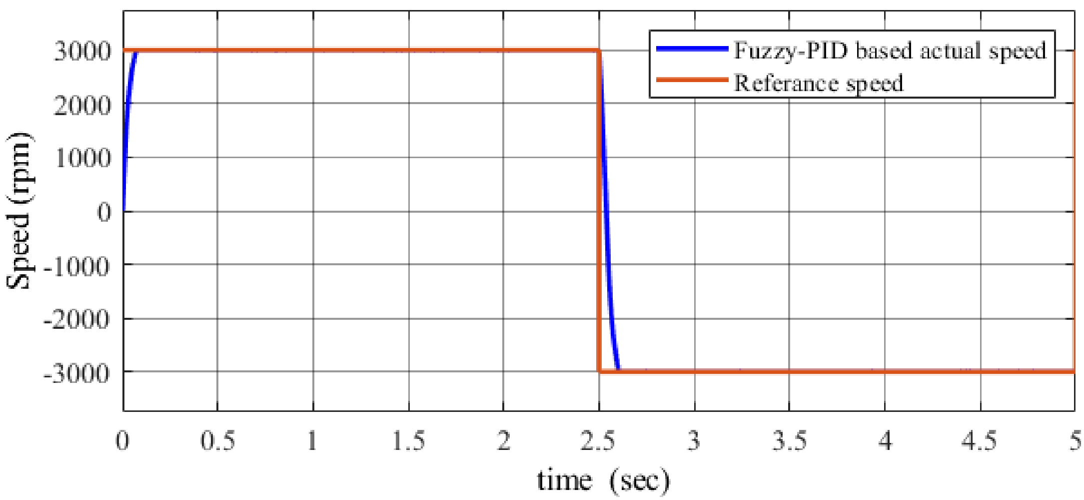

Figure 4.7 Show speed variation during forward motoring to reverse braking

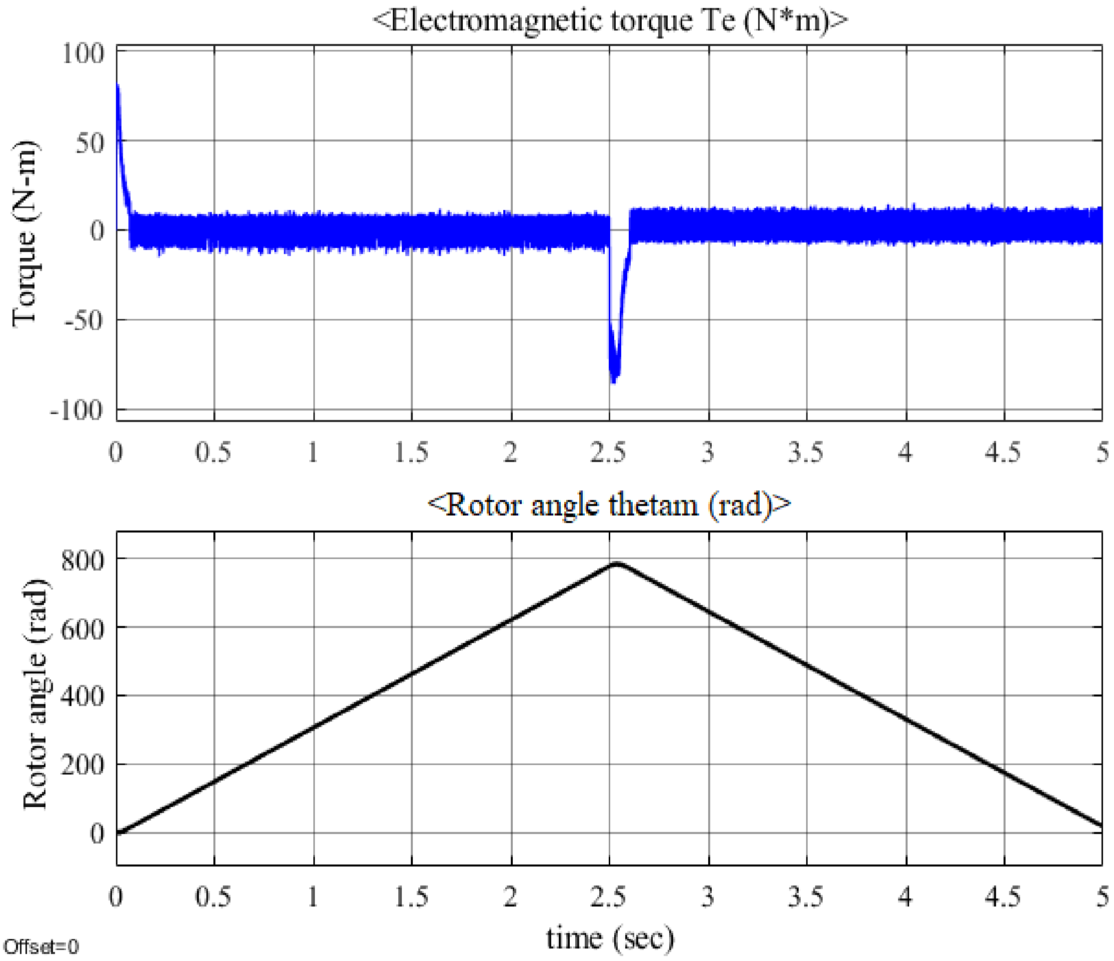

Figure 4.8 Show torque and rotor angle variation during forward motoring to reverse braking

There is a slight variation in electromagnetic torque during the changeover process but it quickly gets backs to normal. When a speed reversal command is issued again, the motor undergoes reverse braking and operates in Forward direction. The variation of motor performance when the motor is changing from reverse braking mode to forward motoring mode are shown in Figure 4.9.

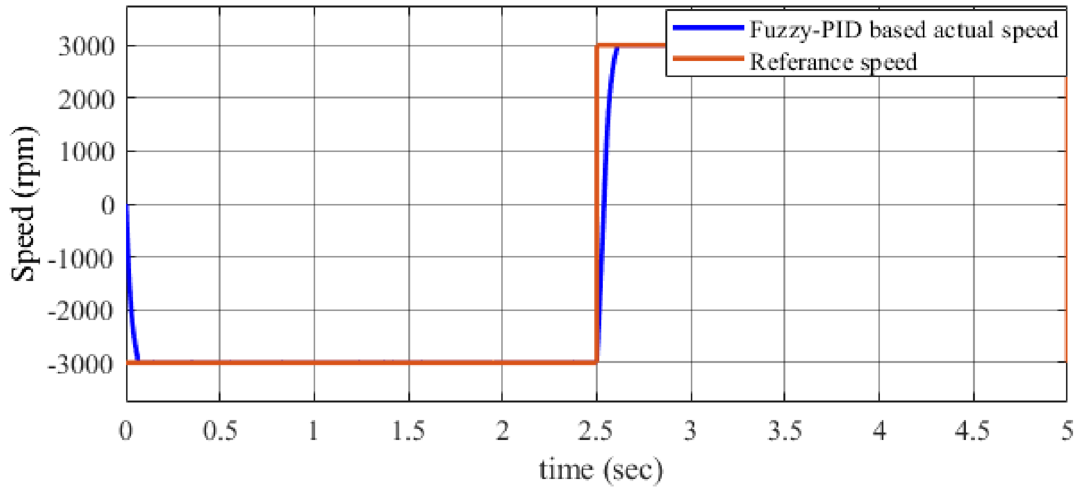

Figure 4.9 Show speed variation during reverse braking to forward motoring

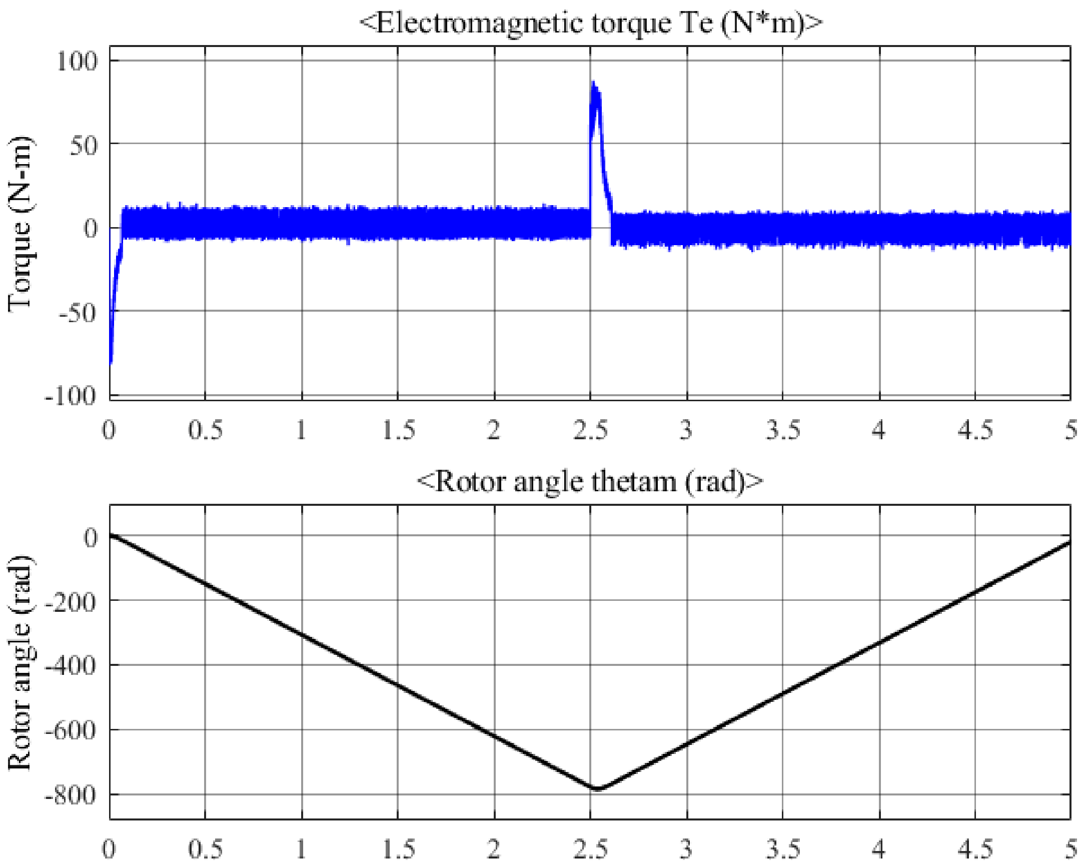

Figure 4.10 Show torque and rotor angle variation during reverse braking to forward motoring

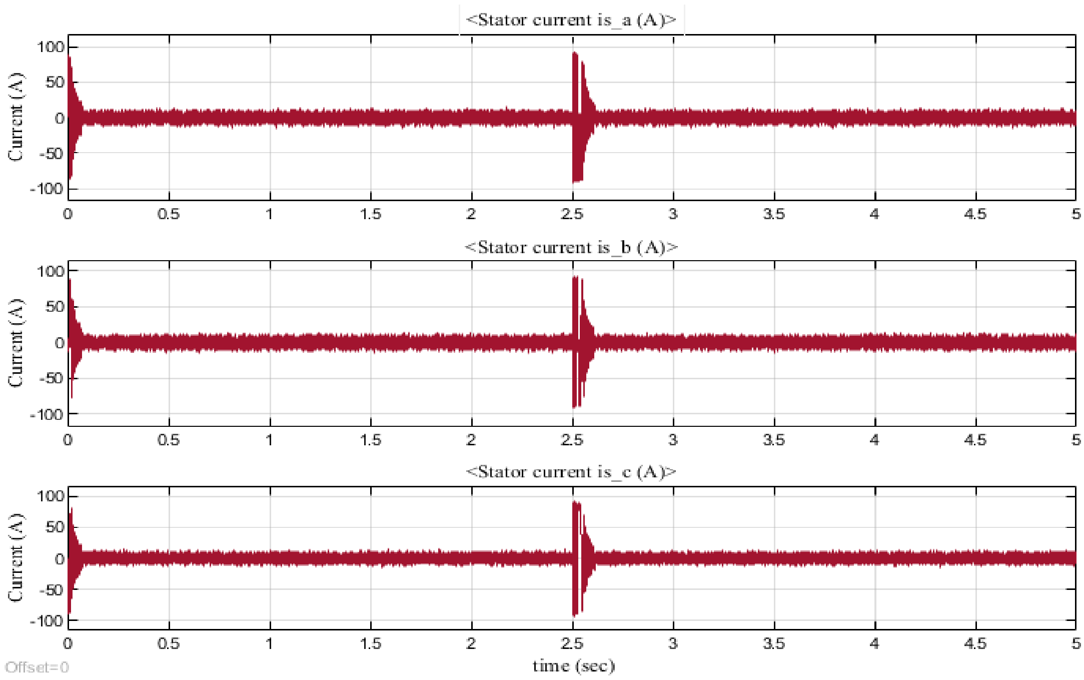

Figure 4.11 Phase a, b, and c current variations during forward motoring and reverse braking

4.1.2. PWM Based Nonlinear BLDCM Drive Output Results

In Figure 4.12 shows the 3-phase signals generated from hall sensor. Figure 4.13 and Figure 4.14 shows the 3-phase signals generated from hall effect decoder and hall effect signal zoom out part from 0.4s to 0.43. Figure 4.15 shows the back electromotive force (emf) of the BLDC motor. In this Figure, X and Y axis represented the time in second (secs) and back emf value in Volt (V) of the BLDC motor respectively. Figure 4.16 shows the stator current of the BLDC motor. In this Figure X-axis represented the time in second (secs) and Y-axis the motor stator current in Ampere (A) respectively. It is also observed that the stator currents are fixed for 0.2s which is the same as electromagnetic force time of the result as shown in Figure 16. In Figure 4.17 show the 3-phase get pulse signals generated from hysteresis current controller.

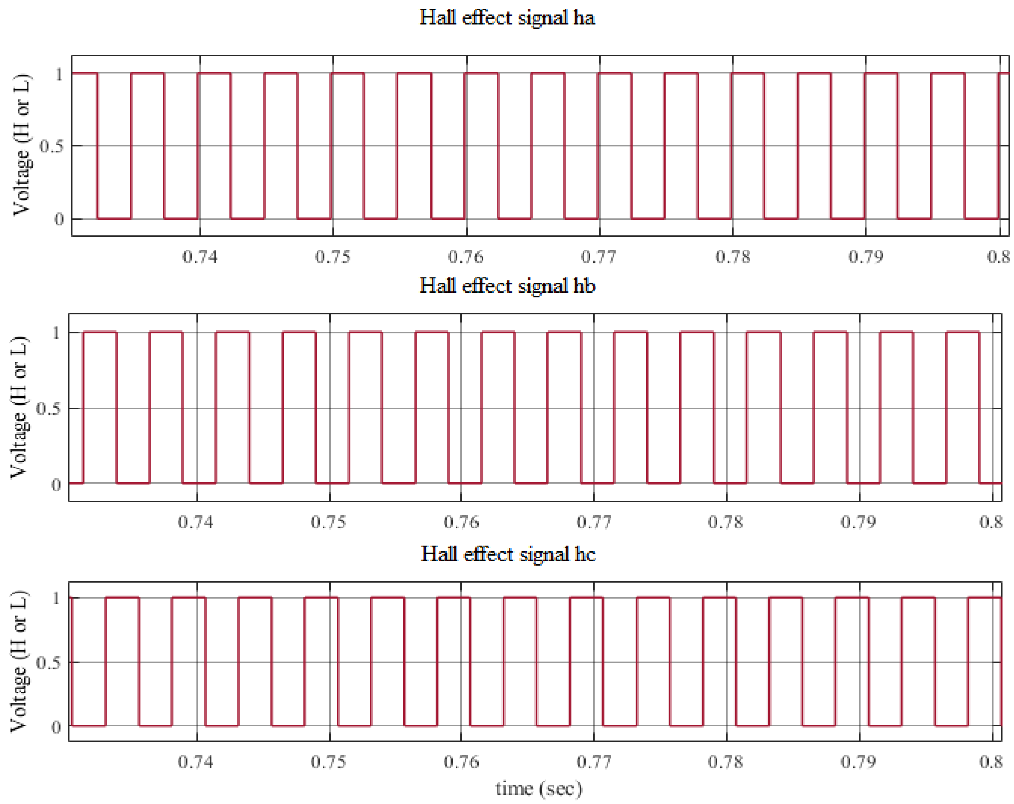

Figure 4.12 shows the 3-phase signals generated from hall sensor

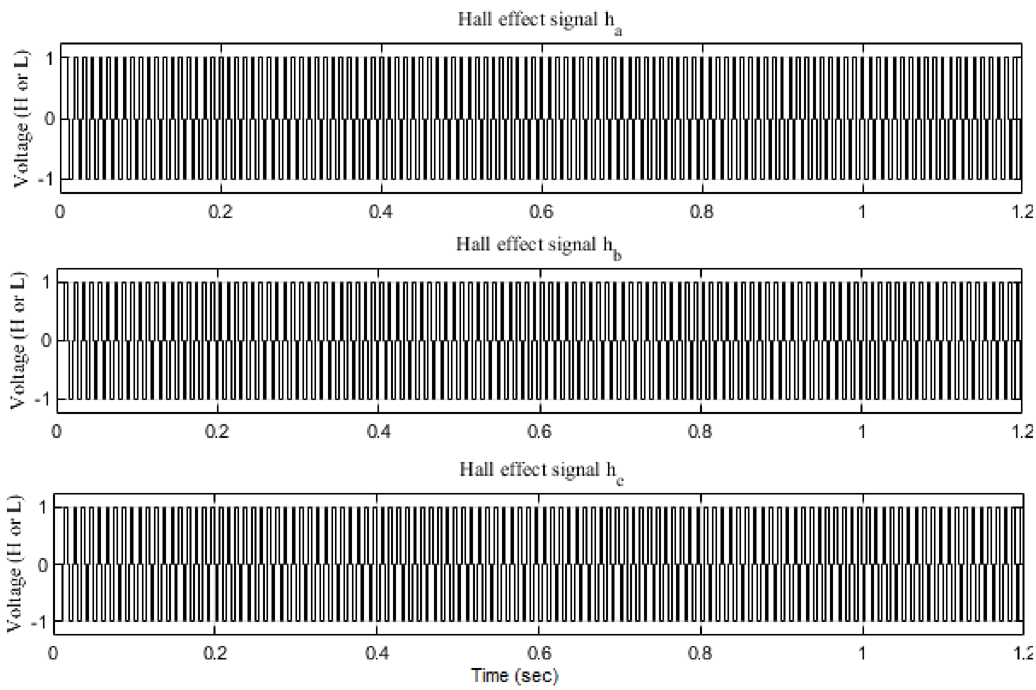

Figure 4.13 BLDC motor hall effect decoded signal

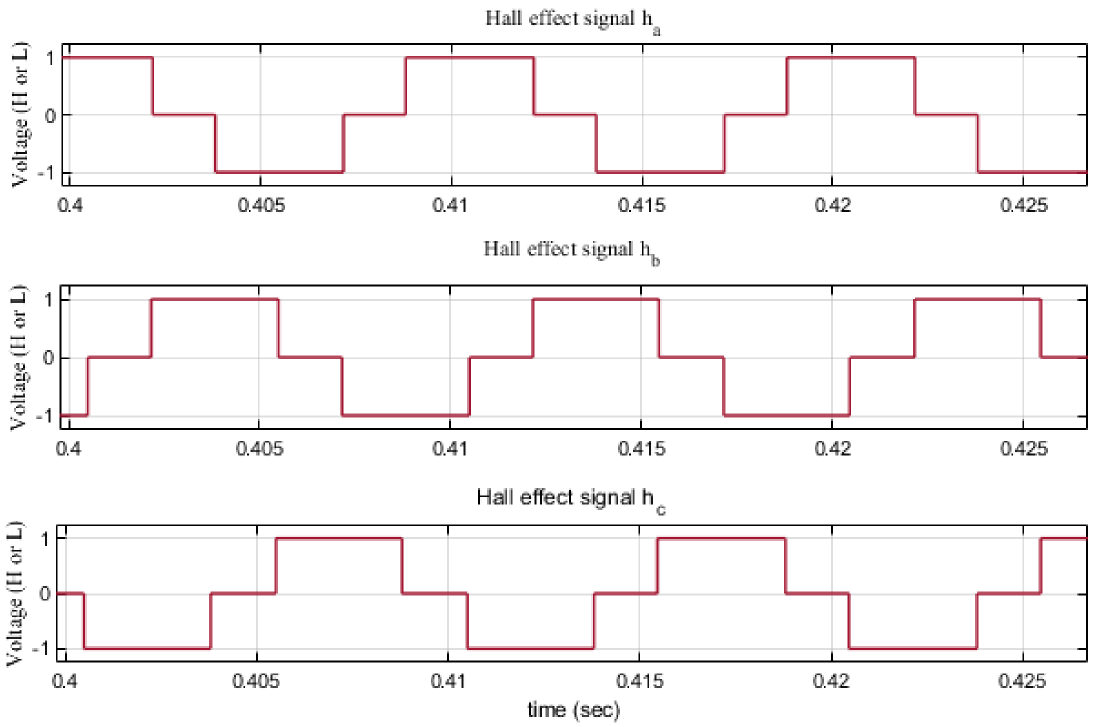

Figure 4.14 BLDC motor hall effect decoded signal zoom out part

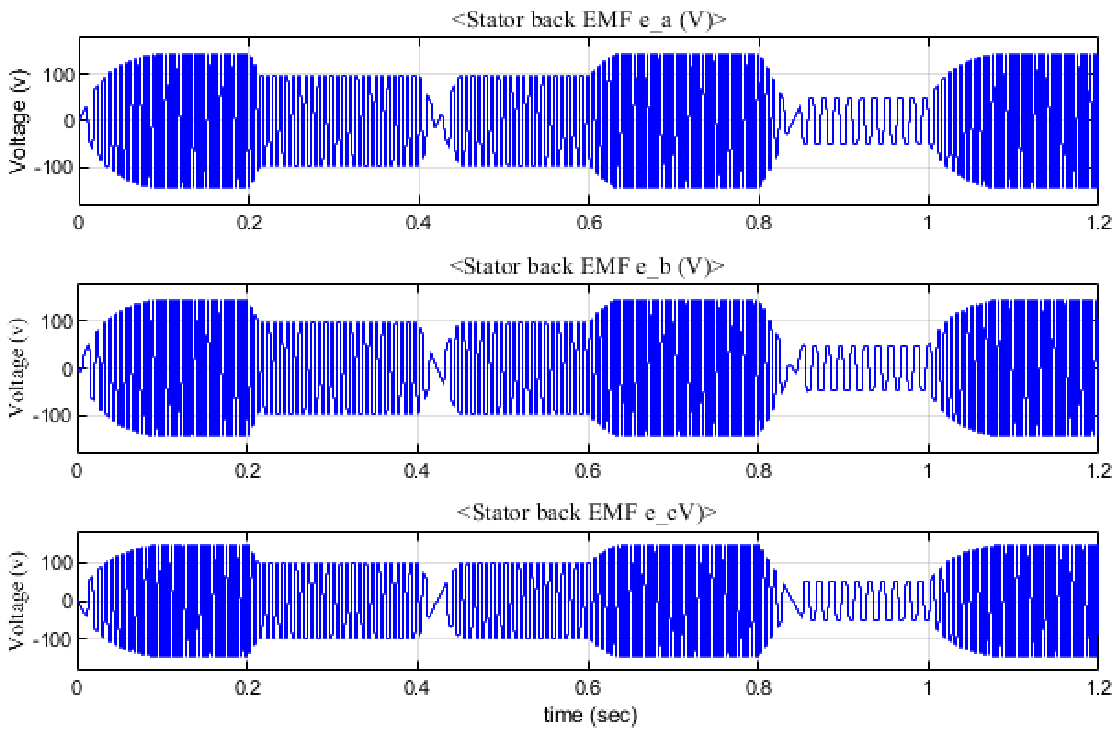

Figure 4.15 BLDC motor 3-phase back electromotive force

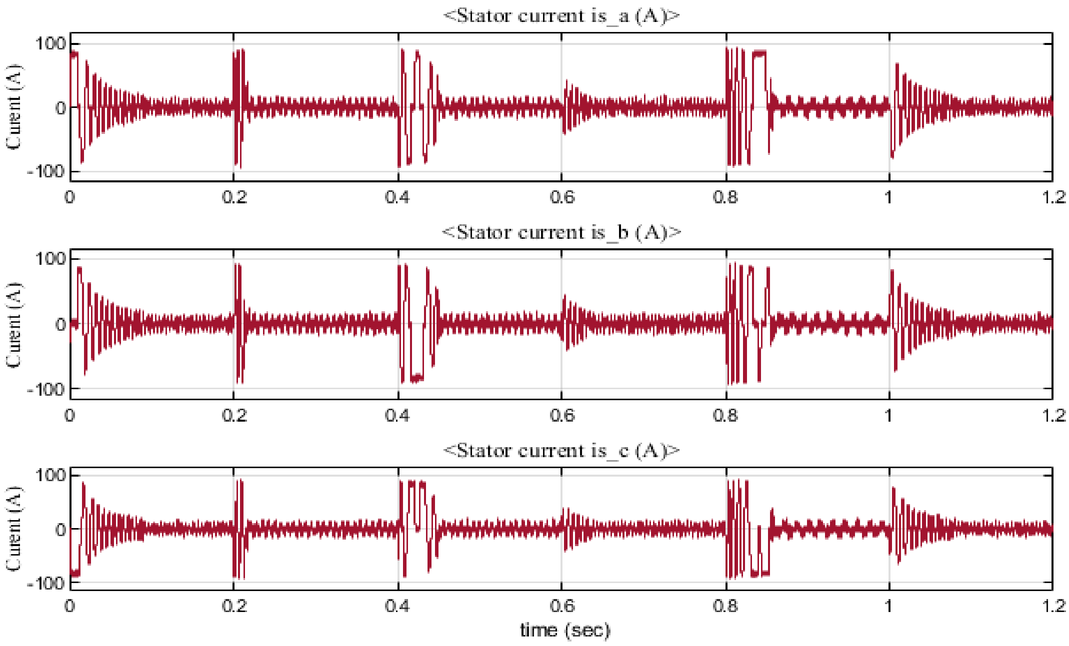

Figure 4.16 Phase stator current of the BLDC motor

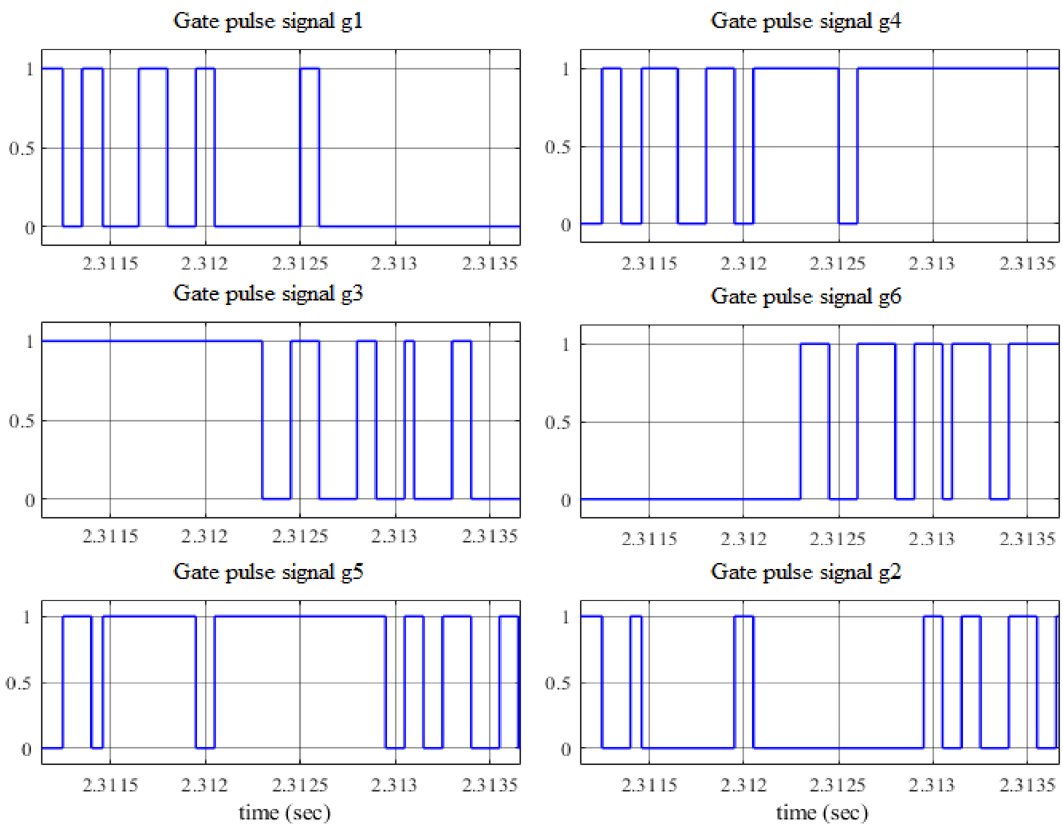

Figure 4.17 3-phase inverter get pulse signals

4.1.3. Fuzzy-PID Speed Controller-Based BLDC Motor Driving Output Results

The simulation of fuzzy-PID based speed control of brushless dc motor using bidirectional converter is performed using MATLAB/Simulink model. The fuzzy logic controller is used as speed controller is used as speed control circuit. The output of the controller is fed to a controlled voltage source which feeds the inverter. The fuzzy logic controller is designed through fuzzy inference system (FIS) editor and is exported to the MATLAB workspace. Mamdani type of inference engine is used in the FIS editor. By setting positive and negative speed get two modes of operation of Brushless motor. The simulation results provide the necessary wave forms for the analysis of speed control of BLDC motor drive.

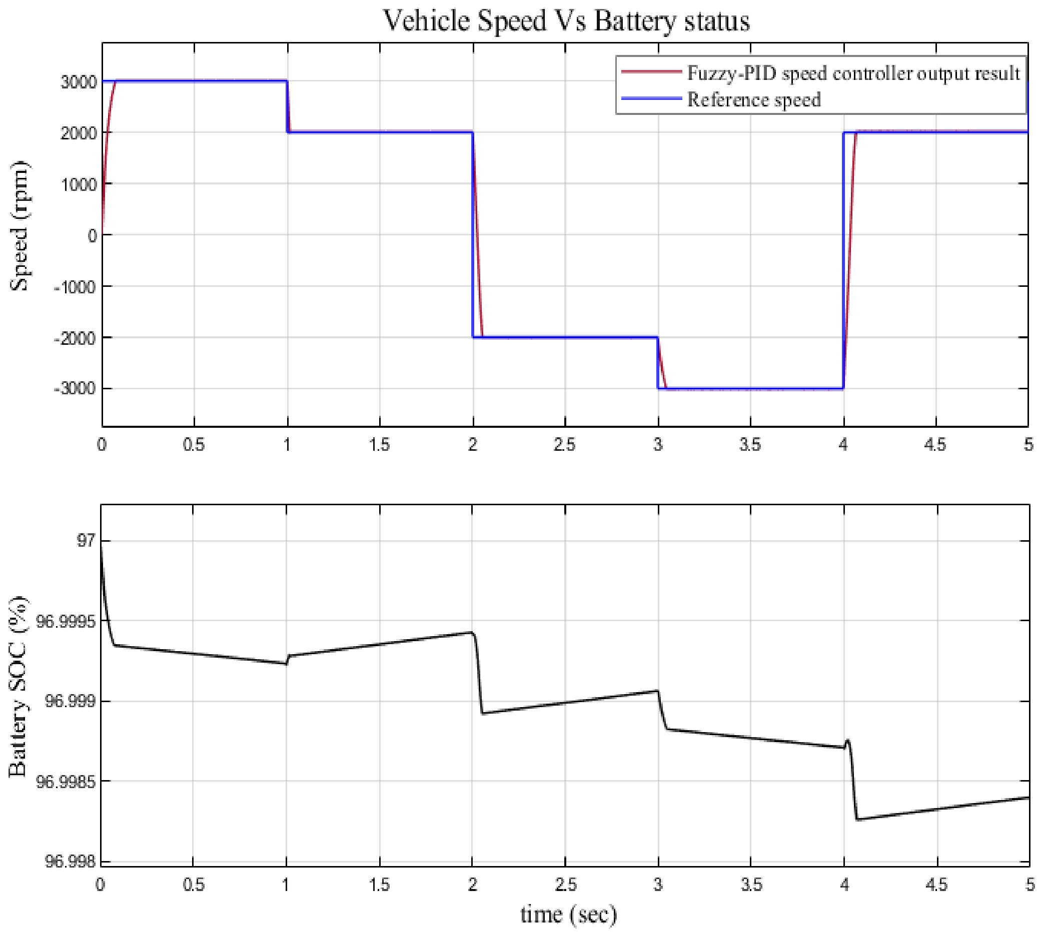

Figure 4.18 Fuzzy-PID based speed control of BLDC motor vs battery state of charge

For the first 1sec speed and torque have positive, then converter operates in boost mode. The BLDC motor act as a normal motoring mode and the power flow from the battery to the motor as seen in the Figure 4.18. After 1sec the speed decreasing but still positive. The motor produces a negative torque, then converter operates in a buck mode regenerating the electrical energy from the motor to the battery. So as to realize the vehicles downhill motion. For next 2sec applied negative speed and the motor produce negative torque and the converter operates in a buck mode regenerating the electrical energy from the motor to the battery. For last 1sec second speed goes to positive and the motor act as normal.

4.1.4. Battery State of Charge

During motoring, the battery is providing the power to the motor and hence the battery SOC (state of charge) decreases. During regeneration the battery current goes negative since the converter is operating in the buck mode and hence the SOC of the battery starts increasing (after .45s up to 0.6s and 0.085s up to 1s) as seen from Figure 4.19.

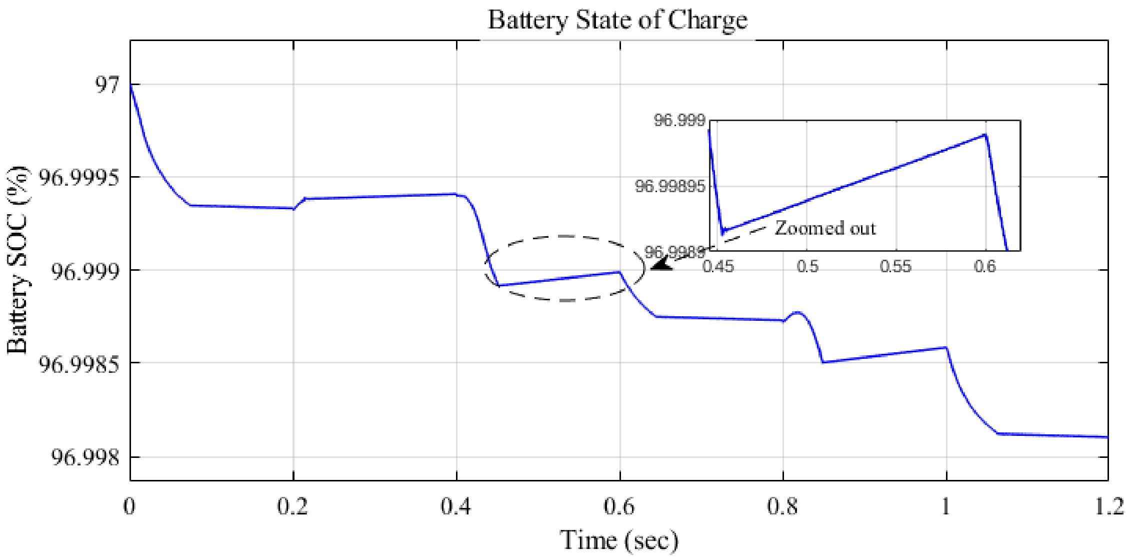

Figure 4.19 Battery state of charge

CHAPTER FIVE

CONCLUSIONS AND RECOMMENDATIONS

5.1. Conclusions

In this thesis, the fuzzy-PID control scheme for the speed control of Brushless motor using a bidirectional converter is proposed. In braking modes of operation, instead of wasting kinetic energy it can be stored in a battery. The excess energy is effectively stored in the battery based on the mode of operation of the bidirectional converter. Simulation studies were conducted to evaluate the performance of both proportional integral controller and fuzzy-PID speed control method. The advantages of this proposed method are excellent speed control, smooth transition between the quadrants and efficient conservation of energy.

The speed control of a BLDC Motor is using both PID controller, and Fuzzy-PID Controller. Fuzzy-PID controller is proposed which combines the fuzzy controller with the conventional PID controller and has the benefit of two methods. Based on the simulation results, the execution of the two controllers are analyzed on the premise of different control system parameters, for example, maximum overshoot, rise time and settling time. It is clearly shown that for the same operating conditions the control concept using a Fuzzy tuned PID controller has better speed regulation and performance than the conventional PID controller. This mean is that developing system can be easily applied to real area. As a result, at no load and high load condition, performance of fuzzy-PID controller shows that there isn't no overshoot on the speed response of BLDC motor and fluctuations of torque response are reduced.

The BLDC motor is fed by a lithium battery via bidirectional DC-DC converter, the vehicle dynamics is considered. The two modes of operation motor and generator are explained. The designed system has only one direction of rotation, but allows regenerative braking. The simulation results show that the speed regulator gives good performance on the speed tracking, accuracy and the rejection of disturbance load. The mode generator operating permits to transform the kinetic energy in electrical energy which is stored in the battery;

this is useful to resolve the problems relevant to the battery energy storage system and increase the autonomy of the vehicle.

5.2. Recommendations

In this research, work attempts have been made to use the best components. Because of a shortage of time don't compare current control methods use hysteresis current controller but, this controller has a limitation. There are superior to that method to control current of BLDC motor.

To add current control function to the proposed speed controller in order to keep the current within a certain range for a specific speed, could be a work for future. The proposed future work would thereby enhance the motor start-up current, reduce the motor current ripples and overall enhance the motor torque characteristics performance. Current control methodology will also reduce the speed and torque variations caused due to any sudden changes in the motor current value.

REFERENCES

[1] P. J. Grbovic, P. Delarue, P. Le Moigne, and P. Bartholomeus, "A bidirectional three-level dc-dc converter for the ultra-capacitor applications," *IEEE Trans. Ind. Electron,* Vols. 57, no. 10, p. 3415–3430, Oct. 2010.

[2] F. Wang, X. Yin, H. Luo, and Y. Huang, "A series regenerative braking control strategy based on hybrid-power," *in Proc. Int. Conf. CDCIEM,* p. 65–69, 2012.

[3] N. Mutoh and Y. Nakano, "Dynamics of front-and-rear-wheelindependent-drive-type electric vehicles at the time of failure," *IEEE Trans. Ind. Electron,* vol. 59, p. 1488–1499, Mar. 2012.

[4] E. Bostanci, Z. Neuschl, and R. Plikat, "No-load performance analysis of brushless dc machines with axially displaceable rotor," *IEEE Trans. Ind. Electron*, Vols. 61, no. 4, p. 1692–1699, Apr. 2014.

[5] J. Zhang, X. Lu,J. Xue and B. Li, "Regenerative Braking System for Series Hybrid Electric City Bus," *The World Electric Vehicle Journal,* vol. 2, p. 4, 2008.

[6] A. A. R, "Control of Three Phase BLDC Motor using Fuzzy Logic Controller," *International Journal of Engineering Research & Technology (IJERT),* Vols. 2, no. 7, 2013.

[7] Pennycott, L. De Novellis,P. Gruber,A. Sorniotti and T. Goggia, "Enhancing the Energy Efficiency of Fully Electric Vehicles via the Minimization of Motor Power Losses," *IEEE International Conference on Systems, Man, and Cybernetics.,* 2013.

[8] Wikipedia contributors, "Electric motor," Wikipedia, The Free Encyclopedia. Wikipedia, The Free Encyclopedia. [Online]. [Accessed 19 March 2020].

[9] J.B.Gupta., "Theory & Performance of ELECTRICAL MACHINES," *S.K.Kataria& Sons.*

[10] X. D. Xue, K. W. E.Cheng and N. C. Cheung, "Selection of Electric Motor Drives for Electric Vehicles," *Australasian Universities Power Engineering Conference (AUPEC'08),* 2008.

[11] Cheng He, Chen Hao, Wang Qianlong, Xu Shaohui and Yang Shunyao, "Design and Control of Switched Reluctance Motor Drive for Electric Vehicles," *14th International Conference on Control, Automation, Robotics & Vision Phuket, Thailand (ICARCV),* November 2016.

[12] RuiEstevesAraújo, Henrique Teixeira,José Barbosa and Vicente Leite, "A Low Cost Induction Motor Controller for Light Electric Vehicles in Local Areas," *IEEE ISIE,* June 20-23, 2005Dubrovnik, Croatia..

[13] X. D. Xue, K.W.E.Cheng and N. C. Cheung, "Selection of Electric Motor Drives for Electric Vehicles," *Australasian Universities Power Engineering Conference (AUPEC),* vol. 08, 2008.

[14] M.V.Ramesh, J.Amarnath,S.Kamakshaiah,B.Jawaharlal and Gorantla.S.Rao, "Speed Torque characteristics of Brushless DC motor in either direction on load using ARM controller," *IEEE Transactions on Industry Applications,* Vols. 36, no. 1, January/February 2000.

[15] D. van Niekerk, M. Case and D.V. Nicolae, "Brushless Direct Current Motor EfficiencyCharacterization," *978-1-4763-7239-8/15/$31.00,IEEE,* 2015.

[16] Sachin S. Bharatkar, Raju Yanamshetti, D. Chatterjee, A.K. Ganguli, "Performance Comparison of an efficient IM Controller and BLDC Drive for Vehicular Applications," *Journal of Modelling and Simulation of Systems,* vol. 1, no. 3, 2010.

[17] Cuneyt Karacan, Comparison Of Performance Of Switched Reluctance Motors,Induction Motors And Permanent Magnet Dc Motors, Middle East Technical University, Middle East Technical University, April 2010.

[18] Stijn Derammelaere, Michiel Haemers, Jasper De Viaene and Florian Verbelen, "A quantitative comparison between BLDC, PMSM, Brushed DC and Stepping Motor Technologies," *IEEE Transactions on Industrial Electronics,* 2016.

[19] C Iclodean, B Varga, N Burnete, D Cimerdean and B Jurchiș , "Comparison of Different Battery Types for ElectricVehicles," *IOP Publishing,IOP Conf. Series: Materials Science and Engineering 252,* pp. 103 - 105, 2017.

[20] Markus Einhorn, Valerio Conte, Christian Kral and Jurgen Fleig, "Comparison of electrical battery models using a numerically optimized parameterization method," *2011 IEEE Vehicle Power and Propulsion Conference, IEEE,* October 2011 , Chicago, IL, USA .

[21] Lu L.,Han X.,Li J.,Hua J. and Ouyang M., "A review on the key issues for lithium-ion battery management in electric vehicles," *Journal of Power Sources,* no. 0378-7, p. 272–288, 2012.

[22] Bhajana, V. V., and Pavel Drabek, "A novel ZCS bidirectional buck-boost DC-DC converters for energy storage applications," *Industrial Technology (ICIT), International Conference on IEEE*, 2015.

[23] Gupta, Gaurav, and Prerna Gaur, "GFuzzy logic controlled-power factor corrected bridgeless buck boost converter-fed brushless DC motor drive," *Computer, Communication and Control (IC4), International Conference on. IEEE,* 2015.

[24] Atul Kumar, Dr. Prerna Gaur, "Bidirectional DC/DC Converter for Hybrid Electric Vehicle," *IEEE Transactions on Advances in Computing, Communications and Informatics (ICACCI),* pp. 839-843, sep 2014.

[25] R.Kandiban, and R. Arulmozhiyal, "Design of Fuzzy PID Controller for Brushless DC Motor," *International Conference on Computer Communication and Informatics (ICCCI),* p. 1, Jan. 10 – 12, 2012, Coimbatore, INDIA.

[26] K.C.Donev and J.M. "Regenerativebraking,https://energyeducation.ca/encyclopedia/Regenerative_braking.", Energy Education, 2018. [Online]. [Accessed 20 November 2019].

[27] M.K, Y.H Gan,et al, "Studies of Regenerative Braking in Electric Vehicle," *Sustainable Utilization and Development in Engineering and Technology (STUDENT),IEEE,* 2010.

[28] Soniya.K, Malode and R.H.Adware, "Regenerative Braking System in Electric Vehicles," *International Research Journal of Engineering and Technology (IRJET),* vol. 03, no. 03, 2016.

[29] Pulkit, Anchal,et al, "Regenerative Braking Systems (RBS) (Future of Braking Systems)," *International Journal of Mechanical And Production Engineering,* vol. 2, no. 05, pp. 2320-2092, 2014.

[30] Kayaalp and R. Ilker, "Modeling and Analysis of Bidirectional DC-DC Converter," *2015,* no. 2411-3123, pp. 2411-2933.

[31] L. Habtamu, "Modeling and Analysis of Regenerative Braking of an Induction Motor," 2012.

[32] Joshi and Mahendra Chandra, "Modeling and Control of Bidirectional DC-DC Converter Fed PMDC Motor," *Annual IEEE India Conference (INDICON),* 2013.

[33] R.W. Erickson and D. Maksimovic, "Fundamental of power electronics," Kluwer, Norwel, MA, 2nd edition, 2011.

[34] N. Mohan, T.M. Undeland and W.P. Robbins, "Power converters," Wilkey New York,2nd edition, 2003..

[35] S. Yang, K. Goto,Y, Imamura and M. Shoyama, "Dynamic characteristics model of bidirectional DC/DC converter using state space averaging method," *IEEE, Int. Telecommunication energy Conf (INTELEC),* pp. 1-5, 2012..

[36] Y. Imamura, H. A. Ramadan,S. Yang , G. M.Dousoky and M. Shoyama Seamless, "dynamic model of bidirectional DC/DC converter," *IEEE, Power electronics and drive systems Conf (PEDS),* pp. 1109- 1113, 2013.

[37] P. Xuewei and A. K. Rathore, "Novel Bidirectional Snubberless Naturally Commutated Soft-Switching Current-Fed Full-Bridge Isolated DC/DC Converter for Fuel Cell Vehicles," *IEEE. Trans. Ind. Electron,* vol. 61, pp. 2307-2315, May 2014.

[38] Y. B. T. I. B. Axelrod, "Steep conversion ratio Cuk, Zeta and Sepic converters based on a switched coupled-inductor cell," *IEEE 39th Power Electronics Specialists Conf. (PESC),* pp. 3009-3014, 2008.

[39] Liang, Chen, Yang,J. F. Chen and A. Ioinovici, "Ultra large gain step-up switched-capacitor DC-DC converter with coupled inductor for alternative sources of energy," *IEEE. Circuits Syst,* vol. 59, pp. 864-874, Apr 2012.

[40] B. Axelrod, Y. Berkovic,S. Tapuchi and A. Ioinovici, "Improved circuit of the switched coupled-inductor cell for dc-dc converters with very large conversion ratio," *Proc. 13th European Conf. on Power Electronics and Applications (EPE),* pp. 1-10, 2009.

[41] Premananda Pany, R K Singh and Ramesh K., "TripathiBidirectional DC-DC converter fed drive for electric vehicle system," *International Journal of Engineering, Science and Technology.*

[42] Kumar, V. Vijaya,V. Udayakumar and J. Muruganandham., "Speed control of BLDC motor for four quadrant operation without loss of power," *Computation of Power, Energy Information and Commuincation (ICCPEIC), 2015 International Conference on. IEEE,* 2015.

[43] Siong, T. C.,Ismail, B,Siraj, S. F.,Mohammed, and Tajuddin , "Implementation of Fuzzy Logic controller for permanent magnet brushless DC motor drives," *In Power and Energy (PECon), International Conference on IEEE,* pp. 462-467, 2010.

[44] Blessy, M. S and M. Murugan, "Modeling and controlling of BLDC motor based fuzzy logic," *In Information Communication and Embedded Systems (ICICES),International Conference on IEEE.,* pp. 1-6, 2014.

[45] Krishnan, P. Hari and M. Arjun, "Control of BLDC motor based on adaptive fuzzy logic PID controller," *Green Computing Communication and Electrical Engineering (ICGCCEE),2014 International Conference on. IEEE,* 2014.

[46] GRUNDITZ and EMMA ARFA, "BEV Powertrain Component Sizing With Respect to Performance, Energy Consumption and Driving Patterns," pp. 3-11, 2014.

[47] Mehrdad Ehsani, Yimin Gao,Sebastien E. Gay and Ali Emadi, "Modern Electric, Hybrid Electric, and Fuel Cell Vehicles Fundamentals, Theory, and Design," *United States of America : CRC PRESS,* 2005.

[48] T.Porselvi, Srihariharan .M. K,Ashok.J and Ajith Kumar.S, "Selection of Power Rating of an Electric Motor for Electric Vehicles," *International Journal of Engineering Science and Computing,,* Vols. 7, no. 4, pp. 6469- 6472,, 2017.

[49] T.D.Gillespie, "Fundamentals Of Vehicle Dynamics," *1st ed. Society of Automotive Engineers, Inc,* 1992.

[50] X. Xin and C. Zhang, "Optimal Design of Electric Vehicle Power System with thePrinciple of Minimum Curb Mass," *ELSEVIER ScienceDirect,* vol. 105, pp. 2629-2634, 2017.

[51] M. Zhou, L. Zhao,Y. Zhang, Z. Gao and R. Pei, "Pure Electric Vehicle Power-train Parameters Matching Based on Vehicle Performance," *International Journal of Control and Automation,* Vols. 08,no. 9, pp. 53-62, 2015.

[52] S. Borthakur and S. C. Subramanian, "Parameter Matching and Optimization of a Series Hybrid Electric Vehicle Powertrain System," *In Proceedings of the ASME 2016 International Mechanical Engineering Congress & Exposition, Arizona, USA,* 2016.

[53] K. S. Amit, D. Ankit and K. Praveen, "Analysis of Induction Motor for Electric Vehicle Application Based on Drive Cycle Analysis," *In IEEE International Conference on Power Electronics, Drives and Energy Systems (PEDES),* 2014.

[54] M. G. Geda, "SpeedControl of BLDC Motor by using PWM current controller technique for electric vehicle propulsion," *Adama Science and Technology University, Adama, Ethiopia,* pp. 27-33, September,2018.

[55] W. He, N. Williard, C. Chen and M. Pecht, "State of Charge Estimation for Electric Vehicle Batteries using Unscented Kalman Filtering," *ELSEVIER: Microelectronics Reliability* , pp. 1-8, 201..

[56] A. Purna Chandra Rao, Y. P. Obulesh and Ch. Sai Babu, "Mathematical modeling of bldc motor with closed loop speed control using pid controller under various loading conditions," *ARPN Journal of Engineering and Applied Sciences,* Vols. 7, NO. 10,, no. 1819-6608, pp. 2-3, OCTOBER, 2012.

[57] T. Kim, Sensorless Control of the BLDC Motors from Near-Zero to Full Speed, Texas, USA.: PhD. Thesis, Texas A&M University, 2003.

[58] Eindhoven, Brushless DC Motor Control using the LPC2141, Netherlands: Application Note; AN10661, NXP Semiconductors, October 2007.

[59] M. sandeep and B. Lachulal, "Design of A Closed Loop Speed Control For BLDC Motor," *International Refereed Journal of Engineering and Science,* Vols. 3, no. 11, p. 7, Nev. 2014.

[60] T.Saarulatha, V.Yaknapriya, T.Muthukumar, and S.Saravanan , "Proportional Integral &Derivative Controller for BLDC Motor," *International Journal of Advances in Engineering Research (IJAER),* vol. No. 8, no. 2231-5152, November, 2014.

[61] Arman Jaya, et al , "Design of PID-Fuzzy for Speed Control of Brushless DC Motor in Dynamic Electric Vehicle to Improve Steady-State Performance," *International*

Electronics Symposium on Engineering Technology and Applications (IES-ETA), pp. 180-181, 2017.

[62] S. K. Lakhanwal and A. Gill, "S. K. LakhanFuzzy logic Technique Based Speed Control of a Permanent Magnet Brushless DC Motor Drive," *Int. J. Mod. Eng. Res,* Vols. 4, no. 8, pp. 1–12, , 2014.

[63] A. A. Zanjade and J. W. Bakal, "A. A. ZanjHardware / Software Implementation of Fuzzy - Neural - Network Self - Learning Control Methods for Brushless DC Motor Drives," *A. A. Zanjade and J. W. Bakal, "Hardware / Software Implementation of Fuzzy - Neural - Network Self - LearInt. J. Eng. Res. Technol,* Vols. 2, no. 4 , p. 717–720, 2015. .

[64] A. A. Zanjade and J. W. Bakal, "A. A. ZanjHardware Implementation of Fuzzy Logic Controller for Sensorless Permanent BLDC Motor Drives," *A. A. Zanjade and J. W. Bakal, "Hardware Implementation of Fuzzy Logic ControInt. J. Eng. Res. Technol,* Vols. 2, no. 4, p. 717–722, 2013.

[65] M. A. Shamseldin and A. A. El-samahy, "M. A. ShamseldSpeed Control of BLDC Motor By Using PID Control and Self-tuning Fuzzy PID Controller," *15th Int. Work. Res. Educ. Mechatron,* 2014..

[66] Rubaai, MJ Castro-Sitiriche, and AR Ofoli, "Rubaai, MJ Castro-SiDSP-based laboratory implementation of hybrid fuzzy-PID controller using genetic optimization for high-performance motor drives," *Rubaai, MJ Castro-Sitiriche, and AR Ofoli, "DSP-based laboratory implementation of hybrid fuzzy-PID controller using genetic optimi IEEE Transactions on Industry applications,* vol. 44, p. 1977–1986, 2008.

[67] C.Saurabh, "Motor Torque Calculations For Electric Vehicle," *International journal of scientific & technology research,* Vols. 4, no. 08, p. 2, 2015.

[68] A.Tashakori and Etal, "Direct Torque Controlled Drive Train for Electric Vehicle," *Proceedings of the World Congress on Engineering,* vol. 2, p. 1, 2012.

[69] M. Ravi Tereja Reddy and Etel, "Investigation of Capacity of Motor and its Simulation for an Electric Vehicle," *Journal of Chemical and Pharmaceutical Sciences,* no. no. 5, p. 2, Oct. 2016..

[70] Rubi Batham and Rameshwar Singh, "Speed Control of Brushless DC Motor Using Different Intelligence," *International Research Journal of Engineering and Technology (IRJET),* vol. 4, p. 1, 2017.

[71] A. Gaurav, A. Chandak and A. Bhole, "A Review on Regenerative Braking in Electric Vehicle," *International Conference on Innovations in Power and Advanced Computing Technologies,* 2017.

Reference links: L

[L1]https://www.google.com/search?q=electric+motors&tbm=isch&hl=en&chips=q:electric+motors,g_1:diagram:UJBwZBmbxx4%3D&client=firefoxbd&hl=en&sa=X&ved=2ahUKEwjvgL2ugc3rAhWs8IUKHYouBGkQ4lYoAHoECAEQFA&biw=1686&bih=818

[L2]https://www.google.com/search?q=Bidirectional+DCDC+Converter&tbm=isch&chips=q:bidirectional+dc+dc+converter,g_1:buck+boost:tXsnTBRm2Jg%3D&client=firefoxbd&hl=en&sa=X&ved=2ahUKEwjRuoeVic3rAhVaLxoKHYYkD0QQ4lYoAHoECAEQFA&biw=1686&bih=818#imgrc=_uvoQeOmWeKt7M

[L3]https://www.google.com/search?q=Four%20Quadrant%20Operation&tbm=isch&hl=en&hl=en&tbs=rimg%3ACVczGvMgp_1I4YRRolo9xtw4y&client=firefoxbd&sa=X&ved=0CBsQuIIBahcKEwioj5D38zrAhUAAAAAHQAAAAAQCA&biw=1686&bih=818#imgrc=eqft9U0a3mynM&imgdii=yu34N4d29vhCVM

[L4]https://www.google.com/search?q=Inverter+Circuit&tbm=isch&ved=2ahUKEwjOk_qsis3rAhUS04UKHf_1CDsQ2cCegQIABAA&oq=Inverter+Circuit&gs_lcp=CgNpbWcQAzICCAAyAggAMgIIADICCAAyAggAMgIIADICCAAyAggAMgIIADICCABQwcAMWMHADGC7xwxoAHAAeACAAbECiAGxApIBAzMtMZgBAKABAaoBC2d3cy13aXotaW1nwAEB&sclient=img&ei=Iu5QX856kqaXBP_ro9gD&bih=818&biw=1686&client=firefox-b-d&hl=en&hl=en#imgrc=z9ZuLCp_gr0IOM

[L5]https://www.google.com/search?q=equivalent+circuit+of+BLDC+motor&client=firefox-b-d&sxsrf=ALeKk00CfJ3jr-RqMBbe_GaBX5eh8ZEM0Q:1602666122929&source=lnms&tbm=isch&sa=X&ved=2ahUKEwiAhc3H3LPsAhUa4OAKHYmTCxoQ_AUoAXoECBAQAw&biw=1252&bih=600

[L6]https://www.google.com/search?q=Bidirectional+cascaded+buckboost+converter&tbm=isch&chips=q:bidirectional+cascaded+buck+boost+converter,online_chips:electric+vehicle&client=firefoxbd&hl=en&sa=X&ved=2ahUKEwibo3K1_vrAhUT8RoKHcvrBvkQ4lYoAnoECAEQFw&biw=1686&bih=818#imgrc=5PN5m9lqNXtweM&imgdii=RctxdFpSJ31IkM

APPENDIXES

APPENDIX A: APPENDIXES RELATED TO ANALYSIS OF DATA

- **MATLAB** code for the analysis of aerodynamics dragging force versus speed of the car in Km/hr (Figure 3.5)

```
clear all; close all;

m=1500; fric=0.01; g=9.81; a=1; r=0.25324; K_friction=0.01; F_tot=0; v=16.67;Tot_effcen.M=0.95; Adnsty=1.2; Af=2; vo=0; Cw=0.2; Vkph=0; Vkph1=0; d_Vkph=1e-2; Vkph_final=130;  x=1; n=1;

while(Vkph<Vkph_final),

Vmps=Vkph*(1000/3600);

Fadyna=0.5*Adnsty*Cw*Af*(Vmps+vo)^2;

if Vkph<=100*d_Vkph;

statfric=0.2;

else

statfric=0;

end

F_tot=m*g*(K_friction+statfric)+Fadyna+m*a; % Total force(Nm)

Power=F_tot*Vmps/0.95; Torque=(Power*r/Vmps);% Nm

Vkph=Vkph+d_Vkph;

Vkph1=Vkph1+d_Vkph;

if x>16,

F_totn(n)=F_tot;

Torquen(n)=Torque;

Powern(n)=Power/1000; %Power in KW

Fadynan(n)=Fadyna;

Vkphn(n)=Vkph;

n=n+1; x=1;

end
```

```
x=x+1;
end
Figure();
plot(Vkphn,Fadynan,'r');
axis([0 130 0 350]);
grid
xlabel('Speed of the car(Km/hr)')
ylabel('Aerodynamic dragging force (N)')
```

……………………………………………………………………………………………

- **MATLAB** code for the analysis motive force versus approaching angle of the vehicle (Figure 3.6)

```
clear all; close all;
m=1500; fric=0.01; g=9.81; a=0.5; r=0.25324; K_friction=0.01; F_tot=0; vkph=100; Tot_effcen.M=0.95; Adnsty=1.2; Af=2; vo=0; Cw=0.2; apangle=0; apangle1=0; d_apangle=1e-2; apangle_final=30; x=1;n=1;
while(apangle<apangle_final),
vmps=vkph*(1000/3600);
theta=apangle*(2*pi/360);
FA=0.5*Adnsty*Cw*Af*(vmps+vo)^2;
if apangle<=100*d_apangle;
statfric=0.001;
else
   statfric=0;
end
Frolling=m*g*(K_friction+statfric)*cos(theta);
Fgradient=m*g*sin(theta);
F_tot=Frolling+Fgradient+FA+m*a; % Total force (Nm)
apangle=apangle+d_apangle;
apangle1=apangle1+d_apangle;
if x>16,
```

```
F_totn(n)=F_tot;
Fgradientn(n)=Fgradient;
Frollingn(n)= Frolling; %Power in KW
FAn(n)=FA;
apanglen(n)=apangle;
n=n+1; x=1;
end
x=x+1;
end
Figure(1);
plot(apanglen, F_totn,'k',apanglen,Fgradientn,'b--',apanglen,Frollingn,'k:',apanglen,FAn,'r')
axis([0 30 0 9000]);
grid
xlabel('Approaching angle')
ylabel('Motive forces (N)')
```

………………………………………………………………………………………

- **MATLAB** code for the analysis driving power vs speed of the electric vehicle (Figure 3.7)

```
clear all; close all;
m=1500; fric=0.01; g=9.81; a=1; r=0.25324; K_friction=0.01; F_tot=0; v=16.67; Tot_effcen.M=0.95; Adnsty=1.2; Af=2; vo=0; Cw=0.2;Vkph=0; Vkph1=0; d_Vkph=1e-2; Vkph_final=150; x=1; n=1;
while(Vkph<Vkph_final),
Vmps=Vkph*(1000/3600);
Fadyna=0.5*Adnsty*Cw*Af*(Vmps+vo)^2;
if Vkph<=100*d_Vkph;
statfric=0.2;
else
statfric=0;
end
```

```
F_tot=m*g*(K_friction+statfric)+Fadyna+m*a; % Total force(Nm)
Power=F_tot*Vmps/0.95; % Required input power (Watt)
Torque=(Power*r/Vmps);% Nm
Vkph=Vkph+d_Vkph;
Vkph1=Vkph1+d_Vkph;
if x>16,
F_totn(n)=F_tot;
Torquen(n)=Torque;
Powern(n)=Power/1000; %Power in KW
Fadynan(n)=Fadyna;
Vkphn(n)=Vkph;
n=n+1; x=1;
end
x=x+1;
end
Figure(1);
plot(Vkphn,Powern,'r','LineWidth',2);
set(gca,'FontSize',12)
axis([0 130 0 100]);
grid
xlabel('Speed of the car(Km/hr)')
ylabel('Power (KW)')
```

……………………………………………………………………………………………………

- **MATLAB** code for torque versus speed characteristics curve (Figure 3.8)

```
clear
Ratedpower=60000; wrpm=0; wrpm1=0; wb=187.5; d_wrpm=1e-2; wrpm_final=12000;  x=1; n=1;
while(wrpm<wrpm_final),
wm=wrpm*(2*pi)/60;
```

```
Torque= Ratedpower/wm;
if Torque>=320,
Torque=320;
end
if Torque<320,
Torque= Torque;
end
Power=Torque*wm;
wrpm=wrpm+d_wrpm;
wrpm1=wrpm1+d_wrpm;
if x>16,
wrpmn(n)=wrpm;
Torquen(n)=Torque; Powern(n)=Power/1000;
n=n+1; x=1;
end
x=x+1;
end
Figure(1);
[AX,Torque,Power]=plotyy(wrpmn,Torquen, wrpmn,Powern);
axis([0 12000 0 350]);
set(get(AX(1),'ylabel'), 'string','Torque(Nm)')
set(get(AX(2),'ylabel'), 'string','Power(KW)')
set(Torque,'LineStyle','--')
set(Power,'LineStyle','-')
set(gca, 'FontName','TimesNewRoman')
set(gca, 'FontSize',12)
set([Torque,Power],'LineWidth',0.5)
xlabel('Motor Speed(rpm)')
```

```
grid

legend('Torque','Power')
```

……………………………………………………………………………………………………

- **MATLAB** code for analysis of the effect of the approaching angle in the power of the vehicle (Figure 3.9)

```
clear all; close all;

m=1500; fric=0.01; g=9.81; a=0; r=0.25324; c_ofriction=0.01; d=0.25324; v=16.67; Tot_effcen.M=0.95; Adnsty=1.2; Af=2; vo=0; Cw=0.2; angleR=0; angleR1=0; d_angleR=1e-6; angleR_final=40;  x=1; n=1;

while(angleR<angleR_final),

Fadyna=0.5*Adnsty*Cw*Af*(v+vo)^2;

theta=angleR*2*pi/360; %Degree to radian conversion

F_tot=m*g*(sin(theta)+c_ofriction*cos(theta))+Fadyna+m*a; % Total force(Nm)

Power=F_tot*v; Torque=(Power*r/v)/0.95;

angleR=angleR+d_angleR;

angleR1=angleR1+d_angleR;

if x>16,

F_totn(n)=F_tot;

Torquen(n)=Torque; Powern(n)=Power/1000; %Power in KW

Fadynan(n)=Fadyna;

thetan(n)=angleR;

n=n+1; x=1;

end

x=x+1;

end

plot(thetan,Powern,'b','LineWidth',2);

axis([0 40 0 200]);

grid

xlabel('The approaching angle in degree')

ylabel('Power (KW)')
```

APPENDIX B: RELATED TO THE LINEAR BLDC MOTOR MATLAB/SIMULINK MODEL

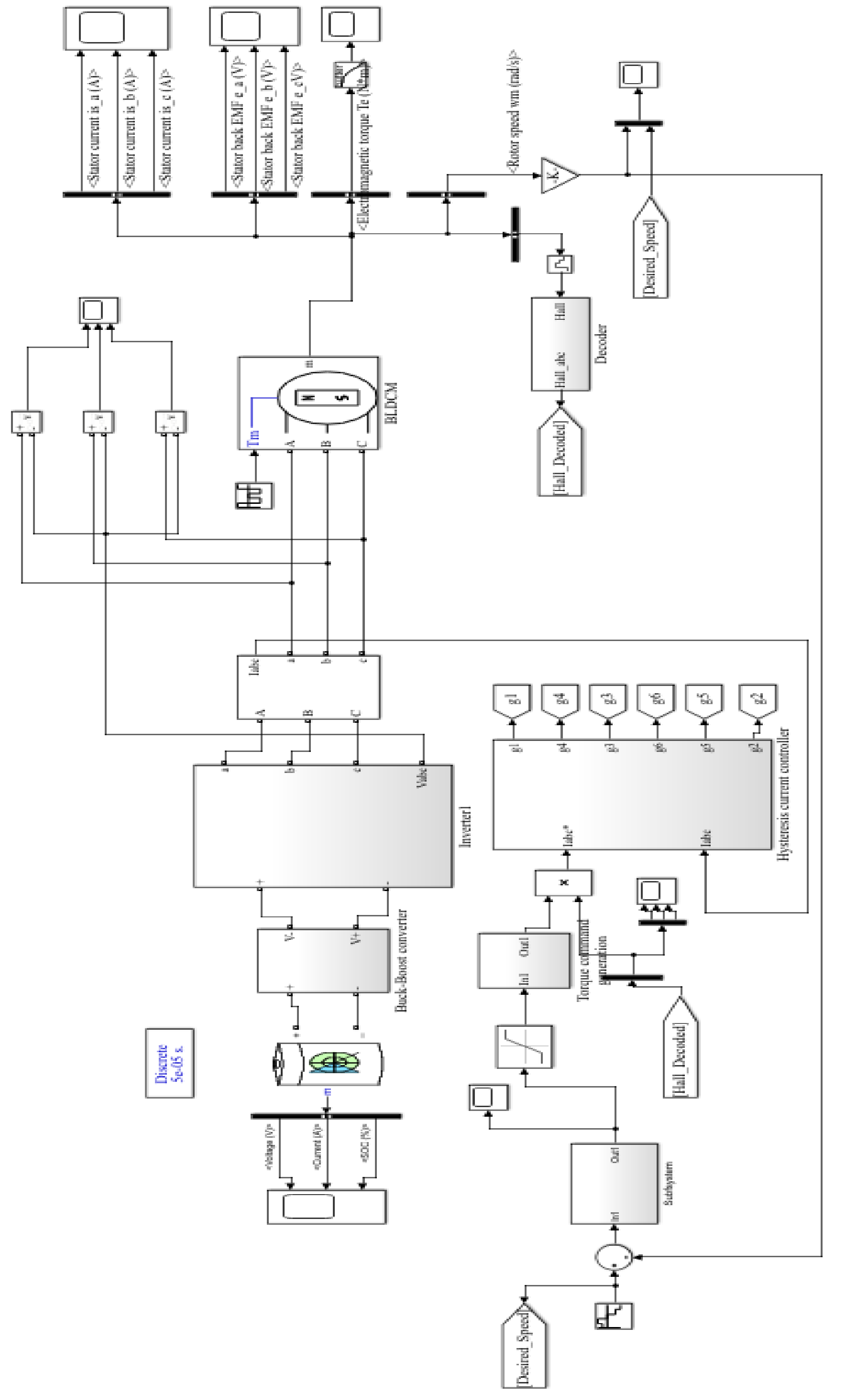

Fuzzy-PID Simulink block for BLDC motor model

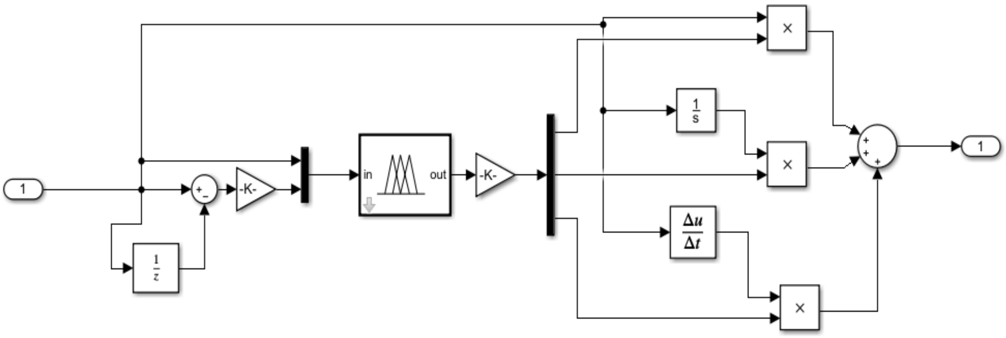

Torque generation command Simulink block for BLDC motor model

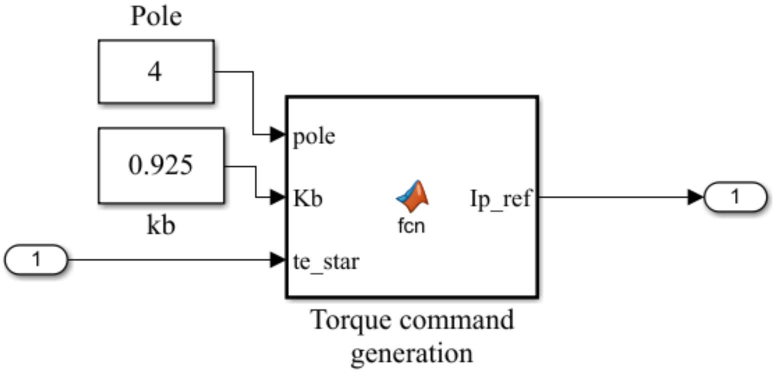

MATLAB code for Torque generation command

```
function Ip_ref  = fcn(pole, Kb,te_star)

te_rate = 160; lamda_p =Kb*(pole/2);

% torque limit => up to 2 [p.u.]

te_lim_p = 2*te_rate; te_lim_n = -2*te_rate;

if (te_star>=te_lim_p)

te_cmd = te_lim_p;

elseif (te_star<=te_lim_n)

te_cmd = te_lim_n; else

te_cmd = te_star;

end

Ip_ref = te_cmd/(2*lamda_p);

end
```

Hysteresis current Simulink block for BLDC motor model

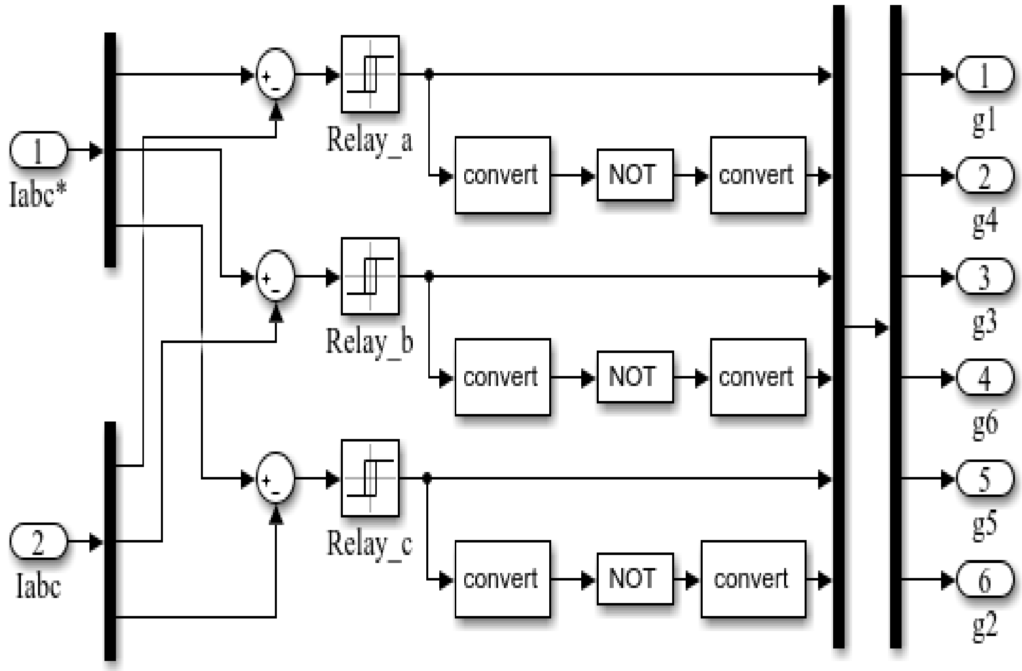

PID design Simulink block for BLDC motor model

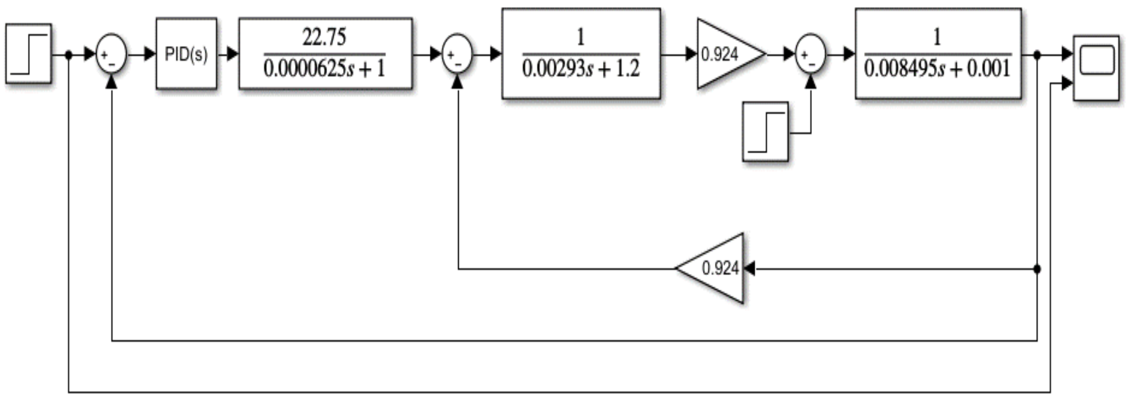

Inverter Simulink block for BLDC motor model

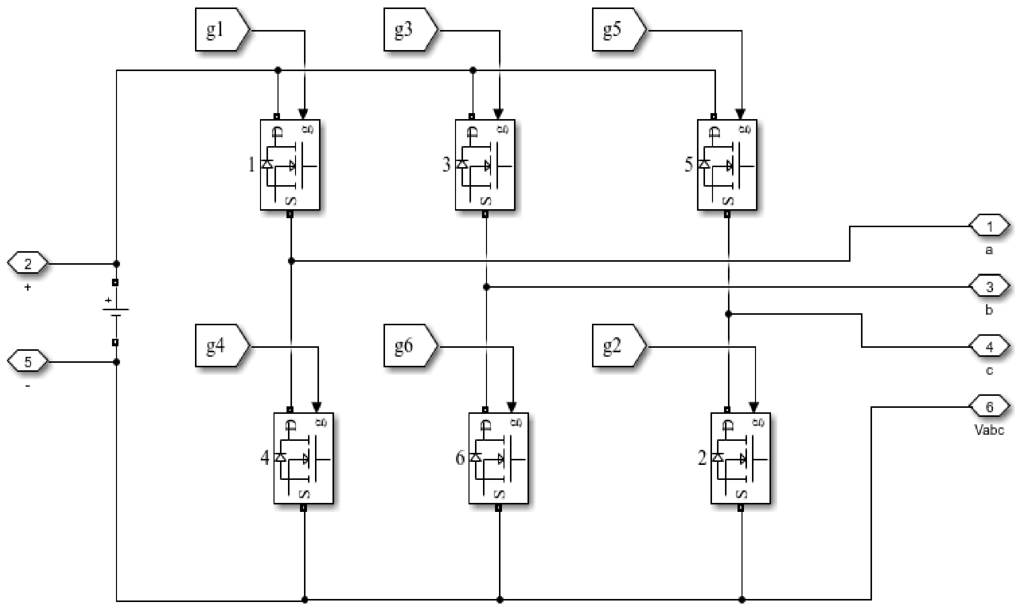

Bidirectional DC-DC using MOSFET and freewheeling diode Simulink block for BLDC motor model

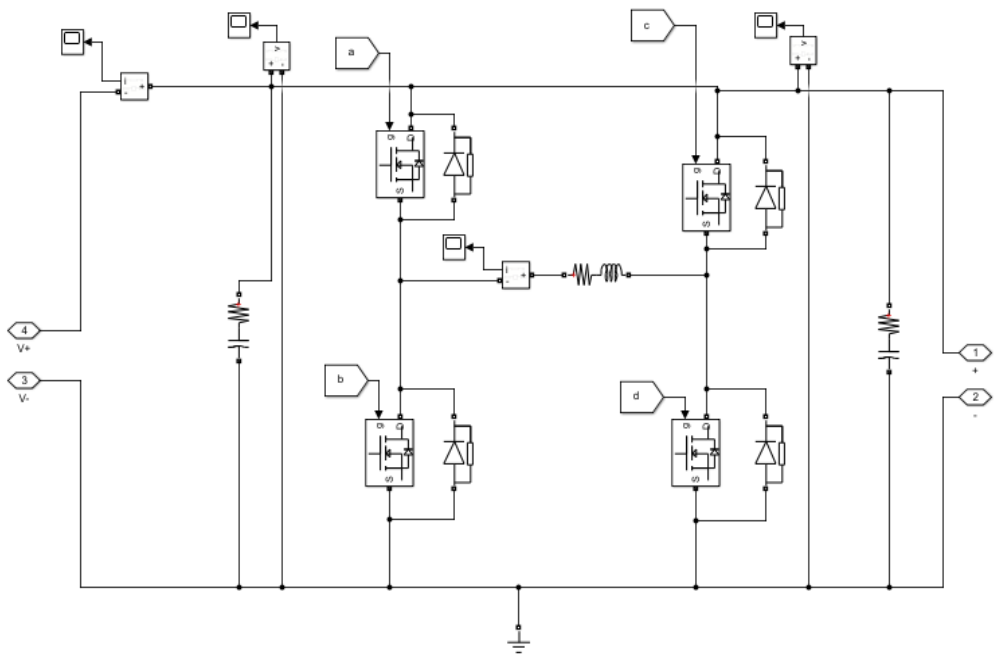

Hall effect decoder Simulink block for BLDC motor model

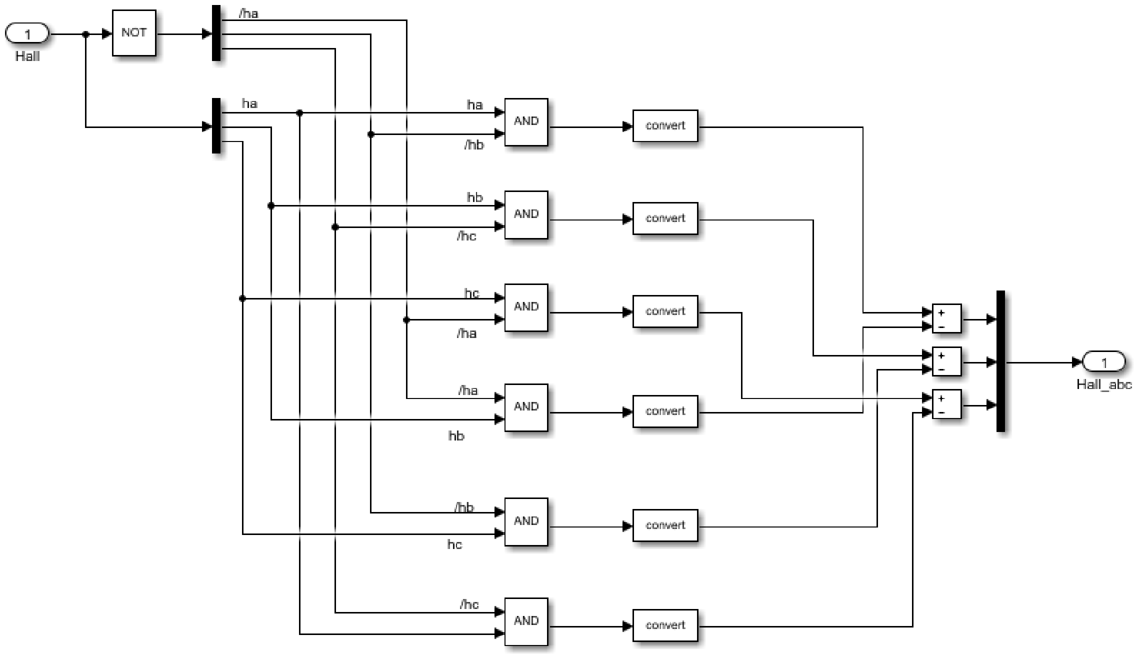

APPENDIX C: APPENDIXES RELATED TO DATA COLLECTION

Data from internet: Data of similar size motor used for EV (accessed on January 05, 2020).

Power	The battery voltage	Speed	Rated torque	Peak torque	Peak power	current	Peak current	Efficiency	Weight
50 kw	360V~540V	3500rpm	136Nm	300Nm	110KW	140A	320A	95.4%	250kg
60 kw	360V~540V	3500rpm	164Nm	350Nm	130KW	172A	380A	95.6%	260kg
75kw	360V~540V	3500rpm	205Nm	260Nm	160KW	212A	430A	95.7%	270kg
100kw	380V~540V	5000rpm	191Nm	400Nm	220KW	289.3A	590A	96.0%	270kg